INCLUSION OF GASES IN SOME CLATHRATE COMPOUNDS

By

Sydney Arnold Allison

A thesis submitted for the degree of

DOCTOR OF PHILOSOPHY in the UNIVERSITY OF LONDON

Chemistry Department,
Imperial College of Science and Technology,
London S.W.7.

OCTOBER, 1966.

ABSTRACT

By vigorous agitation of a small quantity of quinol or phenol crystals with stainless steel ball bearings in an atmosphere of a suitable gas it has been found possible to form the clathrate compound of this host material and the gas by direct solid-gas reaction.

The decomposition pressures of the quinol clathrates could not be accurately found, but those of the phenol clathrates were determined and by application of the Clausius-Clapeyron equation the heat of reaction:

1 mole gas M + n moles α-phenol

$\longrightarrow$ 1 mole M.n β-phenol

was obtained for each phenol-gas clathrate. The values were found to be -5.3_5, -8.1_9, -6.1_8, -8.4_3, -7.6_5, -9.0_6 and -10.7 K cals./mole for the clathrates of krypton, xenon, methane, ethane, ethylene, carbon dioxide and sulphur dioxide respectively.

The uptake of gas was followed volumetrically and the equilibrium occupancy of the cavities determined as a function of temperature and pressure. At constant temperature the fractional occupancy of the quinol clathrates as a function of pressure closely approximates to a Langmuir isotherm. From the variation of the Langmuir

equilibrium constant with temperature, the heats of intercalation of the gases have been calculated to be -6.0_3, -9.8 and -6.1 K cals./mole for krypton, xenon and methane respectively. At constant temperature the fractional occupancy of the phenol clathrates as a function of temperature was not found to follow the equations either of Langmuir or of double Langmuir isotherms. From the temperature coefficients of the isotherms the heats of intercalation of the gases within the cavities of the phenol lattice have been calculated to be -5.9, -10.6, -6.5, -11.4, -14.5 and -15.5, K cals./mole for the gases krypton, xenon, methane, ethane, ethylene and carbon dioxide respectively. The enthalpy differences between the α - and β - modifications of phenol with the different enclathrated guest species have also been calculated and found to be 0.14, 0.80, 0.06_4, 0.88, 2.1 and 1.8 K cals./mole for the gases krypton, xenon, methane, ethane, ethylene and carbon dioxide respectively.

Experiments were made in which the manner of shaking was varied from run to run and the effect on the uptake of gas as a function of time observed. A number of parameters governing the rate and mechanism of these reactions were determined.

ACKNOWLEDGEMENTS

I am deeply indebted to Professor R. M. Barrer, F.R.S., for his patient guidance and encouragement during the course of this work.

I wish to thank my parents for their encouragement and unfailing support during the course of this study.

C O N T E N T S

Page No.

Abstract 2

Acknowledgements 4

I INTRODUCTION 7

I.1 The Nature of Clathrate Compounds 7
I.2 The Nature and Crystalline Structure of the Quinol Clathrate 9
I.3 The Nature and Crystalline Structure of the Phenol Clathrate 15
I.4 The Phase Behaviour and Conditions of Formation of Clathrates 20
I.5 The Thermodynamics of Clathrate Formation 22
I.5.1 Application of the Clapeyron Equation to the Three-Phase Equilibrium α-clathrate-gas 29
I.6 Theories of Clathrates 30
I.6.1 The van der Waals and Platteeuw Theory 30
I.6.2 The Barrer and Stuart Theory 35
I.6.3 Application to Quinol and Phenol Clathrates 39
I.6.4 Evaluation of the Cell Partition Function by the Method of Lennard-Jones and Devonshire 44
I.7 The Motivation and Objectives of the Work Undertaken 53

II EXPERIMENTAL 56

II.1 Materials 56
II.2 Preliminary Experiments 57
II.3 Refinement of the Experimental Method 63
II.3.1 The Thermostat Bath 65

		Page No.
II.4	The Standardised Experimental Technique	.. 69
II.4.1	Calibration of the Volumes of the System	.. 69
II.4.2	The Reaction Bulb and Connecting Arm	.. 71
II.4.3	Introduction of a Sample of Crystals into the Reaction Vessel..	.. 72
II.4.4	Sorption of Gas by the Crystals	.. 73
II.4.5	Determination of Dissociation Pressures	.. 76
III	RESULTS AND DISCUSSION..	.. 77
III.1	Preliminary Results	.. 77
III.2	The Dissociation Pressures of the Quinol and Phenol Clathrates	.. 80
III.2.1	The Dissociation Pressures of the Quinol Clathrates	.. 81
III.2.2	The Dissociation Pressures of the Phenol Clathrates	.. 84
III.3	The Measurement of the Maximum Sorption of Gas by the Quinol Crystals	.. 97
III.4	The Measurement of the Maximum Sorption of Gas by the Phenol Crystals	..116
III.5	Kinetic Measurements of the Formation of the Quinol and Phenol Clathrates	..141
III.5.1	The Initiation Time ..	..142
III.5.2	The Rate of Formation of the Clathrate	..154
III.5.3	Kinetic Runs with Interrupted Shaking	..164
III.5.4	Kinetic Runs with No Shaking	..165
III.5.5	The Effect of Shaking on the Reaction	..174

I INTRODUCTION

I.1 The Nature of Clathrate Compounds

In the present work the clathrate compounds formed by quinol and phenol with a number of different gases were studied.

The term clathrate is used to describe a type of molecular inclusion compound in which molecules of one compound known as the "host" compound form a three-dimensional network which encloses cavities, in which molecules of another compound know as "guest" molecules may be trapped. The molecules of the guest compound are enclosed in such a way that they cannot escape except by decomposition of the surrounding host network. The only restrictions on the nature of the guest molecules are that they are neither too large to fit into the cavity nor too small to be prevented from escaping, and that the guest species does not react chemically with the host.

There is thus no chemical bonding between the host and guest molecules but there are weak van der Waals interactions capable of stabilising the clathrate lattice structure. In general the host lattice is unstable when

no guest molecules are trapped in the cavities. If a certain fraction of the cavities is occupied in a certain region of temperature and pressure then the clathrate structure may be thermodynamically stable with respect to the normal crystal structure of the host.

Chemical equations implying bonds and stoichiometry do not apply to these phases and the degree of filling of the cavities is dependent on the conditions of temperature and pressure under which the clathrates were formed.

Compounds capable of forming a host lattice cover a wide range of compounds from organic molecules such as quinol and phenol through water to inorganic complexes such as monoammine nickel(II) cyanide and Dianin's compound. Urea adducts and zeolite complexes have also been referred to as clathrates. Guest species have also been found to cover a wide range including inert gases, inorganic gases such as carbon dioxide and sulphur dioxide,and organic molecules such as methane, ethane and methanol.

In the next chapter a more detailed description of the nature and crystal structure of the quinol and phenol clathrates will be given.

I.2 The Nature and Crystalline Structure of the Quinol Clathrate

It has long been known that quinol forms complexes with certain volatile compounds, these complexes having the general limiting formula

$$3C_6H_4(OH)_2.M$$

Mylius[1] in his investigations concluded that no ordinary chemical combination existed. He suggested that during the crystallisation of these compounds the quinol molecules were in some way able to lock the volatile component into position.

Palin and Powell[2] investigated the structure of these compounds to discover their exact nature. They prepared the SO_2 compound by slow crystallisation from an aqueous solution of quinol saturated with SO_2 and showed that it was not stoichiometric since the ratio of SO_2 to quinol was lower than the 1:3 suggested, and was variable. They subjected the SO_2 compound to a detailed X-ray study and determined the crystalline structure as described below. Powell[3] postulated the general nature of this type of compound and suggested the name clathrate to describe them.

Palin and Powell[4] then examined the crystalline structure of the quinol compound which is obtained by

crystallising quinol from a solution in methanol. This crystalline structure had been termed β-quinol by Caspari[5,6] to distinguish it from the normal structure which he termed α-quinol. They showed that β-quinol had the same structure as the SO_2 complex, and was therefore also a clathrate compound with molecules of methyl alcohol occupying the same position as the SO_2 molecules in the SO_2-quinol complex.

Palin and Powell[7] prepared and examined a wide range of these quinol complexes and were able to show that they were all of the same kind. They suggested that the term β-quinol be now used for quinol in the crystalline structure of the host lattice, and not for the methanol complex alone.

The structure of β-quinol

In β-quinol the quinol molecules are linked through hydrogen bonds to form a giant molecule extending in three dimensions.

Six oxygen atoms are linked by hydrogen bonds to form a plane hexagon with sides 2.75Å long. The corresponding six quinol molecules project alternately up and down from the plane of the oxygen hexagon, the O-O axis of the quinol molecule making an angle of about 45° with the plane of the oxygen hexagon.

The second oxygen atom of each quinol molecule is connected in a similar way with another oxygen hexagon parallel to but above or below the first. This is illustrated in Fig. 1. The O-O axis of a quinol molecule is inclined at a small angle of about 3^{o} to the line joining the centre of the axis to the centre of a connected oxygen hexagon as it would be viewed in the projection shown in Fig. 1A. This results in the O-O axis making two slightly different angles of average value 111^{o}, nearly the tetrahedral angle with the hydrogen bonds at its ends. The plane of the benzene ring of the quinol molecule is inclined at an angle of 45^{o} to its oxygen-carbon bond line.

Since the benzene rings of the quinol molecule have sides of 1.4Å this lattice structure constitutes a very open framework into which an identical second framework may be substituted. This is so arranged that an oxygen hexagon of the second structure lies halfway between the top and bottom oxygen hexagons of Fig. 1. No small gaps now exist between the two structures, but two oxygen hexagons lying parallel, one above the other, create, with their respective quinol benzene ring planes, a cavity as seen in Fig. 2. An appropriately sized molecule may now fit into this cavity and be trapped. The atoms

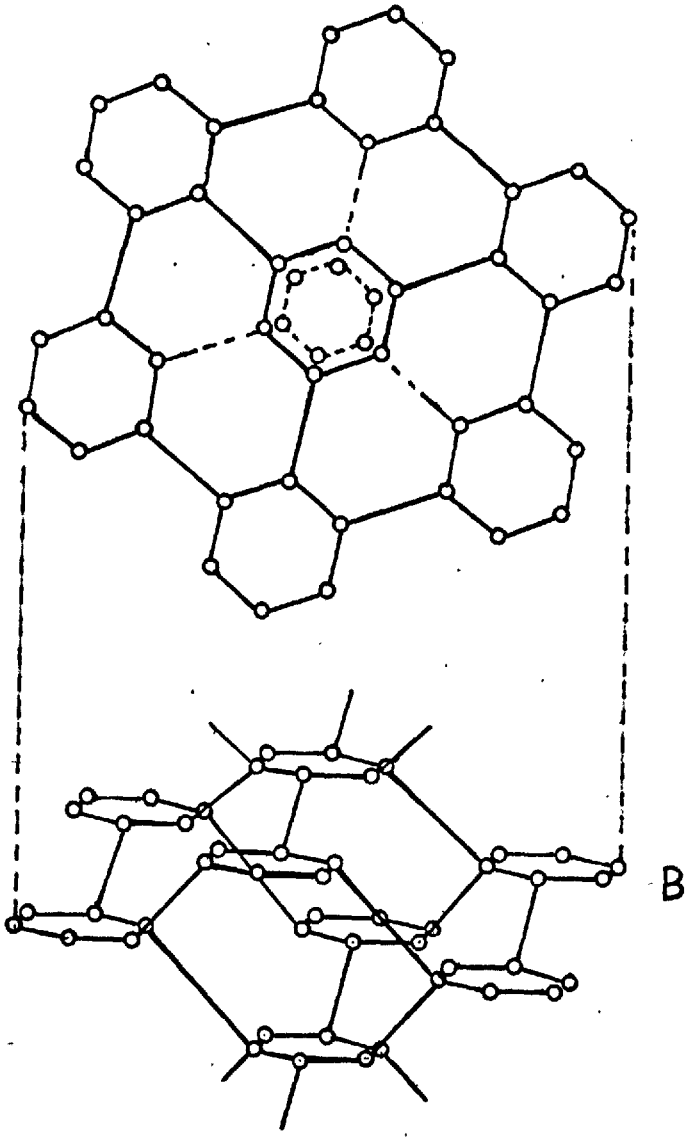

Fig. 1

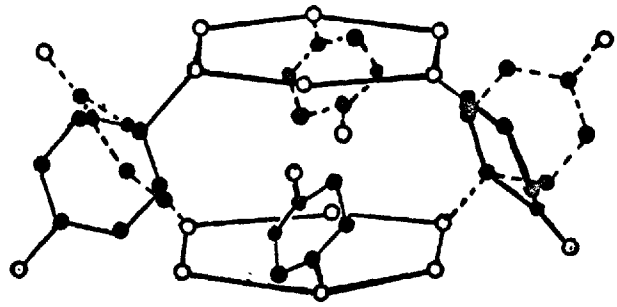

Fig. 2

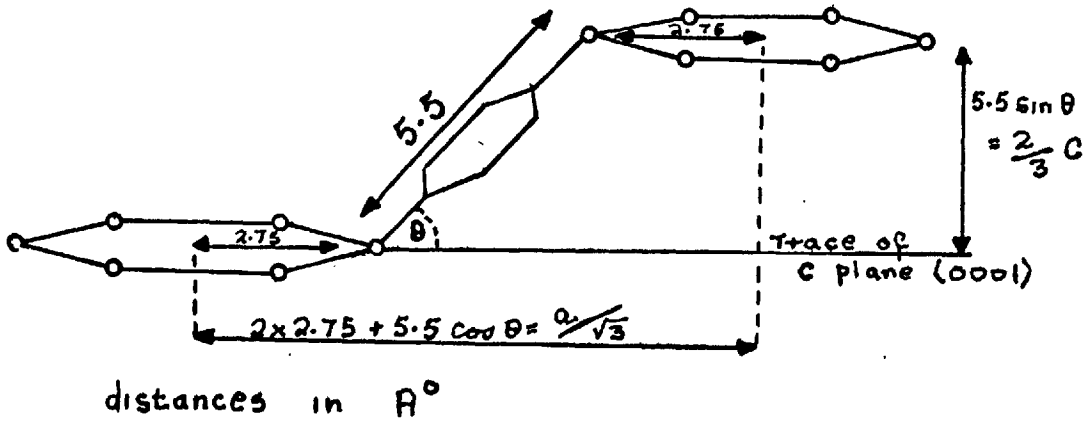

distances in A°

Fig. 3

surrounding the cavity centres are spread over a sphere of diameter about 8Å, and the cavity has a diameter of about 4Å. There is one such cavity for every three quinol molecules.

Palin and Powell[7] showed that the structure is not completely rigid.but is capable of distortion from the form of the empty lattice as the size of the caged molecule increases. As the size increases the angle θ increases, the C-dimension increases and the α -dimension decreases in the relationship given in Fig. 3. The size of θ varies from $41^{\circ}28'$ for the acetylene-quinol clathrate, through 45° for the SO_2-quinol clathrate, to $49^{\circ}10'$ for the clathrate formed by quinol with the large methyl cyanidë molecule. The degree of filling increases as the distortion increases, indicating that the greater the distortion the greater the degree of filling necessary to stabilise the structure. Although the empty β -quinol structure can be prepared it is not stable.

If each cavity is occupied by a guest species M the clathrate has the limiting formula

$$3C_6H_4(OH)_2.M \ .$$

I.3 The Nature and Crystalline Structure of the Phenol Clathrates.

That phenol, like quinol, forms complex compounds with a wide range of volatile compounds has also been known for a long time.

Terres and Volmer[8] made a phenol complex with CO_2 and Nikitin[9], and Nikitin and Kovalskaya[10] made similar compounds with a wide range of gases including the noble gases radon and xenon. That these compounds were clathrate compounds analogous to the quinol clathrates seemed probable.

Von Stackelberg, Hoverath and Scheringer[11] undertook a detailed X-ray structural analysis of these compounds and found that they were clathrate compounds having the crystal structure described below. As with quinol the clathrate crystal structure is referred to as β-phenol and the normal phenol crystal structure as α-phenol.

The structure of β-phenol

The oxygen atoms of six phenol molecules are joined by hydrogen bonds to form a regular hexagon with sides 2.7Å long. The phenol molecules project alternately up and down from the plane of the oxygen hexagon and at angles of 44° to it. The plane of the benzene ring

of the phenol molecules is bent at an angle of 42° to its oxygen-carbon bond line. Two such hexagons lie parallel and one above the other at a distance of 5.6Å apart as illustrated in Fig. 4. The space between the two hexagons constitutes a small cavity capable of containing a molecule up to about 5Å in free diameter. Eight such cavities lie at the corners of a rhombohedrally shaped elementary cell as shown in Fig. 5. The plane of the oxygen hexagons is at right angles to the axis of the cell, and the phenol molecules lie in line with the lines joining the corners of the cell. The sides of the cell have a length of 12.05Å, the rhombohedral angle being 86°. These eight small cavities enclose a large cavity three times as long as a small cavity, having a length of about 15Å. The positions of the two types of cavity are shown in Fig. 5. If a molecule having a free diameter of greater than 4.5Å is contained in the small cavity then the cell is distorted along the cell axis, the rhombohedral angle being made smaller.

Construction of a scale model of the clathrate unit cell shows that there is a "window" between two adjacent large cavities through which a trapped molecule might be able to pass, suggesting the possibility

of mobility of guest molecules between the large cavities.

Maximum composition formulae for phenol clathrates have been described and given as:[12]

(i) $12C_6H_5OH.5M_1$, where M_1 is a molecule the size of HCl, four such molecules being located in the large cavity;

(ii) $12C_6H_5OH.4M_2$, where M_2 is a molecule the size of SO_2;

(iii) $12C_6H_5OH.2M_3$ where M_3 is a molecule the size of carbon disulphide, only two carbon disulphide molecules can be located in the large cavity and none in the small;

(iv) $12C_6H_5OH.2M_3.M_1$(or M_2) for a double clathrate.

It is suggested, however,[13] that in the carbon disulphide-phenol clathrate the small cavity was occupied by a molecule of oxygen or nitrogen from air which would have made it a double clathrate of the limiting formula above.

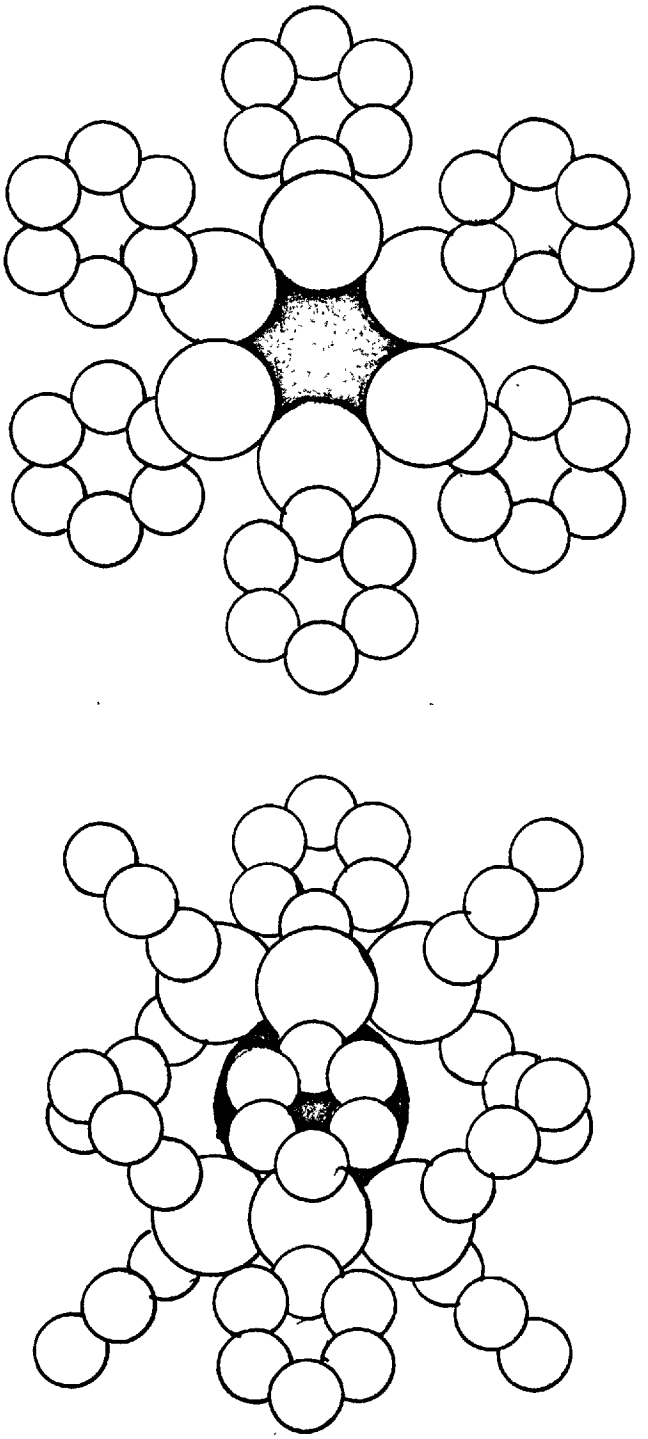

Fig. 4

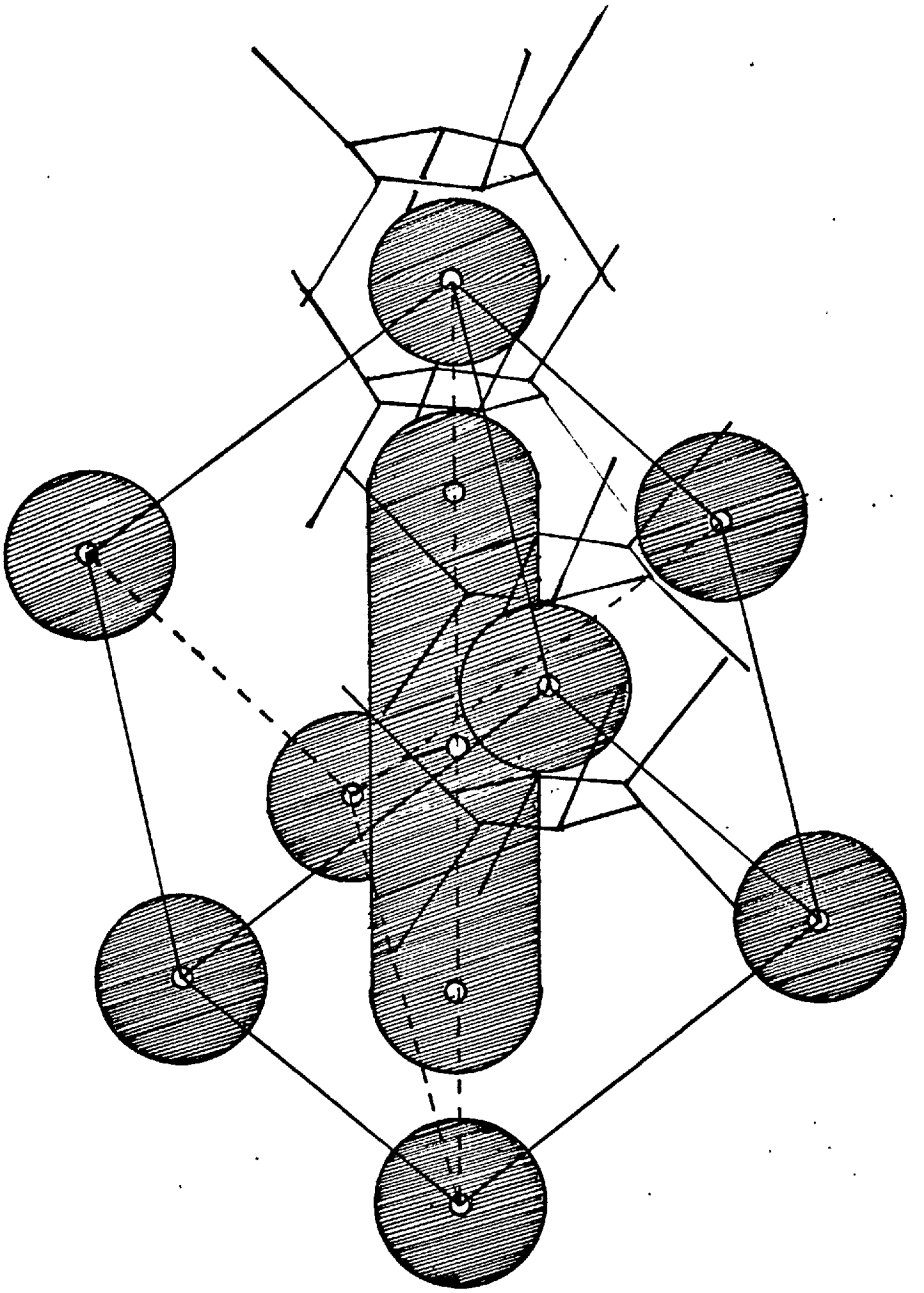

Fig. 5

I.4 The Phase Behaviour and Conditions of Formation of Clathrates

The P-T-x diagram for the binary system quinol-argon is shown in Fig. 6.

At ordinary temperatures the three-phase equilibria in which clathrates play a role are

$$\alpha\text{-host} + \text{gas} \rightleftharpoons \text{clathrate}$$

$$\alpha\text{-host} + \text{clathrate} \rightleftharpoons \text{liquid}$$

$$\text{liquid} + \text{gas} \rightleftharpoons \text{clathrate.}$$

The liquid phase is liquid host in which a small amount of gas is dissolved.

The clathrate is formed if the pressure and temperature are such that they are represented by a point in the shaded area.

Consider the three phase equilibrium α-quinol-clathrate-gas. When the temperature rises the gas content drops. For a given temperature there is a pressure below which the clathrate is no longer stable but decomposes or is metastable. This pressure is known as the dissociation pressure, or decomposition pressure.

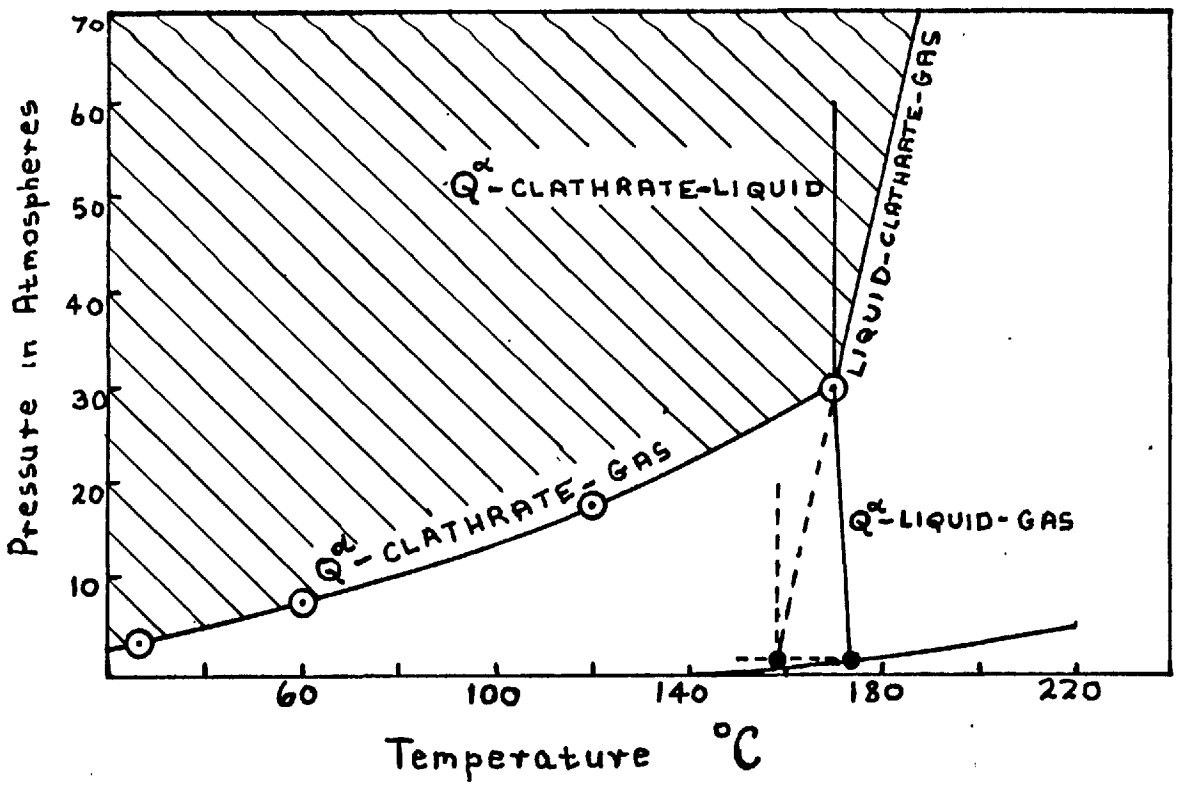
Pressure in Atmospheres
70
60
50
40
30
20
10
60
100
140
180
220
Temperature °C
Q$^{\alpha}$ - CLATHRATE-LIQUID
LIQUID-CLATHRATE-GAS
Q$^{\alpha}$ - CLATHRATE - GAS
Q$^{\alpha}$ - LIQUID - GAS

Fig. 6

I.5 The Thermodynamics of Clathrate Formation

In order to examine the factors influencing the formation and stability of the clathrate, a hypothetical clathrate of guest species M enclosed in a host lattice having one type of cavity only will be considered. The limiting composition of the clathrate, when every cavity contains one molecule, is M.n, n being the number of host molecules per cavity. Let quinol here be considered as the host compound.

At temperature T and pressure P assume that the clathrate has the composition, $M.^{n}/\theta$ (β -quinol), where θ is the fraction of cavities occupied by guest molecules.

The clathrate may be considered to have been formed in the following reactions:

$^{n}/\theta$ moles. α-quinol $\rightarrow$ $^{n}/\theta$ moles. β-quinol (as empty host lattice) $\quad \Delta G_1$

1 mole of gas M + $^{n}/\theta$ moles. β -quinol

$\longrightarrow$ 1 mole. $M.^{n}/\theta$ moles. (β -quinol) $\quad \Delta G_2$

---

1 mole gas M + $^{n}/\theta$ moles. α -quinol

$\longrightarrow$ 1 mole. M. $^{n}/\theta$ moles (β -quinol)

$$\Delta G = \Delta G_1 + \Delta G_2$$

ΔG, ΔG_1 and ΔG_2 are free energy changes in the above reactions.

ΔG_1 may be considered as:-

$$\Delta G_1 = {}^{n}/\theta \; \Delta G_{\alpha \rightarrow \beta}$$

where $\triangle G_{\alpha \rightarrow \beta}$ is the molar free energy change accompanying the conversion of α -quinol into the empty β -quinol lattice. In view of the fact that empty β -quinol is unstable it is reasonable to assume that $\triangle G_{\alpha \rightarrow \beta}$ is a positive quantity.

$$\triangle G = {}^{n}/_{\theta} \triangle G_{\alpha \rightarrow \beta} + \triangle G_2$$

Similarly for the enthalpy change accompanying the above reactions

$$\triangle H = {}^{n}/_{\theta} \triangle H_{\alpha \rightarrow \beta} + \triangle H_2$$

$\triangle G_2$ may be expressed in terms of the enthalpy change $\triangle H_2$ and entropy change $\triangle S_2$

$$\triangle G_2 = \triangle H_2 - T \triangle S_2$$

Assuming that for a spherical guest molecule the molecules comprising the lattice cavity react with it according to the Lennard-Jones 12:6 potential, then the potential energy $\varepsilon(r)$ of the guest molecule can be calculated as a function of the distance r of the centre of the molecule from the centre of the cavity. This is illustrated in Fig. 7. Curve (i) represents a very small guest molecule. Curve (ii) a molecule fitting comfortably into the cavity with a little space to spare and curve (iii) is for a large molecule

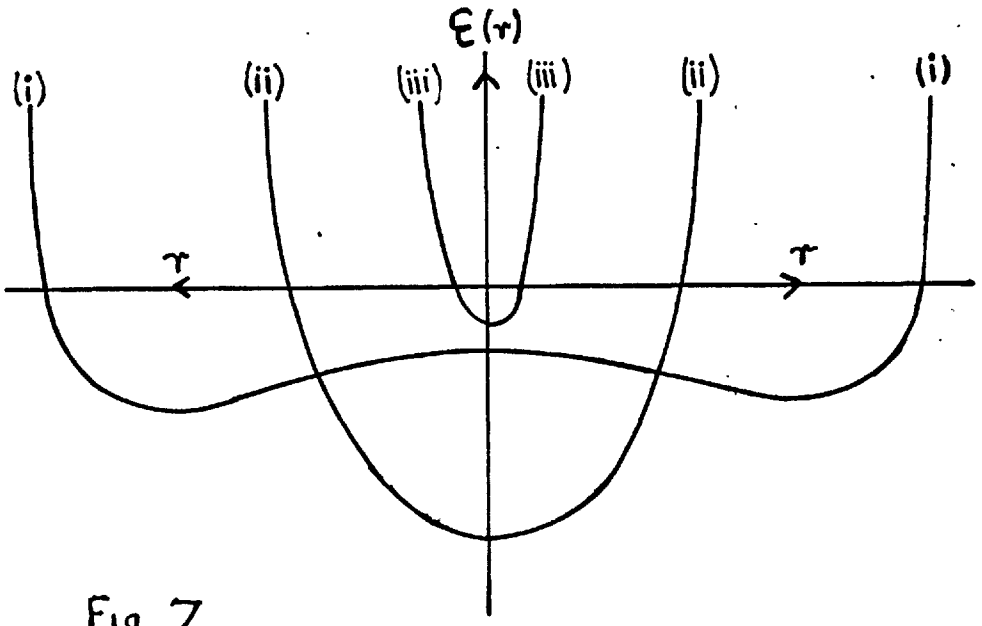
ε(r)
(i)
(ii)
(iii)
(iii)
(ii)
(i)
r
r

Fig. 7

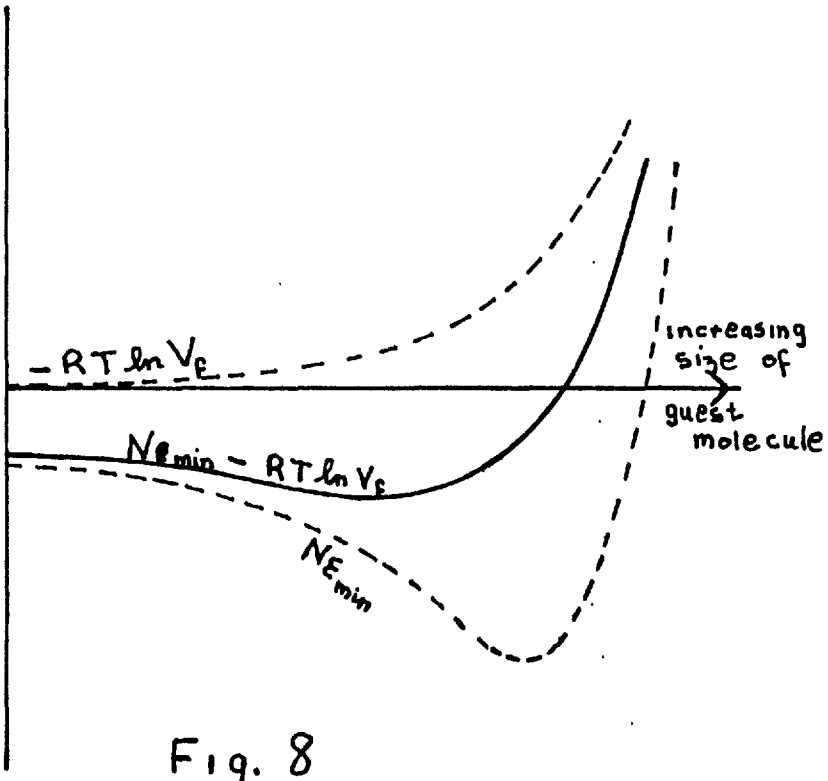
$-RT\ln V_E$
increasing size of guest molecule
$N\varepsilon_{min} - RT\ln V_E$
$N\varepsilon_{min}$

Fig. 8

only just able to fit into the cavity with resultant large repulsive energy even at the centre of the cavity.

Assuming that the guest molecules behave classically and that the internal degrees of freedom for the encaged and gaseous molecules are the same, then ΔH_2 will be equal to the energy required to remove 1 mole of guest molecules from the minimum energy level $\varepsilon_{min.}$ of the potential energy well into the gas phase. Therefore

$$\Delta H_2 = N\varepsilon_{min.} - RT$$

where N is Avogadro's number and RT is an external work done by the system through the evolution of 1 mole. of gas in the gas phase.

The effective volume over which the centre of the molecule is free to move in the cavity may be defined as V_f where

$$V_f = \int_{cavity} 4\pi r^2 \exp\left[\frac{-(\varepsilon(r) - \varepsilon_{min.})}{kT}\right].dr$$

where $4\pi r^2 dr$. is the element of volume over which the interaction energy lies between $\varepsilon(r)$ and $\varepsilon(r) + d\varepsilon(r)$. The exponential term is a measure of the

accessibility of the element of volume relative to that when $\varepsilon(r) = \varepsilon_{min.}$

The molar volume of the enclathrated guest molecule is $V_f.N$. In the gas phase it is $\frac{RT}{P}$. The contribution to the entropy change ΔS_2 due to this reduction in molar volume may be expressed as

$$\Delta S_2 = R \ln \left[\frac{NP.V_f}{RT}\right] - R + S_c$$

-R represents the loss in communal entropy in enclathrating one mole of gas with one molecule per cavity. S_c is the configurational entropy and arises from the number of ways of arranging the occupied and empty cavities

$$S_c = - R \left[\ln\theta + \frac{1 - \theta}{\theta} \ln(1 - \theta)\right]$$

Thus by substituting for ΔH_2 and ΔS_2 in the expression for ΔG.

$$\Delta G = {}^{n}/_{\theta} \left(\Delta G_{\alpha\rightarrow\beta} \right) + N\varepsilon_{min.} - RT \left[\ln\frac{NP.V_f}{RT} - \left\{\ln\theta + \frac{1 - \theta}{\theta} \ln(1 - \theta)\right\}\right]$$

For the clathrate to be thermodynamically stable ΔG must have a negative value. The most favourable conditions

for the formation of the clathrate will thus be found when

1. $\varepsilon_{min.}$ has a large negative value;
2. V_f is large;
3. P is large;
4. T is small.

Since θ is determined by $\varepsilon_{min.}$, V_f, P and T, it should not be considered separately. The above conditions imply that θ is large for stable clathrate formation. As θ tends to one, the numerical value of the configurational entropy term S_c tends to zero. This decreases the negative value of ΔG. This is offset by the large values of P and small values of T required for large θ and by the decrease in value of the term $^{n}/\theta\ \Delta G_{\alpha\rightarrow\beta'}$. $\varepsilon_{min.}$ and V_f are also not independent, a high value of $\varepsilon_{min.}$ generally accompanying a small value of V_f. A large guest molecule with large repulsive interactions results in $\varepsilon_{min.}$ being numerically small as well as V_f. The clathrate is then rendered unstable. Fig. 8 shows how $N\varepsilon_{min.}$ and $-RT\ln V_f$ are expected to vary with increasing size of the maximum dimension of a guest molecule. Maximum stability occurs before $-\varepsilon_{min.}$ is a maximum due to the effect of V_f.

This expected behaviour applies when the guest molecules have different radii but the same force constant. In general, however, the larger the molecule the larger the force constant.

As the size of the guest molecule increases the increase in repulsion may lead to distortion of the host lattice and anomalously large values of $\Delta G_{\alpha \rightarrow \beta}$, contributing to decreased stability.

If the host lattice has escape holes from its cavities then small guest molecules require only a small activation energy for their escape and the ensuing decomposition of the clathrate structure. This reason in addition to low thermodynamic stability accounts for the non-existence or very low stability of clathrates with very small guest molecules.

In general, therefore, as the size of the guest molecules increases the stability of the clathrate increases to a maximum after which stability rapidly decreases until a size of guest molecule is reached above which no clathrate may be formed.

I.5.1 Application of the Clapeyron Equation to the Three-Phase Equilibrium α-Clathrate-gas

The Clapeyron equation may be applied to the univariant two-component system of the three-phase equilibrium existing for the clathrate of species M to give

$$\frac{dP}{dT} = \frac{\Delta H}{T\,\Delta V}$$

where ΔH is the heat of the reaction:

1 mole. gas M + $^{n}/_{\theta}$ moles. α-quinol $\rightarrow$ 1 mole.M.$^{n}/_{\theta}$ β-quinol

and ΔV is the corresponding volume change.

Since the volume change accompanying the conversion of $^{m}/_{\theta}$ moles. α-quinol to $^{n}/_{\theta}$ moles β-quinol is usually less than 0.1% of the volume change in enclathrating 1 mole. of gas then ΔV may be replaced by the volume of 1 mole of gas M at pressure P and temperature T.

Assuming ideal gas behaviour

$$\frac{dP}{dT} = \frac{-\Delta H.P}{RT^{2}}$$

If ΔH remains constant along the three phase equilibrium the above can be integrated to give:

$$\ln P = C + \frac{\Delta H}{RT}$$

A plot of lnP against $\frac{1}{T}$ will then be a straight line the slope of which will be equal to $\frac{\Delta H}{R}$.

At large pressure the departure of the behaviour of the gas from ideal behaviour makes this simple treatment inapplicable.

However in the pressure region less than one atmosphere of the P-T-x three phase equilibrium the Clapeyron equation may be thus simply applied to yield a value for the heat of overall formation of the clathrate.

I.6 Theories of Clathrates

I.6.1 The van der Waals and Platteeuw Theory

Van der Waals[14] gave a statistical mechanical description of clathrate compounds in which a partition function was derived and thermodynamic considerations discussed. The partition function derived was based on a simple model in which the following physical considerations held:

(i) The contribution of the host molecules to the partition function is the same for the empty β-lattice

as it is when the lattice is occupied by guest molecules to any fractional occupancy θ.

(ii) Each cavity holds only one guest molecule.

(iii) The contribution of each encaged guest molecule to the partition function is independent of the fractional occupancy θ, i.e. interaction between guest molecules is neglected.

Consider an assembly of Nm molecules of host and $N\theta$ molecules of guest A, having one cavity per m host molecules and having a fractional occupancy of these cavities of θ.

The partition function may then be represented by

$$(1) \quad \exp\left(\frac{-F}{kT}\right) = \exp\left(\frac{-F^{o}}{kT}\right) \frac{N!}{[N\theta]![N(1-\theta)]!} h_{A(T)}^{N\theta}$$

or in terms of the free energy F

$$(2) \quad \frac{F}{kT} = \frac{F^{o}}{kT} + N\left\{\theta\ln\theta + (1-\theta)\ln(1-\theta)\right\} - N\theta\ln h_{A}(T)$$

where F^{o} is the free energy of Nm molecules of host in the empty β - form at temperature T.

The combinatorial factor in (1) expresses the number of distinct ways in which A molecules can be distributed over the cavities, and $h_{A}(T)$ is the contribution of an encaged A molecule to the partition function.

If now μ_A^x and μ_H^x are the chemical potentials of the two components in the clathrate (x) they are obtained as follows.

The assembly contains $N_A = N\theta$ molecules of A

$N_H = mN$ molecules of host.

For a change at constant temperature and pressure

(3) $$dF = \mu_A^x dN_A + \mu_H^x dN_H$$

or

(4) $$dF = \mu_A^x(Nd\theta + \theta dN) + \mu_H^x m dN$$

therefore

(5) $$\mu_A^x = \left(\frac{1}{N}\right)\left(\frac{\partial F}{\partial \theta}\right)_N$$

and

(6) $$\mu_H^x = \left(\frac{1}{M}\right)\left(\frac{\partial F}{\partial N}\right)_\theta - \left(\frac{\theta}{mN}\right)\left(\frac{\partial F}{\partial \theta}\right)_N$$

substitution of (2) for F into (5) and (6) yields

(7) $$\frac{\mu_A^x}{kT} = \ln\frac{\theta}{1-\theta} - \ln h_A(T)$$

and

(8) $$\frac{\mu_H^x}{kT} = \frac{\mu_H^\beta}{kT} + \frac{1}{m}\ln(1-\theta)$$

where $\mu_H^\beta = \left(\frac{1}{m}\right)\left(\frac{\partial F^\circ}{\partial N}\right)$ is the chemical potential of the β- modification.

Consider now the equilibrium vapour pressure of a gas over a clathrate. The chemical potential μ_A^G of a perfect gas A at a temperature T is related to the partial pressure p_A according to the relation

$$(9) \quad \frac{\mu_A^G}{RT} = \ln \frac{p_A}{kT} - \ln \phi_A(T)$$

where $\phi(T)$ is the partition function of a gaseous molecule A with the volume factor removed. Thermodynamic equilibrium will exist if

$$\mu_A^{\alpha} = \mu_A^G$$

Substituting in equations (7) and (9) yields

$$(10) \quad p_A = kT \frac{\phi_A(T)}{h_A(T)} \cdot \frac{\theta}{1-\theta}$$

which may be written

$$(11) \quad p_A = C_A \cdot \frac{\theta}{1-\theta} .$$

Consider now the three phase equilibrium S^{α} and S^{α} and G, where the solid clathrate S^{β} is simultaneously in equilibrium with the α- form of the host and the gas phase G, then in addition to the requirement implicit in (10) we have the condition

$$\mu_H^x = \mu_H^\alpha$$

where μ_H^α denotes the chemical potential of the α-form of the host. Substituting in (8) yields

$$(12) \qquad \mu_H^\alpha = \mu_H^\beta + \left(\frac{kT}{m}\right)\ln(1 - \theta)$$

or

$$(12a) \qquad \Delta\mu_{\alpha\to\beta} = -\frac{kT}{m}\ln(1 - \theta)$$

This theory for the simple case was extended by van der Waals and Platteeuw[15] for the general case of a cage forming substance Q and a number of encaged compounds A, B ....M encaged in different types of cavities 1 ....n.

Equations (10) and (12) become the more general formulas.

$$(13) \qquad p_k = \frac{kT\phi_{K_1}(T)}{h_{K_1}(T,V)} \cdot \frac{\theta_{K_1}}{1-\sum_J \theta_{J_1}}$$

$$= \frac{kT\phi_{K_2}(T)}{h_{K_2}(T,V)} \cdot \frac{\theta_{K_2}}{1-\sum_J \theta_{J_2}} = \cdots$$

or

$$(14) \qquad p_K = C_{K_1}\frac{\theta_{K_1}}{1-\sum_J \theta_{J_1}} = C_{K_2}\frac{\theta_{K_2}}{1-\sum_J \theta_{J_2}} = \cdots$$

$$(15)\quad \mu_Q = \mu_Q^{\beta} + kT \sum_i \nu_i \ln\left(1 - \sum_K \theta_{K_i}\right)$$

or

$$(15a)\quad \Delta\mu_{\alpha\rightarrow\beta} = -kT \sum_i \nu_i \ln\left(1 - \sum_K \theta_{K_i}\right).$$

ν_i being the number of cavities of type i per molecule of Q.

I.2 The Barrer and Stuart Theory[16]

Independently Barrer and Stuart[16] attempted a similar statistical thermodynamic treatment of the general case. Making the same fundamental assumptions as van der Waals and Platteeuw they deduced relationships (16) and (17) which are analogous to equations (15) and (13) respectively.

$$(16)\quad \frac{\mu_Q}{kT} = \frac{\mu_Q^{\beta}}{kT} + \sum_i \left\{\left(\frac{N_i}{\sum_i N_i}\right)M \cdot \ln\left(1 - \sum_{A,B,\ldots m} \theta_i^M\right)\right.$$

and

$$(17)\quad p_K = \frac{kT\,\phi_K(T)}{h_M^1(T)} \cdot \frac{\theta_i^M}{\left(1 - \sum_{AB\ldots m} \theta_i^M\right)}$$

where A,B...m refer to the different guest species comprising the multi component gas phase. The other

symbols have the same significance as in equations (13) and (15).

At the dissociation pressure for the multi-component gas phase

$$\mu_Q = \mu_Q^{\alpha}$$

where again μ_Q^{α} refers to the chemical potential of the host species in its α -form.

One can deduce from (16) that along the three phase P-T equilibrium line for gas, clathrate and α -form

$$(18)\quad \frac{1}{m\,{}_i N_i} \cdot \frac{d}{dT}\left[\sum\left\{N_i \ln\left(1 - \sum_{AB\ldots M} \theta_i^{\,m}\right)\right\}\right]$$

$$= \frac{d}{dT}\left[\frac{\mu_Q^{\alpha} - \mu_Q^{\beta}}{kT}\right]$$

$$= -\frac{\Delta H_{\alpha-\beta}}{RT^2} + \frac{\Delta V_{\alpha\to\beta}}{RT} \cdot \frac{dP}{dT}$$

where $\Delta H_{\alpha\to\beta}$ is the molar heat of the reaction

β -modification empty $\rightarrow$ α -modification

and $\Delta V_{\alpha\to\beta}$ is the corresponding volume change

P is the total pressure, the vapour pressure of Q and the partial pressures of gaseous species A,B,C ....M.

i.e. $P = P_Q + P_A + P_B + P_C + \ldots\ldots\ldots + P_M$

at temperature T.

It may be seen that equations (11) and (14) are Langmuir's isotherm and (12) and (15) are generalisations of Raoult's law. This is not surprising considering the nature of the model used in the derivation. The situation may be illustrated by the following qualitative argument. Consider a clathrate having one type of cavity. If a gaseous molecule K is encaged in a cavity this corresponds to the process

$$\text{empty cavity} + K \longrightarrow \text{occupied cavity.}$$

The empty cavity "binds" the molecule K to form an occupied cavity. If an empty cavity is denoted by X and an occupied one by Y this can be described as a reversible reaction.

$$X + K \rightleftharpoons Y$$

neglecting interactions of neighbouring K molecules the reaction has an equilibrium constant

$$C_K \simeq [Y] / [X] [K]$$

where square brackets denote concentrations.
Assuming K is the only solute present one further has

$$[Y] \simeq \theta_K \ , \quad [X] \simeq 1 - \theta_K \ , \quad [K] \simeq P_K$$

which yields in the above relationship.

$$C_K = \theta_K / (1 - \theta_K) P_K$$

or

$$(19) \qquad P_K = C_K^{-1} \theta / (1 - \theta_K)$$

which is equation (11).

Langmuir's isotherm entails the generalised form of Raoult's law as a necessary thermodynamic consequence. This can be seen from the Gibbs-Duhem equation.

$$(20) \qquad N_Q d\mu_Q + N_K d\mu_K = 0$$

From equation (19)

$$(21) \qquad d\mu_K = kT d\ln P_K = kT \left\{ \theta_K (1 - \theta)_K \right\}^{-1} d\theta_K$$

and from the definition of θ_K

$$(22) \qquad N_K = \nu N_Q \theta_K$$

where as before ν is the number of cavities per mole of Q.

On substituting (21) and (22) into (20)

$$N_Q \int d\mu_Q = -kT \nu N_Q \int \frac{d\theta_K}{1-\theta_K}$$

which is equation (12).

I.6.3 Application to Quinol and Phenol Clathrates

The simple model first derived by van der Waals applies directly to the quinol clathrate having one species of guest with one molecule per cavity and a fractional occupancy of θ. For the difference of α- and β-modifications in the Gibbs function for quinol we have from equation (12a)

$$\Delta\mu = \tfrac{1}{3} kT \ln(1 - \theta)$$

and for the equilibrium pressure at temperature T from equation (11).

$$p_A = C_A \frac{\theta}{1-\theta}$$

From equation (18) we have for quinol

$$(24) \quad \frac{1}{m} \frac{d \ln(1-\theta)}{dT} = -\frac{\Delta H_{\alpha\to\beta}}{RT^2} + \Delta V_{\alpha\to\beta} \frac{dP}{dT}$$

From the Clapeyron equation we had

$$\frac{dP}{dT} = \frac{\Delta H}{T \Delta V}$$

where as before ΔH is the heat of the reaction:

1 mole. gas M + $\frac{n}{\theta}$ moles. α-quinol

$$\rightarrow \quad 1 \text{ mole. M. } \frac{n}{\theta} \beta\text{-quinol}$$

and ΔV is the corresponding volume change. Substituting in equation (24) gives

$$\frac{1}{m}\frac{d}{dT}\ln(1-\theta) = -\frac{\Delta H_{\alpha\rightarrow\beta}}{RT^2} + \frac{\Delta V_{\alpha\rightarrow\beta}}{RT} + \frac{\Delta H}{T\Delta V}$$

on rearrangement

$$\frac{\Delta V_{\alpha\rightarrow\beta}}{\Delta V}\cdot\Delta H = \frac{RT^2}{m}\cdot\frac{d}{dT}\ln(1-\theta) + \Delta H_{\alpha\rightarrow\beta}$$

and since

$$\frac{d}{dT}\ln(1-\theta) = \frac{-1}{1-\theta}\frac{d\theta}{dT}$$

then

$$(25)\qquad \frac{\Delta V_{\alpha\rightarrow\beta}}{\Delta V}\cdot\Delta H = \frac{-RT^2}{m}\,\frac{1}{1-\theta}\,\frac{d\theta}{dT} + \Delta H_{\alpha\rightarrow\beta}$$

If now the volume change occurring in the conversion of host from the α- to the β-modification is negligibly small relative to the difference ΔV in volume of guest molecules in gaseous and enclathrated form then

$$\frac{\Delta V_1}{\Delta V} \simeq 0 \quad \text{and hence}$$

$$(26) \qquad \Delta H_{\alpha \rightarrow \beta} = \frac{RT^2}{m} \cdot \frac{1}{1-\theta} \frac{d\theta}{dT}$$

In the phenol clathrates in which there are two types of cavity equation (15a) reduced to:

$$(27) \qquad \nu_1 \ln(1-\theta_1) + \nu_2 \ln(1-\theta_2) = - \frac{\Delta \mu}{RT}$$

and equation (14) yields

$$(28) \qquad P_K = C_{K_1} \frac{\theta_1}{1-\theta_1} = C_{K_2} \frac{\theta_2}{1-\theta_2}$$

if only one type of guest species is encaged.

In the derivation of the theory it was assumed that there was only single occupancy of a cavity. This assumption may be approximated to if the large phenol cavity is considered as consisting of three small cavities of one type N_1 and the small phenol cavity as a single cavity of type N_2, then

$$n = \frac{N_1}{N_2} = 3$$

and equation (18) may be expressed as

$$(29)\qquad \frac{1}{m(n+1)}\frac{d}{dr}\left[n\ln(1-\theta_1)+\ln(1-\theta_2)\right] = \frac{-\Delta H_{\alpha\rightarrow\beta}}{RT^2} + \frac{\Delta V_{\alpha\rightarrow\beta}}{RT}\cdot\frac{dP}{dT}$$

which may also be reduced to

$$(30)\qquad \frac{\Delta V_{\alpha\rightarrow\beta}}{\Delta V}\cdot\Delta H = \frac{-RT^2}{m(n+1)}\left[\frac{n}{1-\theta_1}\frac{d\theta_1}{dT}+\frac{1}{1-\theta_2}\frac{d\theta_2}{dT}\right] + \Delta H_{\alpha\rightarrow\beta}$$

and again if $\frac{\Delta V_{\alpha\rightarrow\beta}}{\Delta V}$ is negligibly small to

$$(31)\qquad \Delta H_{\alpha\rightarrow\beta} = \frac{+RT^2}{m(n+1)}\left[\frac{n}{1-\theta_1}\frac{d\theta_1}{dT}+\frac{1}{1-\theta_2}\frac{d\theta_2}{dT}\right]$$

The above equations attribute Langmuir-like behaviour to the adsorption of guest species in the phenol cavities.

Barrer and Rees[17] have shown that if a single sorption centre is capable of holding more than one

molecule then for a single guest species the number of molecules sorbed Ns divided by the total number of sorbtion centres N, $\frac{Ns}{N}$, may be reduced to the term

$$\frac{Ns}{N} = \frac{nr}{(1+r)}$$

where n is the maximum possible number of guests sorbed at a centre, and r is of the form kp. Thus

$$\frac{Ns}{N} = \frac{nkp}{1+kp}$$

which is identical to Langmuir's isotherm, if nN is taken as the total number of sites. This derivation also assumes no interaction between sorbed molecules in the cavity. The approximation that the large phenol cavity can be replaced by three identical small cavities could be a reasonable one provided there is no interaction of guest species in the large cavity.

In the quinol clathrate where a guest molecule is shielded from any other guest molecule by the molecules of the host lattice the assumptions made in the derivation of the theory are met rather well. In the phenol clathrates deviation from the theory may be

expected as interaction between pairs of guest molecules in the large cavity increases, and as the degree of freedom along the axis of the long cavity is restricted by multiple occupancy.

I.6.4 Evaluation of the Cell Partition Function by the Method of Lennard-Jones and Devonshire[15]

The partition functions and resulting expressions for the properties of the clathrate contain the partition function $h_A(T)$ as the only unknown. Construction of these partition functions would allow prediction of the thermodynamic behaviour of the clathrates relative to the empty β-lattice. The application of the Lennard-Jones and Devonshire theory for the study of liquids was described by van der Waals, the essential features of which are outlined below.

Two assumptions further to those made on page 30 for the van der Waals and Platteeuw theory are made.

(iv) The guest molecules can rotate freely in their cavities.

(v) The potential energy of a guest molecule at a distance r from the centre of the cavity is given by the spherically symmetrical potential w(r) proposed by Lennard-Jones and Devonshire.

The last assumption applies strictly only to spherical molecules.

Applying the L-J-D method it is assumed that the average contribution to the potential energy due to interaction of a guest molecule with any of the elements constituting the wall of its cage can be described by the force law

$$(32) \qquad \psi(R) = 4\varepsilon \left\{ \left(\frac{\sigma}{R}\right)^{12} - \left(\frac{\sigma}{R}\right)^{6} \right\} .$$

Consider the cavity as having Z encompassing host molecules, and ε and σ the energy and distance parameters characteristic for host-guest pair interaction. σ is the distance at which

$$\psi(\sigma) = 0$$

The parameter ε is the value of $-\psi(R)$ corresponding to the strongest attraction, which occurs at $R = 2^{\frac{1}{6}}\sigma$. The van der Waals radius of an atom equals $\frac{R}{2} = 0.56\sigma$.

Summing $\psi(R)$ over Z molecules distributed over a sphere yields a function w(r) describing the resultant field within the sphere. This may be expressed as:

$$(33) \qquad w(o) = Z\varepsilon\left\{\alpha^{-4} - 2\alpha^{-2}\right\}$$

$$(34) \quad w(r)-w(o) = Z\varepsilon\left\{\alpha^{-4} l\left(\frac{r^2}{a^2}\right) - 2\alpha^{-2} m\left(\frac{r^2}{a^2}\right)\right\}$$

where l and m are complicated algebraic functions of the dimensionless variable $\frac{r^2}{a^2}$. The parameter measures the cell radius a in terms of the effective molecular diameter σ :

$$(35) \qquad \alpha = \frac{a^3}{\sigma^3\sqrt{2}}$$

The cell partition function can be written as

$$(36) \qquad h = \phi(T) \exp\left[\frac{-w(o)}{kT}\right] \int_{cell} \exp\left[-\frac{w(r)-w(o)}{kT}\right] \cdot 4\pi r^2 dr$$

The function $\phi(T)$ is defined by

$$(37) \qquad \phi(T) = (2\pi mkT)^{3/2} j(T)$$

where m is the mass of the molecule and j(T) its internal partition function including rotations.

$\phi(T)$ represents the contribution due to translational and internal degrees of freedom of the guest molecule. The second term is related to the potential energy $w(o)$ of the guest molecule at the centre of its cage referred to the perfect gas, and the integral is the "free volume" of the guest molecule wandering in its cavity. In the notation of the L-J-D theory the free volume is written as

$$(38) \qquad \int \exp\left[-\frac{w(r)-w(o)}{kT}\right] 4\pi r^2 dr = 2\pi a^3 g$$

where g is the dimensionless integral.

$$(39) \qquad g = \int \exp\left[\frac{Ze}{kT}\left\{\frac{-l(\theta)}{\alpha^4} + \frac{2m(\theta)}{\alpha^2}\right\}\right] \theta^{\frac{1}{2}}\, d\theta$$

hence

$$(40) \qquad h = \phi(T) \exp\left[\frac{-w(o)}{kT}\right] 2\pi a^3 g \quad .$$

Both $\frac{w(o)}{kT}$ and g are completely determined by the dimensionless parameters $\frac{Z\varepsilon}{kT}$ and α. The first is

given by equation (33) while g has to be evaluated by numerical integration of equation (39). Once the values of the two parameters have been determined the vapour pressure and energy of formation of a clathrate may be determined.

Substitution of the above expression for h into equation (2) gives for the free energy of the clathrate relative to empty β -lattice.

$$(41)\quad F-F^{o} = NkT\left[\theta\ln\theta + (1-\theta)\ln(1-\theta) - \theta\left\{\ln\phi_A(T) - \frac{w(o)}{kT} + \ln(2\pi a^3 g)\right\}\right]$$

and for its equilibrium vapour pressure

$$(42)\qquad p_A = kT\,\frac{\exp\frac{w(o)}{kT}}{2\pi a^3 g}\cdot\frac{\theta}{1-\theta}$$

The change in free energy accompanying the reaction.

MQ (solid) + θA (perfect gas) $\longrightarrow$ clathrate can be found by subtraction of the free energy of Nθ molecules of A in the gas phase F^G from equation (41).

$$(43)\quad F^G = -N\theta kT\left\{\ln v_A^o + \ln\phi_A(T) + 1\right\}$$

one obtains

$$(44) \qquad \Delta F = RT\left[\theta \ln\theta + (1+\theta)\ln(1-\theta) + \theta\left\{\frac{w(o)}{kT} + 1 + \ln\left(\frac{v_A^o}{2\pi a^3 g}\right)\right\}\right]$$

ΔF refers to the free energy change in an isothermal reaction of m moles of β with θ moles of the perfect gas having a molecular volume v_A^o. The corresponding energy of reaction ΔU, can be found from (44) by use of the thermodynamic identity.

$$\Delta U = -T^2\left(\frac{\partial\left(\frac{\Delta F}{T}\right)}{\partial T}\right)$$

Thus

$$\Delta U = \theta RT\left\{\frac{w(o)}{kT} + T\,\frac{\partial \ln g}{\partial T}\right\}$$

This may be transformed into

$$(45)\quad \frac{\Delta U_m}{RT} = \frac{\Delta U}{\Theta RT} = \frac{z\varepsilon}{kT}\left[-2\left(1+\frac{g_m}{g}\right)\alpha^{-2} + \left(1+\frac{g_1}{g}\right)\alpha^{-4}\right]$$

where ΔU_m is the energy of reaction per mole of A and g_1 and g_m are integrals related to g, which have also to be calculated numerically.

Van der Waals and Platteeuw[15] used the above derived equations and available experimental data to determine equilibrium pressure and energies of formation of some quinol clathrates. They assumed that the combining rules for the interaction between two unlike particles held,

$$(46)\quad \varepsilon = (\varepsilon_K \varepsilon_Q)^{\frac{1}{2}} \quad \text{"geometric mean approximation"}$$

$$(47)\quad \sigma = \tfrac{1}{2}(\sigma_K + \sigma_Q) \quad \text{"hard sphere approximation"}$$

Here ε_K and σ_K are the force constants for the pure solute K which can be determined from measurements of its second virial coefficient. ε_Q and σ_Q are the similar but unknown constants characteristic for the β-lattice.

For α according to equations (35) and (47)

$$\alpha = \frac{a^3}{\sqrt{2}\sigma^3} = \frac{a^3}{\sqrt{2}(\sigma_{K/2} + \sigma_{Q/2})^3}$$

A value for a, resulting from Powell's X-ray analysis, was taken, i.e., a = 3.95Å. For σ_Q the value

$$\sigma_Q = 2^{\frac{1}{6}}(1.40 + 1.85) = 2.90A$$

was taken, where 1.40Å is the van der Waals radius of a covalently bound oxygen atom and 1.85Å the half-thickness of an aromatic molecule perpendicular to its plane, as suggested by Pauling.

For $\frac{Z\varepsilon}{k}$ according to equation (46)

one has

$$\frac{Z\varepsilon}{k} = Z(\varepsilon_K \varepsilon_Q)^{\frac{1}{2}}/k = Z(\varepsilon_Q/k)^{\frac{1}{2}}(\varepsilon_{K/k})^{\frac{1}{2}}$$

Values for ε_K and σ_K determined by Whalley and Schneider were used for monotomic gases and for the other gases values reported by Hirschfelder, Curtiss and Bird were taken.

The experimental data available was used to assign a value of 294 to the unknown factor $Z(\varepsilon_{Q/R})^{\frac{1}{2}}$ to give the best fit to the theoretical predictions.

Table I[15] below gives the calculated values found by van der Waals and Platteeuw as well as some observed values, at 25°C.

Table I

Guest	P_K in atmospheres		
	Calc.	Observed	Ref.
Argon	3.4	3.4	18
Krypton	0.4	0.4	18
Xenon	0.06		
Methane	0.8		
Nitrogen	5.2	5.8	19
Oxygen	2.6		
HCl	0.02	0.01	20

Guest	Energy of formation ΔU in K. cal		
	Calc.	Observed	Ref.
Argon	-4.5	-5.4	21
Krypton	-6.1		
Xenon	-8.0		
Methane	-5.9		
Nitrogen	-4.5	-5.2	21
Oxygen	-4.8	-4.9	21
HCl	-7.6	-8.6	21

I.7 · The Motivation and Objectives of the Work Undertaken

The crystalline structures of the quinol[2] and phenol[11] clathrates have been accurately determined by X-ray methods. The theory applying to clathrate structures has been derived[14,15,16] and a number of experimental values for the equilibrium vapour pressures and heats of formation found for quinol[15] clathrates and considerably fewer for the phenol[10,22] clathrates. Little experimental data is however available for equilibrium composition as a function of pressure and temperature or for the variation of the dissociation pressure with temperature.

The clathrates of quinol and phenol have been formed by crystallization from solution in some cases at normal

pressures and in others at very high pressures.[2-14]. The direct formation of the clathrate from the α - modification under a very high pressure of guest gas has also been investigated.[22]

In investigating the reaction of xenon with ice crystals to form the type I hydrate Barrer and Ruzicka,[23] found that a very small percentage of the ice crystals were converted to the clathrate at pressures of less than $\frac{1}{2}$ an atmosphere at a temperature of $-78^{\circ}C$. Agitating the ice crystals with glass beads[24] they found that the amount of gas sorbed was tremendously increased. This idea was developed by Barrer and Edge in these laboratories and a suitable agitation technique was found by means of which it was possible to take the reaction to completion.

In this project the method of Barrer and Edge was applied to quinol and phenol in order to attempt to form the gas-clathrates of these two compounds. The successful application of this method would enable the following interesting studies to be attempted:

1. The variation of the composition of the clathrates as a function of temperature and pressure.
2. The dissociation pressures of the clathrates below a pressure of 1 atmosphere as a function of temperature.

3. From the above determinations the fractional occupancy of the cavities at the three phase equilibrium point, θ crit, might also be found.

4. The nature of the kinetics of this method of clathrate formation might be studied.

II EXPERIMENTAL

II.1. Materials

The rare gases employed in the experiments were supplied by the British Oxygen Company Limited. They were claimed to be spectrally pure with the exception of krypton, which contained < 1% of xenon, and xenon which contained < 1% of krypton.

The gases methane, ethane and ethylene were supplied by the National Chemical Laboratory and the purities were stated as follows:

methane	99.98	moles per cent
ethane	99.9	" " "
ethylene	99.92	" " "

Carbon dioxide was supplied by the British Oxygen Company. The purity was stated as better than 99% pure. Sulphur dioxide was obtained from a cylinder supplied by Messrs. Hopkins and Williams. It was purified by passing the gas through a cold trap at -5°C. and then condensing it with liquid oxygen and pumping off any nitrogen and oxygen remaining.

The quinol and phenol used were supplied by Messrs. Hopkins and Williams. The quinol crystals were stored for use in a clean dry bottle. The phenol crystals were crushed in a mortar and stored in an evacuated dessiccator.

II.2 Preliminary Experiments

Previous methods employed for the preparation of quinol and phenol clathrates have already been described.

Barrer and Ruzicka[23] observed that minute ice crystals could react with xenon, at -78°C. and under a pressure of less than half an atmosphere, to form the type I hydrate. However, the maximum amount sorbed corresponded to less than 1% conversion of the ice to the hydrate. On agitating the ice crystals with glass beads they found that the rate of adsorption was dramatically increased, though they did not determine the maximum amount of xenon sorbed.

Barrer and Edge, working in these laboratories, then designed experiments to investigate the potential of this method of preparation of hydrates. The reaction vessel containing ice and gas at -78°C. was so constructed that it could be attached to the arm of a mechanical flask shaker. They found that the vigorous agitation given to

the ice crystals by the mechanical shaking with glass beads caused a very rapid reaction with a maximum conversion of ice to hydrate of about 35%. Since glass beads are very light they substituted lead beads and found that the conversion corresponded to 95%. Since lead beads suffered considerable damage and produced powdered lead in the reaction vessel $\frac{1}{8}$" diameter stainless steel ball-bearings were finally substituted. Although lighter than the lead beads, no appreciable reduction in the rate of reaction or in the maximum amount sorbed was observed.

The first experiments undertaken in this work were designed to test the application of the methods of Barrer and Edge to the production of quinol and phenol clathrates of the noble and other gases.

The apparatus constructed for the experiment is shown in Fig. 9. It is a high vacuum apparatus constructed of Pyrex glass. The vacuum is obtained by a mercury diffusion pump backed by a rotary oil pump. This is capable of reducing the pressure to 10^{-6} mm. of mercury.

The apparatus consists of a volumetric gaseous sorption system, the gas supply, and a Töpler pump for transferring controlled quantities of gas to the sorption

section and for returning gas to the gas reservoir after completing an experiment.

The volumetric sorption system consisted of a 50 ml. gas burette operated by raising or lowering a column of mercury in the tube, a mercury manometer, the pressure difference on which was measured with a cathetometer, and the reaction vessel. The reaction vessel was attached to the rest of the apparatus by means of a flexible rubber connection as shown. The long arm of the reaction vessel could be clamped to a mechanical flask shaker and so vigorously shaken.

The reaction vessel consisted of a bulb of about 20 ml. capacity containing about 250, $\frac{1}{8}$" diameter, stainless steel ball-bearings. This was connected, at the end of a 50 cms.-long glass tube of 0.4 cm. internal diameter, by a B.7 cone and socket joint to the flexible connection. The thin glass tube of 0.4 cm. internal diameter was surrounded by a tube of much wider bore to act as a support when the sorption unit was clamped to the mechanical shaker.

The reaction vessel could be immersed into a thermostat bath, the narrow bore of the connecting arm keeping the volume of gas in which the temperature varied between the temperature of the bath and room temperature,

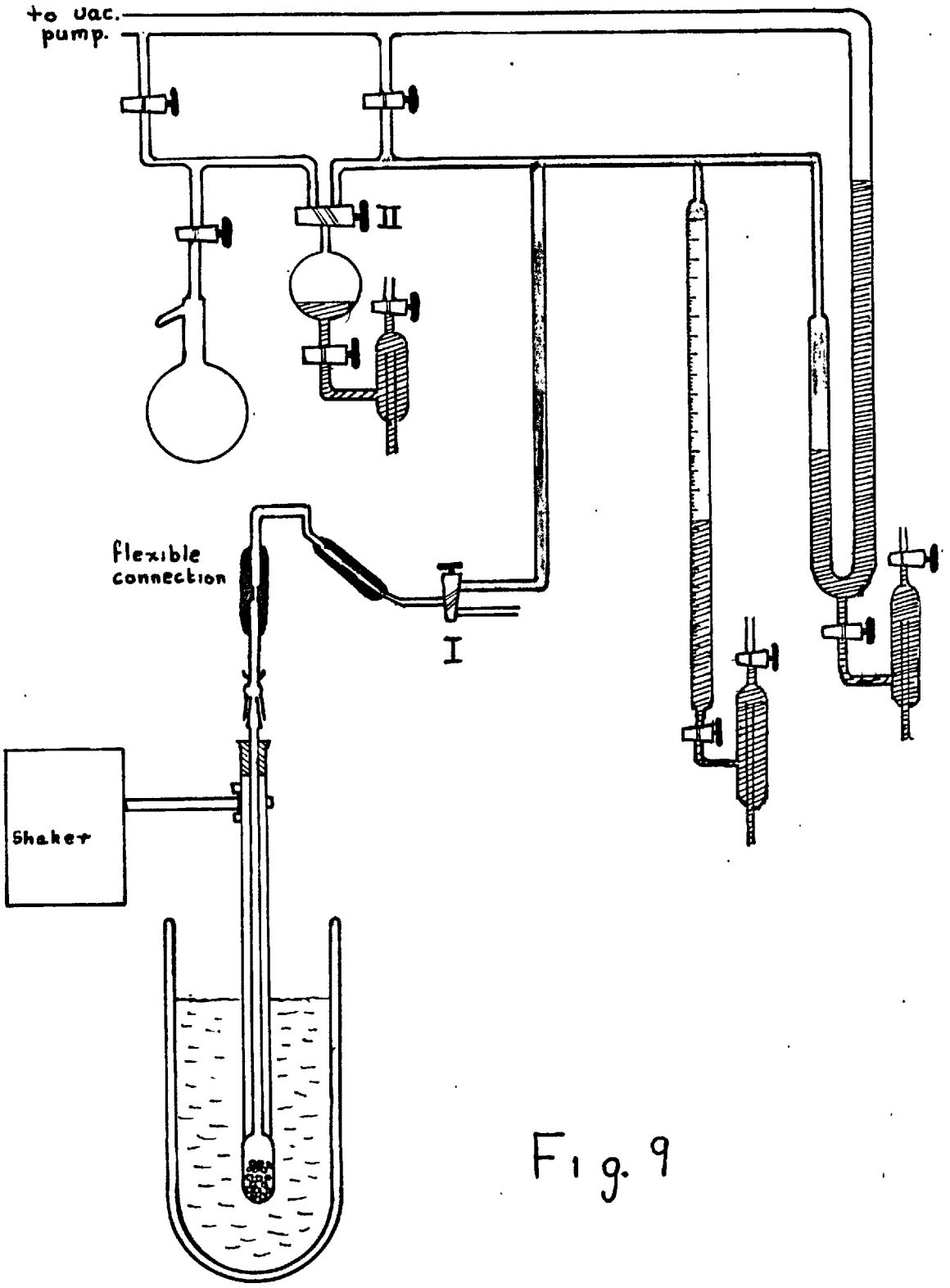

Fig. 9

to a minimum. The B.7 cone and socket joint was firmly held together by small springs attached to "ears" on either side of the joint. The flexible connection first used was made of natural rubber pressure tubing.

The gases used in the experiments were contained in glass flasks of one litre or one half-litre capacity at a pressure of one atmosphere. After attachment to the system and evacuation, the thin glass seals were broken by magnetically operated iron hammers.

For the initial experiments the thermostat bath into which the reaction vessel was immersed, consisted of a Dewar vessel containing a mixture of water and crushed ice to give a temperature of $0^{\circ}C.$ or a mixture of powdered solid carbon dioxide and petroleum ether (100° to 120° boiling range) which gave a temperature of $-78^{\circ}C. \pm 1^{\circ}C.$ 0.25 Gms. of quinol were weighed out and introduced into the reaction vessel with the steel ball bearings. The reaction vessel was attached to the apparatus and immersed in the Dewar vessel containing ice and water. After evacuating the vessel a pressure of 36 mls. of mercury of krypton was introduced into the sorption section. The reading on the gas burette was noted and the experiment begun by setting the shaker in motion and violently agitating the steel ball bearings. It was noticed

that after an initial period in which the pressure dropped very slightly there was a fairly rapid drop in pressure. The column of mercury in the burette was raised to keep the pressure consistently constant and it was found that after 200 minutes, 21.1 mls. of gas at a pressure of 36 cms. of mercury had been sorbed. The experiment was repeated with 0.201 gms. of quinol at a pressure of 22.6 cms. of mercury and after 180 minutes, 17.2 mls. had been sorbed. These two experiments indicated that the method of Barrer and Edge for producing gas hydrates could be applied to quinol clathrates in the region of 0°C.

The experiment was similarly repeated with 0.2 gms. of phenol at 0°C., but at a pressure of 40 cms. of mercury no sorption of krypton was noted after 5 hours. The ice-water bath was replaced with a solid carbon dioxide - petroleum ether bath at -78°C. The experiment was repeated with 0.3 gms. of phenol. After 12 minutes at 30 cms. of mercury a very rapid sorption was noticed which had taken up 36 mls. of gas after 60 minutes. This indicated that the dissociation pressure of phenol krypton clathrate was greater than 40 cms. of mercury at 0°C., but that using the apparatus constructed, phenol clathrates could be produced in the region of -78°C.

These preliminary experiments having successfully tested the applicability of Barrer and Edge's method to quinol and phenol clathrates, the apparatus was slightly modified and the experimental technique standardised.

II.3. Refinement of the Experimental Method

It was now of interest to study the maximum sorption of gas by the host lattice as a function of pressure, the variation of this with temperature, the kinetics of the reaction and the dissociation pressure of the clathrates as a function of temperature.

In order for these to be studied with accuracy, a number of experimental points had to be refined. An accurate and reliable thermostat bath operating in the region 0° to $-78^{\circ}C$. had to be constructed. Possible errors due to change in the room temperature during the course of an experiment and also leakage of air into the system through the flexible rubber connection had to be eliminated or reduced to a negligible minimum.

Error due to change in room temperature could easily be eliminated by calibrating all the separate volumes in the sorption system. Krypton was assumed to behave ideally, and by using the calibrated gas burette a given amount of gas was compressed and by measuring

the corresponding volumes, pressures and room temperature, the unknown volumes were calibrated. Knowing the individual volumes accurately, account could be taken of a change in room temperature during the course of an experiment.

The natural rubber used for the first flexible connection while being sufficiently flexible to accommodate the vigorous shaking of the reaction vessel by the shaker, was considered too permeable to air over the duration of an experiment. Various types of tubing were used to construct flexible connections and the appearance of air in an evacuated connection over a period of time was measured using a McLeod gauge. The types of tubing used were of teflon, neoprene, polyvinyl chloride (P.V.C.) and natural rubber. The leak rates of the various types were found to be in the order

natural rubber $>$ P.V.C. $>$ neoprene $>$ teflon.

Teflon was found, however, to be too rigid to accommodate the vigorous shaking required. Neoprene, although considerably less flexible than natural rubber pressure tubing, was found to be satisfactory if a connection of the design shown in Fig. 9 was constructed.

The neoprene connection was fitted to the system and leakage was found to be undetectable on the mercury manometer over a period of two weeks.

II. 3.1 The Thermostat Bath

A thermostat bath was constructed to meet the following requirements:

1. Constant temperature maintenance within a range 20°C. to -78°C.

2. The temperature set and maintained constant to better than $\pm$ 0.1°C.

3. It should be capable, with attention, of indefinite functioning.

4. It should be capable of functioning for at least 12 hours without attention.

5. It should be economical in the consumption of refrigerant.

The thermostat bath constructed is shown in Fig. 10. It consists of a large silvered Dewar vessel containing a smaller unsilvered Dewar vessel. The inner Dewar vessel contained the bath liquid and was fitted with a glass vacuum tap so that it could either be evacuated or have a desired pressure maintained within it. The space between the two Dewar vessels was filled with the refrigerant.

The heat loss of the bath liquid to the refrigerant should be slightly greater than the heat gained by the bath liquid from the surroundings. To balance this difference a small 25 watt electric lamp was used to heat the liquid. This lamp was connected to a Sunvic control unit and was switched on whenever the bath temperature fell below the required set temperature and was switched off when the temperature had risen to just above the set temperature. The control unit was a bimetallic spiral dipping into the bath liquid, with an adjustable control mechanism to enable it to be set to a required temperature. When the bath temperature dropped below the required temperature the bimetallic spring caused electrical contact to be made in the circuit, activating a relay and switching on the lamp. The contact was broken when the temperature had risen above the set point and the lamp switched off. This mechanism was found to control the temperature to better than $\pm$ 0.1°C.

If the bath was maintained at the same temperature for a period of days it was found that the temperature drifted slightly from the set value, due to electrical sparking corroding the contact point of the bimetallic spiral switching mechanism. The control

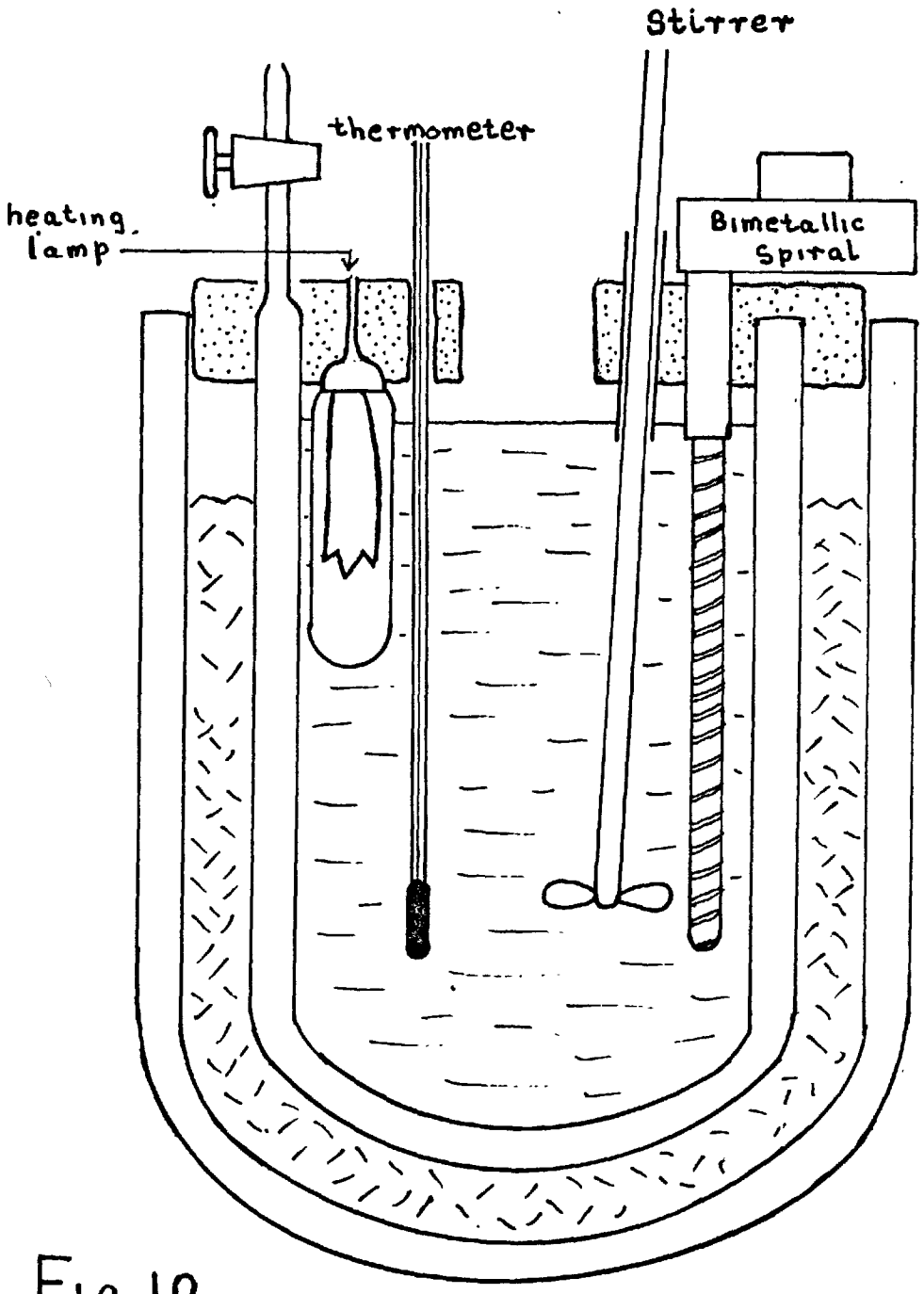

Fig. 10

mechanism allowed this to be corrected. This was not, however, found to be detectable over one day, the general maximum duration of a single experiment.

The bath liquid was stirred with a glass stirrer attached to a small electric motor to ensure a constant temperature at all points in the bath.

In the region 0°C. to 20°C., water was found to be a suitable bath liquid and ice was used as a refrigerant. Between -78°C. and 0°C powdered solid carbon dioxide was used as the refrigerant. In this range a bath liquid having a low viscosity to facilitate stirring and also a fairly non-volatile character was desired. Petroleum ether 100/120 proved to be suitable. Care was taken that a constant volume of liquid was always maintained within the bath.

Between 20°C. and -30°C. the inner Dewar vessel was evacuated but between -30°C. and -78°C. it was found that increasing amounts of air had to be admitted to the inner Dewar vessel to facilitate loss of heat to the refrigerant layer between the two vessels.

Between 0°C. and 20°C. a mercury-in-glass thermometer was used to measure the temperature in the bath. Between 0°C. and -30°C. a mercury-thallium

thermometer was used. Below $-30^{\circ}C$. an ammonium vapour pressure thermometer, constructed in these laboratories, was employed.

II.4 The Standardised Experimental Technique

Having described the final form of the apparatus, it is now of interest to describe the standardised technique used in conducting all subsequent experiments. These may be considered in three parts:

(i) Calibration of the volumes of the volumetric sorption system, and of the reaction vessel

(ii) Introduction of a sample of quinol or phenol crystals into the reaction vessel.

(iii) Measurement of the sorption of gas as a function of time at a particular pressure and temperature, and measurement of the dissociation pressures of the clathrates.

II.4.1 Calibration of the Volumes of the System.

The dead volume V_d in the sorption system is indicated by the shaded area in Fig. 9. To keep this volume constant a calibration line was marked on the left-hand arm of the mercury manometer so that the mercury level could always be brought to this mark before making any pressure measurements.

Having evacuated the system thoroughly, tap I was closed and a quantity of krypton was introduced into the dead volume space through tap II. Tap II was closed and the mercury level in the manometer was adjusted to the calibration mark. The pressure P' and the volume of gas V' in the burette were measured, as was the room temperature T' ^{o}A. The mercury level in the burette was then adjusted to a new level and the new volume V'', the corresponding pressure P'' and room temperature T'' ^{o}A again measured. Since the amount of gas had remained constant, $\frac{PV}{T}$ (assuming ideal gas behaviour) was constant and hence:

$$\frac{P'(V' + V_d)}{T'} = \frac{P''(V'' + V_d)}{T''}$$

which gives on rearrangement:

$$V_d = \frac{\left[\frac{P'V'}{T'} - \frac{P''V''}{T''}\right]}{\left[\frac{P''}{T''} - \frac{P'}{T'}\right]}$$

Several measurements of V_d were made in this way and the mean value determined. It was found that this did not deviate from any individual value by more than $\pm$ 0.02 ml.

II.4.2 The Reaction Bulb and Connecting Arm

The reaction vessel and connecting arm was connected to the rest of the system by a B.7 cone and socket joint and by tap I. It was attached to the remainder of the system and the thermostat bath at the required temperature placed around the bulb. The level of bath liquid was always maintained at the same height on the arm of the reaction vessel. The entire vessel was then evacuated and tap I closed. A quantity of krypton was introduced into the volumetric system through tap II which was then closed and the mercury level in the manometer raised to the mark on the left-hand arm. The pressure "P"' , the volume in the gas burette V"' and the room temperature T"' were noted. The tap I was then opened to allow the gas to enter the reaction vessel and arm. The mercury level was again adjusted to the mark and the new pressure P' and room temperature T' were noted. The volume of gas in

the burette was kept constant. Since the total amount of gas in the system had remained constant:

$$\frac{P'''}{T'''} (V''' + V_d) = \frac{P'}{T'} (V''' + V_d) + P'\phi$$

where $\phi = \sum \frac{\Delta V}{T}$ is the summation of the elements of volume of the reaction bulb and side arm divided by the temperature of the gas in the respective elements. This value ϕ is a constant for each particular temperature at which the thermostat bath has been set and was recalculated for each change in temperature. This function takes into account the change in temperature of the arm as it rises from the bath temperature to that of the room.

II.4.3. Introduction of a Sample of Crystals into the Reaction Vessel

Between 0.1 and 0.2 of a gram of the dry crystals were placed in a weighing vessel and weighed together with a small funnel fitted with a rubber tube connection. The funnel was then attached to the B.7 cone on the end of the reaction vessel arm and the crystals tapped down the funnel into the bulb of the reaction vessel. The funnel and weighing vessel were then

reweighed and the weight of crystals introduced into the bulb found by subtraction. The crystals were of the order of ½ to 1 mm. in length and provided that the funnel and reaction vessel were carefully cleaned and dried before introduction of the crystals, it was found that these crystals did not adhere to the funnel or to the sides of the narrow bore arm, but dropped cleanly to the bottom of the bulb. Using a larger funnel and rubber connecting joint, the washed and dried ball-bearings were then introduced into the bulb of the reaction vessel. The cone was then greased and the reaction vessel attached to the remainder of the system, and the thermostat bath placed around it to the constant level. The system was then evacuated in preparation for an experiment.

II. 4.4 Sorption of Gas by the Crystals

Having evacuated the system, tap I was closed and a quantity of gas admitted into the volumetric section through tap II. The pressure P_o in cms. of mercury, the room temperature, T_o ^oA, and the volume of gas in the burette, V_o mls. were measured. Tap I was then opened and the mechanical shaker started simultaneously. The reaction was thus started at time t_o. As the reaction proceeded, the level of mercury in the

burette was raised so that the height of mercury in the manometer was constant and thus the pressure of gas above the crystals constant.

The amount of gas sorbed at any time t after the start of the reaction is calculated as follows. Suppose that after time t the pressure was P_t, the volume of gas in the burette V_t and the room temperature $T_t\,^{o}K$, then the amount of gas x sorbed by the crystals in mls. per gram at s.t.p. is given by:

$$x = \left\{ \frac{P_o\,(V_o + V_d)}{T_o} - P_t \left[\frac{V_t + V_d}{T_t} + \phi \right] \right\} \frac{273.2}{76w}$$

where w is the weight of crystals introduced into the reaction vessel.

There is a correction necessary to the above relationship. The value of ϕ at the temperature at which the experiment was conducted was determined without crystals present in the reaction vessel, and a correction had to be made for their presence.

If the volume occupied by w grams of clathrate is υ then the corrected value of ϕ is given by

$$\phi = \phi_{\text{calibrated}} - \frac{\upsilon}{T \text{ bath}}$$

The density of the clathrate is obtainable from crystallographic data. This correction should be applied when all the crystals have been converted to the clathrate form and during the course of an experiment, an estimate should strictly be made of the relative amounts of the clathrated and non-clathrated forms. The correction to $\phi_{\text{calculated}}$ is small and this further correction was then negligibly small and could be ignored.

A correction for the amount of host present in the vapour phase should also be made, but at the temperatures at which the reactions were undertaken the amount of quinol and phenol present in the vapour phase, as calculated from vapour pressure data, was extremely small and could be ignored.

A number of readings were made from the start of the experiment over the rapid part of the reaction, fewer being taken as the reaction slowed down. Shaking was continued for a long period until no further sorption of gas took place. This final value was taken to preresent the maximum equilibrium sorption by the crystals at the conditions of temperature and pressure at which the experiment had been conducted.

II.4.5 Determination of Dissociation Pressures

In determining the dissociation pressures, an arbitrary amount of crystals could be placed in the reaction vessel since the dissociation pressure is independent of the amount of host present and depends only on the temperature and pressure. In these experiments the reaction was continued only until the clathrate phase was clearly being formed at a particular pressure. The pressure was then lowered and the reaction continued by resuming shaking. This process was continued until a pressure was reached below which no β -phase would form. This was considered to be the dissociation pressure at that temperature. The dissociation pressure having been found by sorption, it was then found by desorption. This entailed taking a reaction completely to equilibrium and then progressively lowering the pressure and observing the desorption of gas with shaking until a pressure was reached below which all the gas would be completely desorbed. This pressure was again taken to be the dissociation pressure. This constituted a check on the first method.

III RESULTS AND DISCUSSION

III. 1. Preliminary Results

The applicability of the method of Barrer and Edge to the sorption of inert gas by both quinol and phenol having been demonstrated, a number of experiments were performed to determine the nature of the reaction in more detail.

0.141 Gms. of quinol was reacted with xenon at a pressure of 20.5 cms. of mercury at 0°C. The rate of uptake of gas was observed and the final maximum measured. In this quinol-xenon reaction it was found that there was first a small uptake of gas which levelled off before being followed by a second much larger sorption step leading to equilibrium when no further gas was sorbed (Fig. 11). The maximum uptake was 62 mls. of xenon at s.t.p. per gram of quinol. The quinol-xenon experiment was repeated at the much lower temperature of -78°C. and at a pressure of 51 cms. of mercury. The kinetic curve was of the same shape as that found at 0°C. (Fig. 11). The maximum sorption was 67.9 mls. of xenon at s.t.p. per gram of quinol which approximates within experimental error to 67.81 mls. of xenon at s.t.p. per gram of quinol, the theoretical maximum sorption if all the cavities of

β -quinol are occupied by xenon atoms. This was also found at -78°C. at the much lower pressure of 17 cms. of mercury where the maximum sorption was 67. 8 mls. of xenon at s.t.p. per gram of quinol. These results indicated that the sorption of gas was due to enclathration by the β -quinol host lattice as expected.

The first small uptake of gas is possibly the enclathration of gas in cavities in the α -quinol lattice before the formation of β -quinol begins. Powell[3] has suggested that cavities exist in the α -quinol structure which might enclathrate molecules of gas and Helle, Kok, Platteeuw and van der Waals[25] have given evidence of this taking place.

0.1497 Gms. of phenol was reacted with xenon at -78°C. and at a gas pressure of 67.7 cms. of mercury. A short time after the start of the experiment a single-step sorption of gas leading to a maximum uptake of 79.1 mls. of xenon at s.t.p per gram of phenol was observed (Fig. 12). This approximates within experimental error to 79.34 mls. of xenon at s.t.p. per gram of phenol which is the amount of gas enclathrated by the β -phenol lattice with one atom in each of the small cavities and three atoms in each of the large. At a pressure of 12 cms. of mercury at -78°C. the maximum

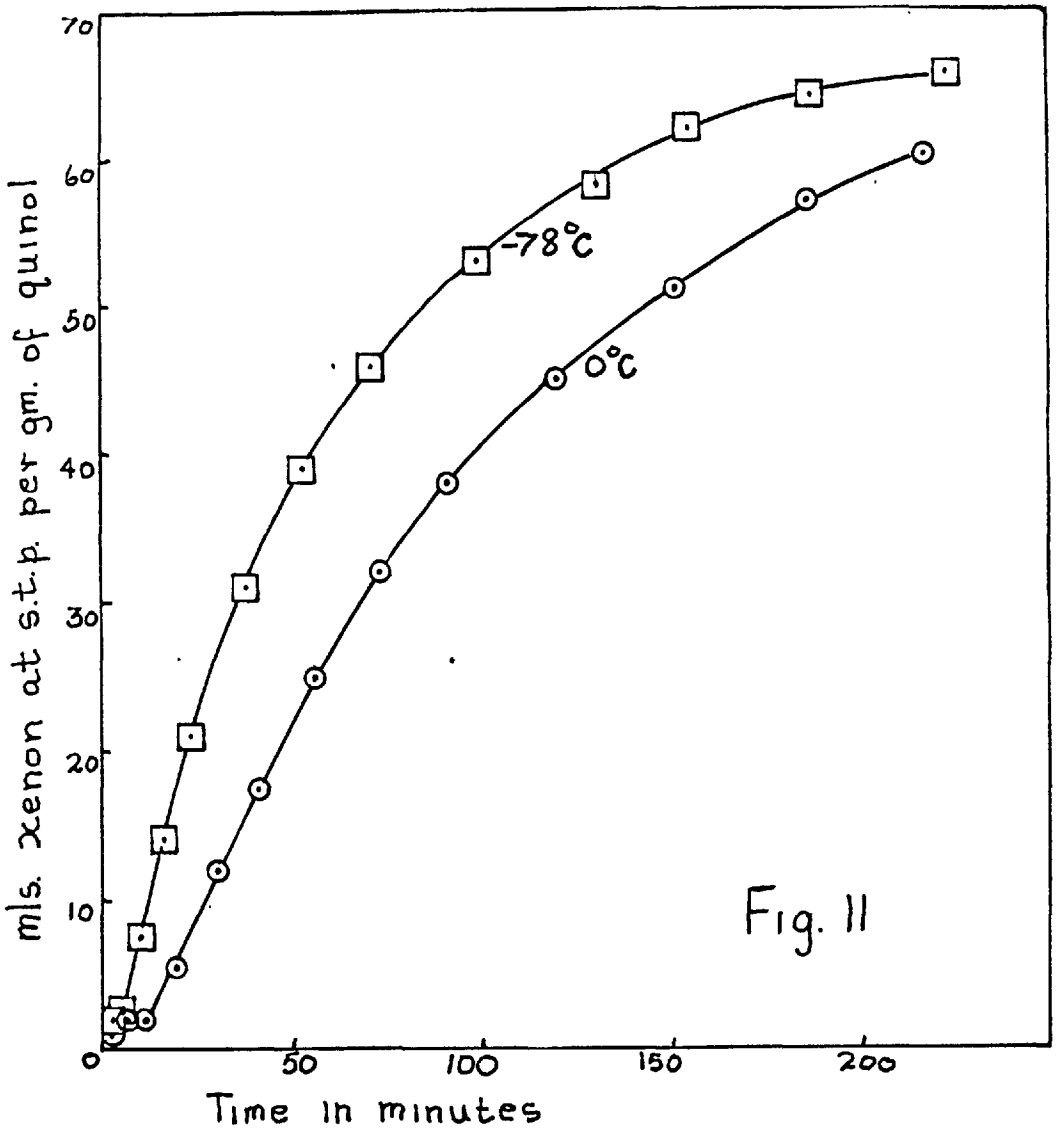
70
60
50
40
30
20
10
0
mls. xenon at s.t.p. per gm. of quinol
-78°C
0°C
50
100
150
200
Time in minutes

Fig. 11

amount sorbed was 78.9 mls. of xenon at s.t.p.. per gram of phenol, again very close to the theoretical maximum. As for quinol, these results indicated that the sorption was due to enclathration in the β-crystal structure of the host compound. At the much higher temperature of -28°C. a single step sorption reaction was again found giving a maximum uptake of 72.5 mls. of xenon at s.t.p. per gram of phenol at a pressure of 40.5 cms. of mercury.

These experiments indicated that by choosing a temperature not so low that the theoretical maximum was reached, the maximum uptake could be measured over a range of pressure and a suitable isotherm constructed.

In the following chapters the determination of the dissociation pressures of the quinol and phenol clathrates, the measurement of the maximum sorption of gas, and the study of the kinetics of these reactions will be described.

III.2 The Dissociation Pressures of the Quinol and Phenol Clathrates.

As has already been described there is a critical pressure known as the dissociation or decomposition pressure below which a clathrate cannot be formed. This dissociation pressure varies considerably with temperature increasing as the temperature increases. As described on

pages 29-30, if the dissociation pressure is determined over a range of temperature the Clapeyron equation may be applied to find ΔH, the heat of the reaction.

1 mole. gas M + $\frac{n}{\theta}$ moles. α-host

$\longrightarrow$ 1 mole. M. $\frac{n}{\theta}$ β-host .

III.2.1 The Dissociation Pressure of the Quinol Clathrates

An attempt was made to determine the dissociation pressures of the clathrate compounds formed by quinol with the following gases: krypton, xenon, methane, ethane, ethylene and carbon dioxide.

A small quantity of quinol, about 0.2 gram, was introduced into the reaction vessel which was then immersed in the thermostat bath set at a temperature T°C. After evacuating the system a pressure of about 60 cms. of mercury of the gas being investigated was admitted to the reaction vessel and shaking started. If no quinol-gas reaction took place at this temperature and pressure, the temperature was progressively lowered until a point was found at which the clathrate would form.

Having found that a reaction would take place the pressure was lowered by about 5 cms. of mercury and the experiment continued to see if the reaction still occurred. In this way the pressure was dropped until a region was reached below which no clathrate could be formed.

A range of pressure was found in this region within which a slow reaction giving a small uptake of gas could be initiated and over which clathrate formed at a higher pressure would decompose. It seemed probable that within this range of pressure the equilibrium isotherm departed from the expected Langmuir-like behaviour and a hysteresis effect occurred. It was not possible to determine the dissociation pressure more accurately than within about ± 2 or ± 3 cms. of mercury, depending on the particular gas. The hysteresis effect is described in more detail in a later chapter.

Values for this approximate dissociation pressure were found over a range in temperature for the clathrate of each gas. Figs. 13 - 18 show plots of Log._{10} dissociation pressure against the reciprocal of the absolute temperature for each gas investigated. The position and slope of the resulting straight-line graph is too uncertain to enable ΔH to be calculated. The

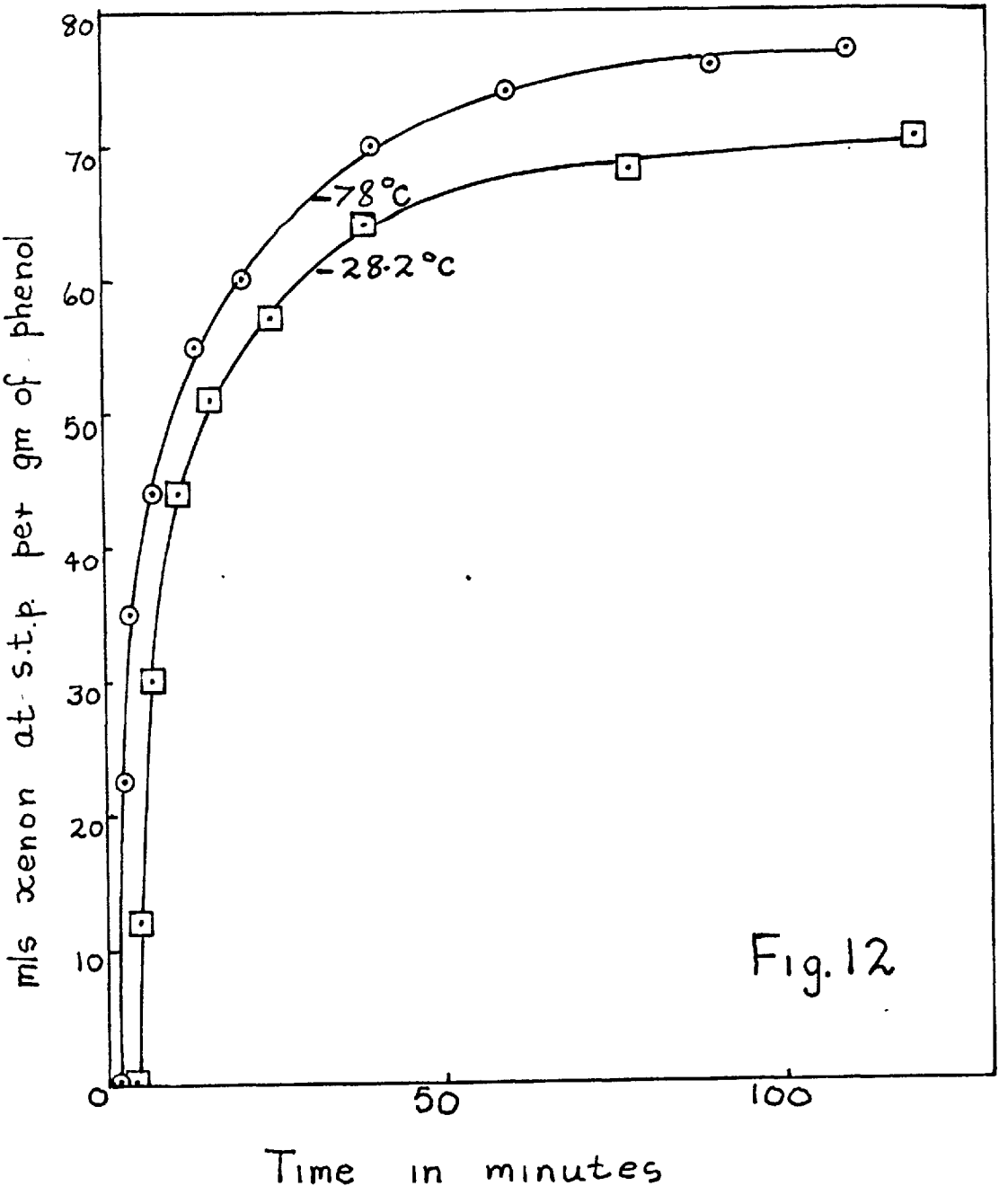
80
70
60
50
40
30
20
10
0
50
100
-78°C
-28·2°C
mls xenon at s.t.p. per gm of phenol
Time in minutes

Fig. 12

values of the dissociation pressures compare reasonably well with those theoretically calculated or experimentally found by other workers, where these are available, Figs. 13, 14 and 15.

III.2.2 The Dissociation Pressures of the Phenol Clathrates

In determining the dissociation pressures of the phenol clathrates of each gas investigated, an arbitrary temperature between 0°C. and -78°C. was chosen to start with. If a clathrate would form at a pressure of about 60 cms. of mercury at this temperature the dissociation pressure was determined as described below. If no reaction took place the temperature was lowered until a value was reached at which the clathrate would form. In this way a satisfactory range of temperature for each gas investigated was found.

At a suitable temperature the pressure at which the clathrate would form was progressively lowered until a point was reached below which no sorption of gases would take place no matter how long shaking was continued. If the reaction was allowed to proceed to equilibrium at a higher pressure and the pressure then dropped and maintained just below the point found as above then all the previously sorbed gas was desorbed. In contrast with the quinol clathrates this point could be determined to

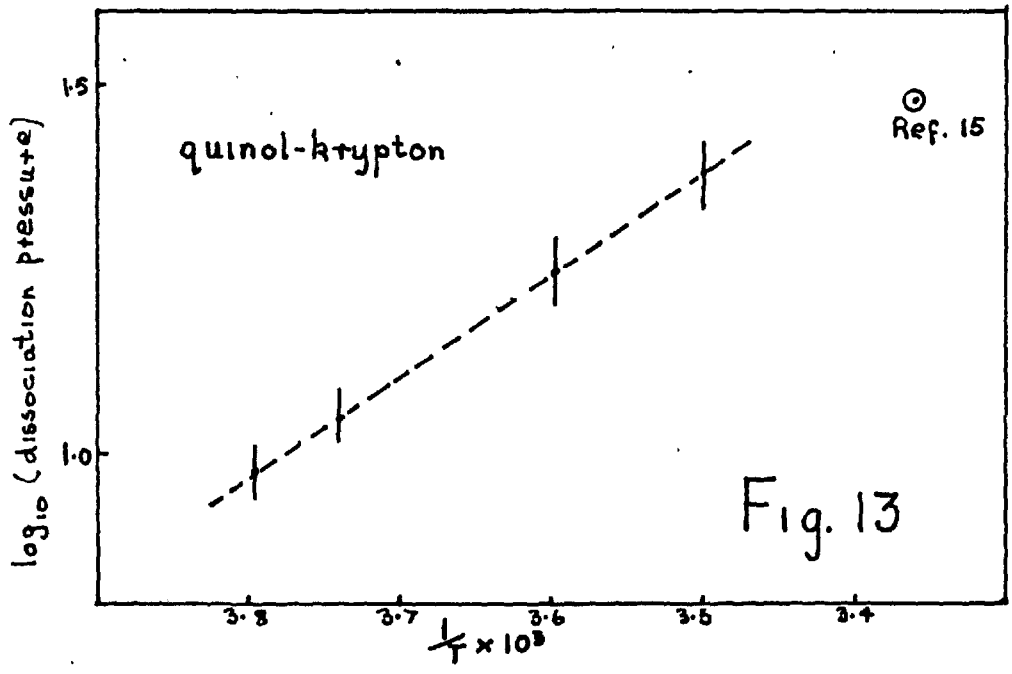
quinol-krypton
Ref. 15
1·5
1·0
log10 (dissociation pressure)
3·8
3·7
3·6
3·5
3·4
1/T x 10³

Fig. 13

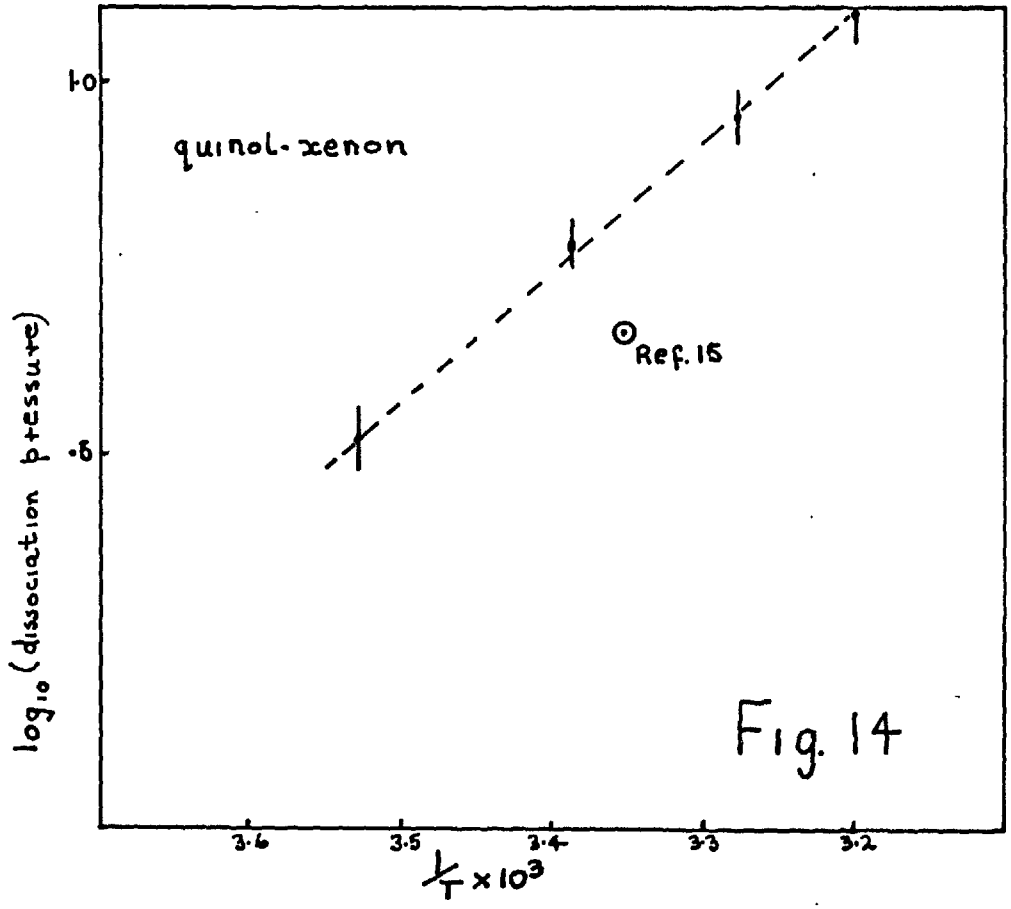
quinol-xenon
Ref. 15
1·0
·5
log10 (dissociation pressure)
3·6
3·5
3·4
3·3
3·2
1/T x 10³

Fig. 14

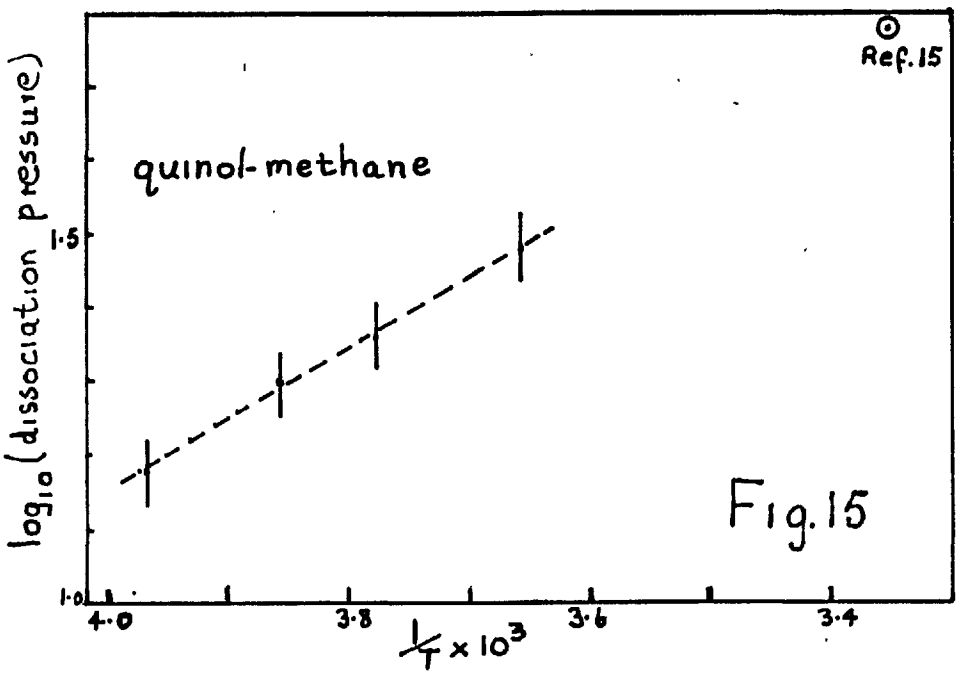
Ref. 15
quinol-methane
$\log_{10}$ (dissociation pressure)
1·5
1·0
4·0
3·8
3·6
3·4
$\frac{1}{T} \times 10^3$

Fig. 15

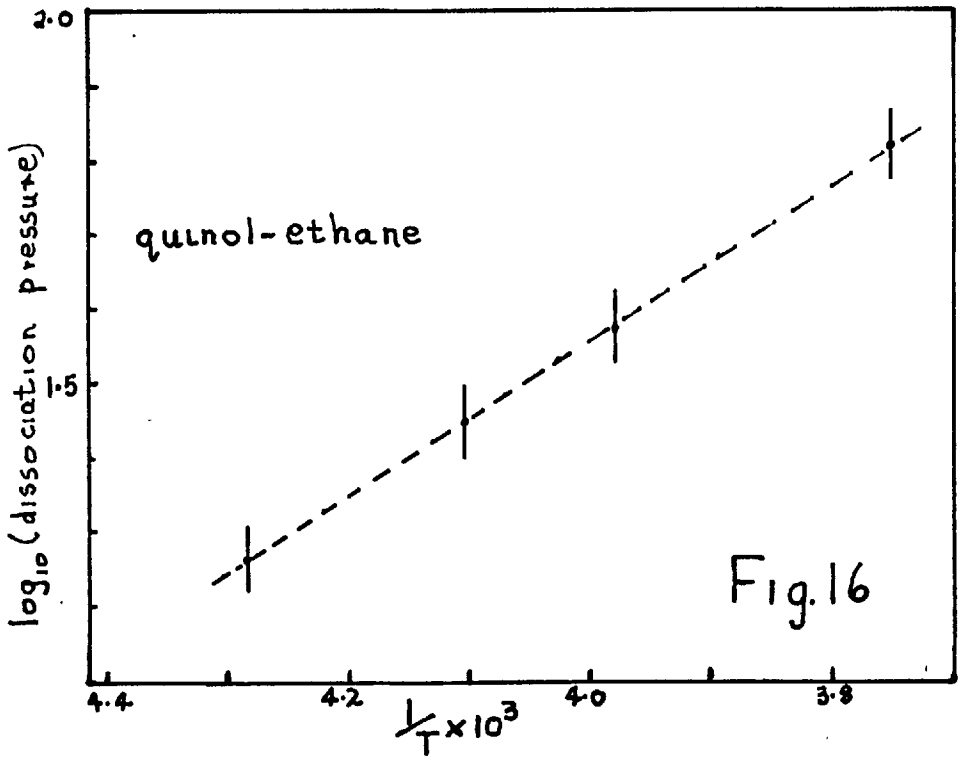
quinol-ethane
$\log_{10}$ (dissociation pressure)
2·0
1·5
4·4
4·2
4·0
3·8
$\frac{1}{T} \times 10^3$

Fig. 16

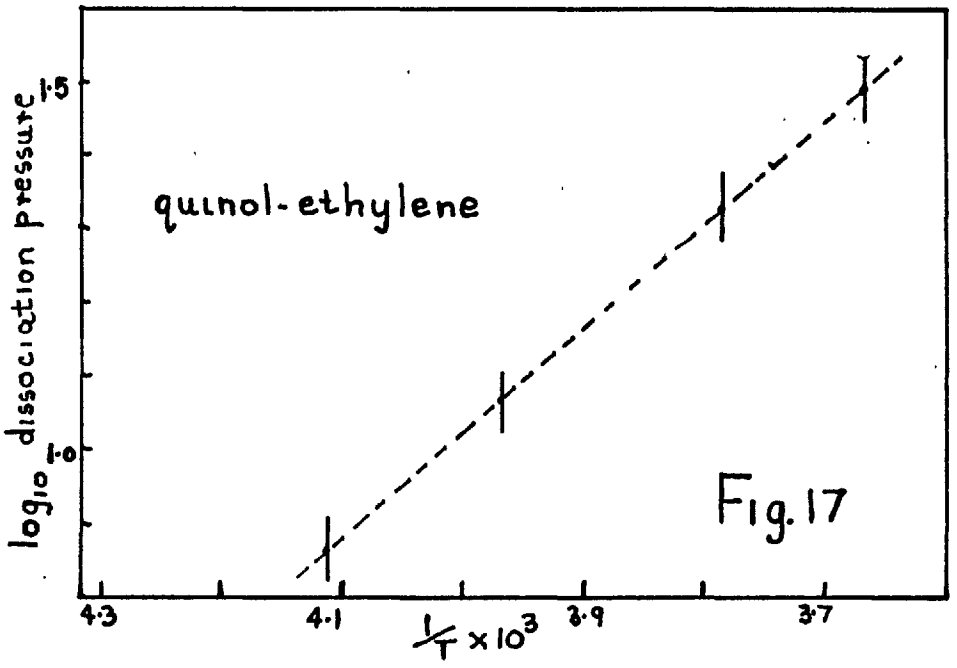
quinol-ethylene
$\log_{10}$ dissociation pressure
1·5
1·0
4·3
4·1
3·9
3·7
$\frac{1}{T} \times 10^3$

Fig. 17

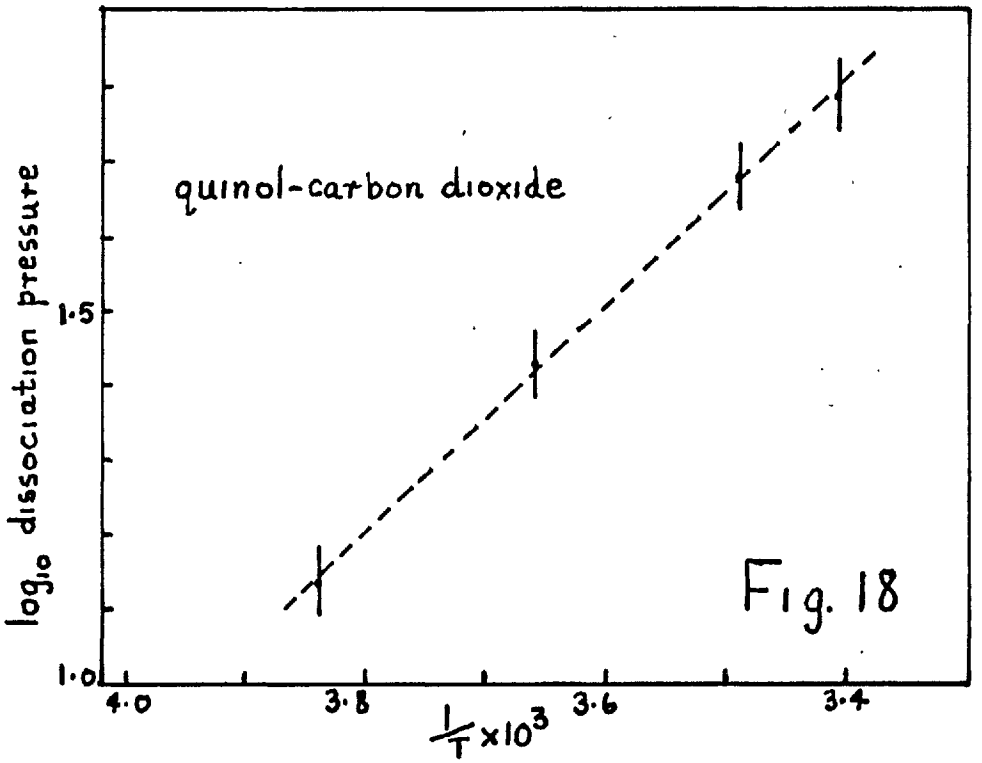
quinol-carbon dioxide
$\log_{10}$ dissociation pressure
1·5
1·0
4·0
3·8
3·6
3·4
$\frac{1}{T} \times 10^3$

Fig. 18

within ±0.1 cms. of mercury with no evidence of any hysteresis effect.

The dissociation pressure was also found by a second method to constitute a check on the first. Gas was admitted to the reaction vessel to a pressure about 1 cm. of mercury above the dissociation pressure found as above. The mercury level in the gas burette was maintained at a constant level. As the reaction proceeded and gas was sorbed, the pressure dropped until a point was reached at which the reaction stopped. This point was taken to be the dissociation pressure. It was found to agree very well with the pressure found by the first method.

Values of the dissociation pressure for each phenol-gas clathrate were found over a range in temperature and are given in Table II.

Figs.19 - 21 show plots of the logarithm to the base 10 of the dissociation pressure against the reciprocal of the absolute temperature. These plots approximate very closely to straight line graphs indicating that the heat of formation of the clathrate remains constant over a wide range of temperature.

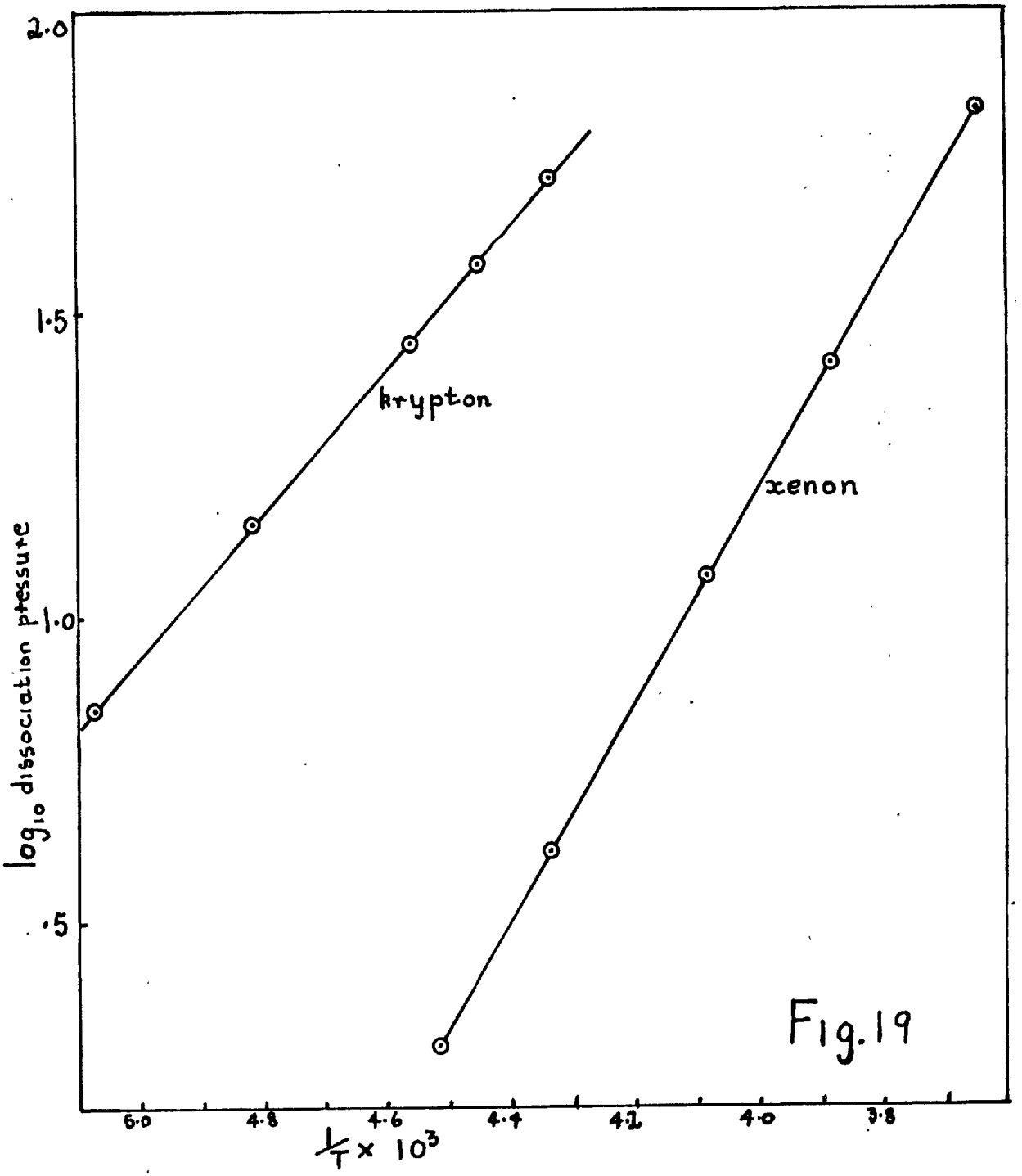

Fig. 19

Phenol Clathrates

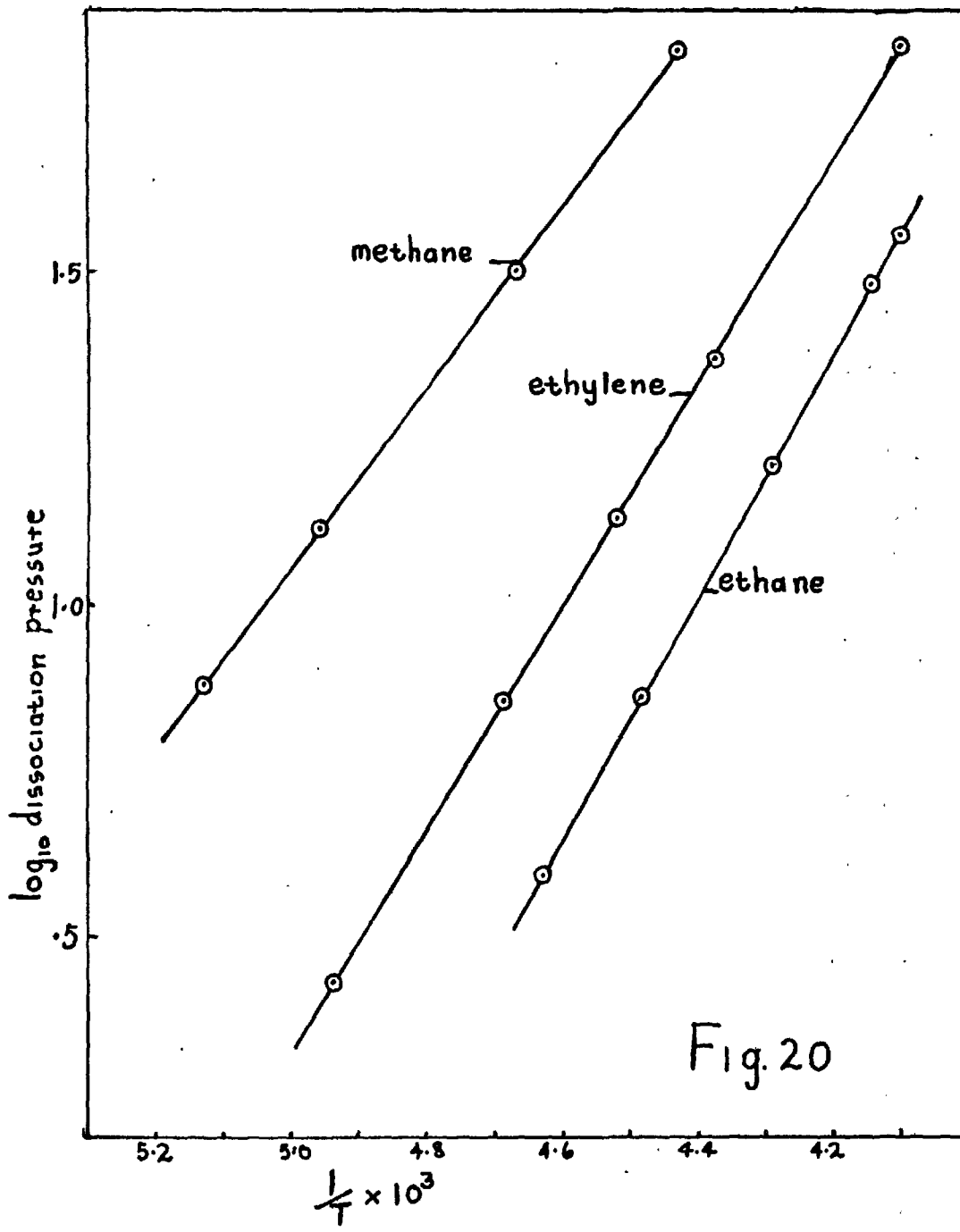

Fig. 20

Phenol clathrates

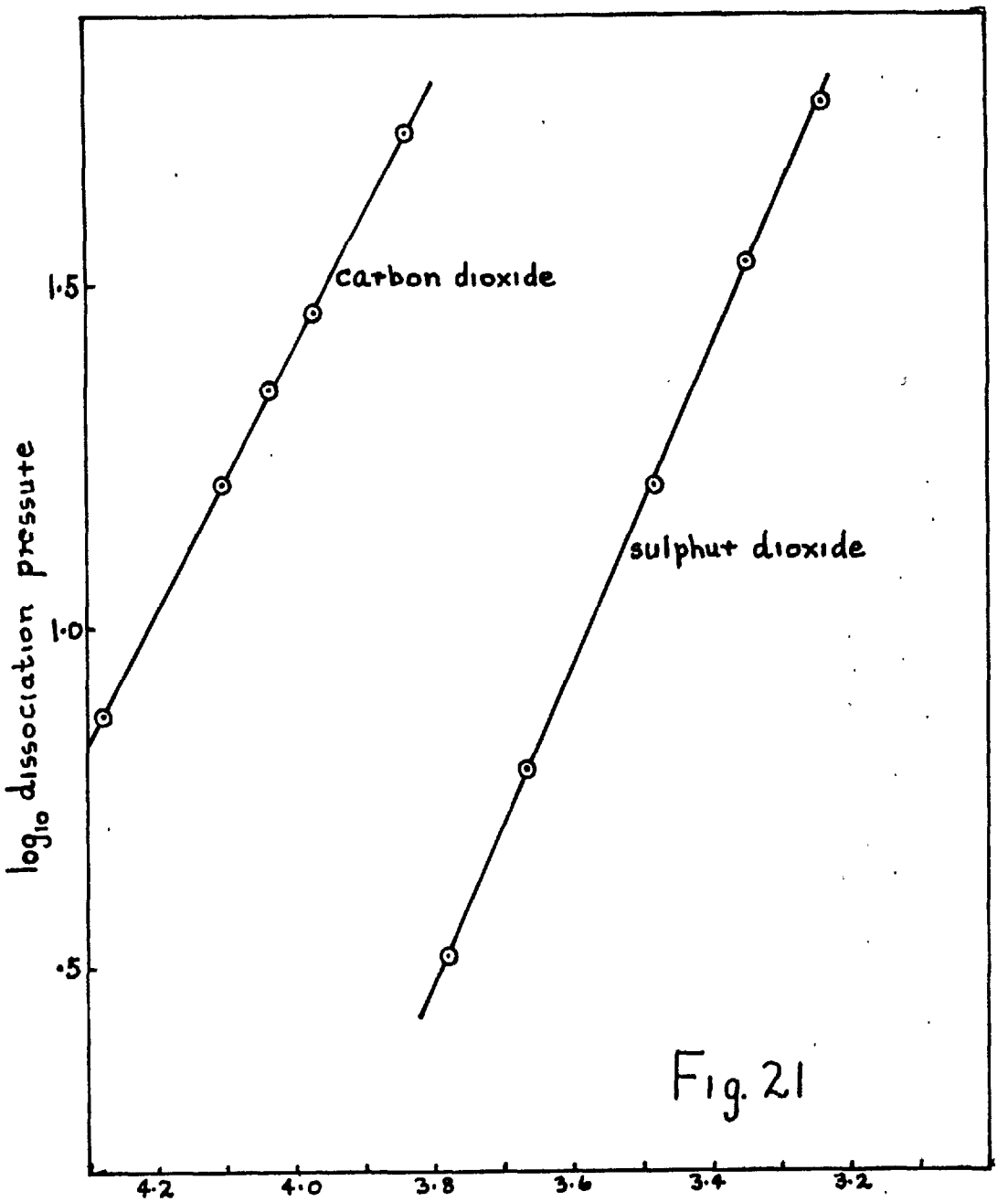

Fig. 21

Phenol clathrates

TABLE II

Phenol-krypton	
Dissociation Pressure in cms. of Hg	Temperature ^{o}A
53.1	230.6
38.0	224.7
28.2	219.3
14.3	208.0
7.2	197.0

Phenol-xenon	
Dissociation Pressure in cms. of Hg	Temperature ^{o}A
69	274.0
25.3	257.4
11.9	244.9
4.2	230.6
2.0	221.5

Phenol-methane	
Dissociation Pressure in cms. of Hg	Temperature ^{o}A
68.5	225.7
31.6	214.1
13.0	201.6
7.6	195.0

Phenol-ethane	
Dissociation Pressure in cms. of Hg	Temperature ^{o}A
36.7	243.6
30.2	241.0
16.2	232.9
7.3	223.2
3.9	216.0

Phenol-ethylene	
Dissociation Pressure in cms. of Hg	Temperature ^{o}A
69.0	243.9
24.0	228.8
13.5	221.0
7.2	213.2
2.7	202.4

Phenol-carbon dioxide	
Dissociation Pressure in cms. of Hg	Temperature ^{o}A
54.5	260.9
28.8	251.9
22.4	247.9
16.2	243.9
7.4	233.9

Phenol-sulphur dioxide	
Dissociation Pressure in cms. of Hg	Temperature ^{o}A
59.5	306.6
34.3	299.0
16.2	287.4
6.3	273.0
3.3	264.6

Application of the Clapeyron equation enables $\triangle H$ to be calculated. $\triangle H$ is given by the slope of the straight line in Figs. 19-21 multiplied by 2.303 R. Values of $\triangle H$ for the various gases investigated were found to be:

Gas	$-\triangle H$ K cals./mole.
krypton	5.3_5
xenon	8.1_9
methane	6.1_8
ethane	8.4_3
ethylene	7.6_5
carbon dioxide	9.0_6
sulphur dioxide	10.7

In Figs. 22 - 25 the values of the dissociation pressures for the gases krypton, xenon, carbon dioxide and sulphur dioxide are compared with the values found by Nikitin and Kovalskaya[18] and by Lahr and Williams,[22] on a plot of Log. $_{10}$ dissociation pressure against reciprocal of the absolute temperature.

The results found for xenon by the present method compare well with those of both Lahr and Williams[22], and Nikitin and Kovalskaya,[10] as do the sulphur dioxide results with those of Nikitin and Kovalskaya.[10] There is however divergence from Nikitin and Kovalskaya's[10]

results for carbon dioxide and considerable difference from Lahr and Williams'[22] results for krypton. The values found for $\triangle H$ are compared in Table III below.

Table III

Gas	$-\triangle H$ k cals./mole.		
	Present work	Lahr and Williams	Nikitin and Kovalskaya
argon		9.85	
krypton	5.3_5	8.97	
xenon	8.1_9	8.8	7.33
carbon dioxide	9.0_6		7.32
sulphur dioxide	10.7		9.00

It may be seen that the heat of overall reaction found by Lahr and Williams[22] for the formation of the phenol clathrates of argon, krypton, and xenon decreases numerically with increasing size and condensability of the gas. For the sizes of these guest molecules this would be in contradiction to the result expected from the discussion on pages 22 - 28 and the increase in numerical value of $\triangle H$ in going from krypton to xenon found by the present method seems more probable.

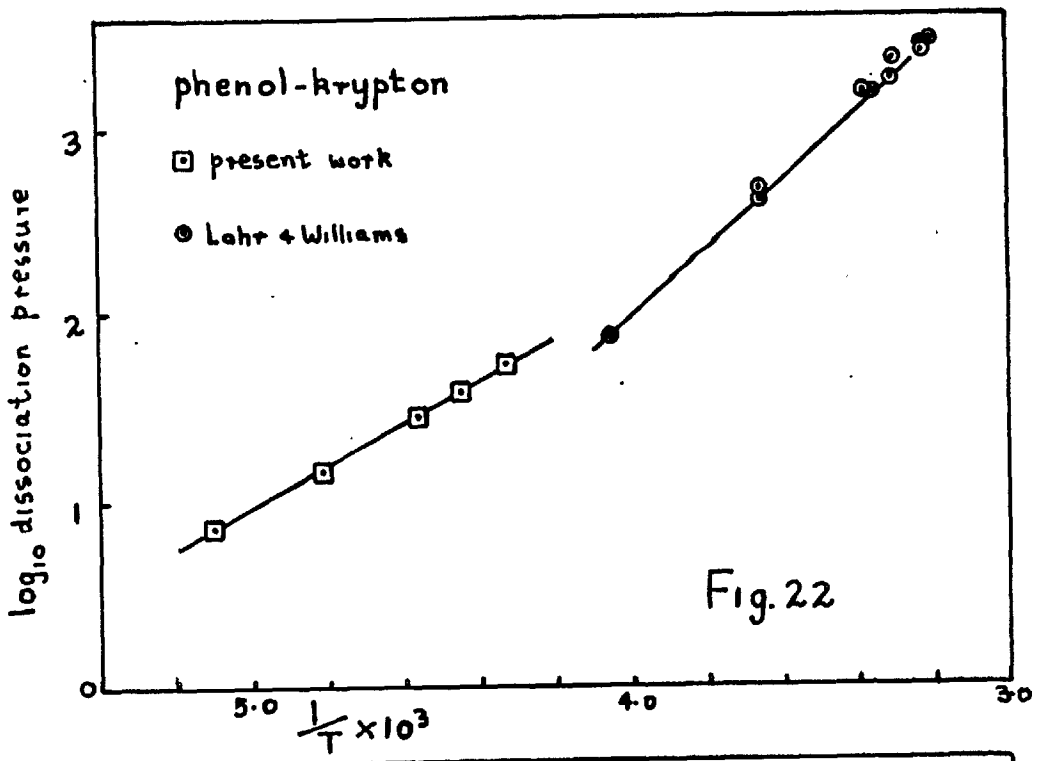
phenol-krypton
present work
Lahr + Williams
log10 dissociation pressure
0
1
2
3
5·0
4·0
3·0
1/T x 10³

Fig. 22

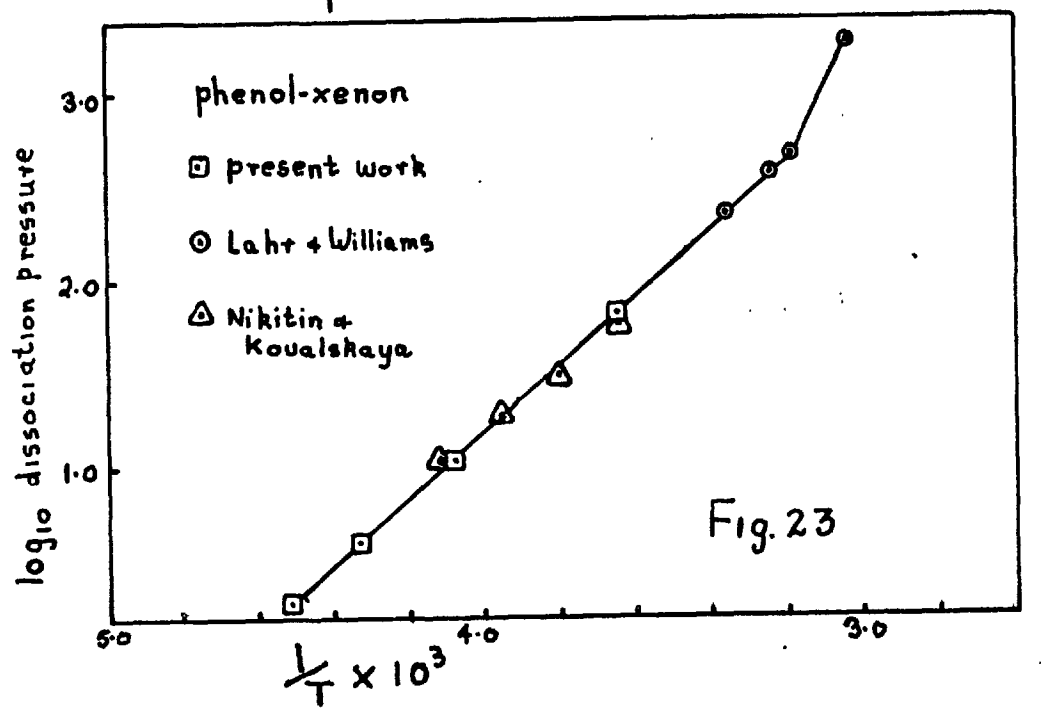
phenol-xenon
present work
Lahr + Williams
Nikitin + Kovalskaya
log10 dissociation pressure
1·0
2·0
3·0
5·0
4·0
3·0
1/T x 10³

Fig. 23

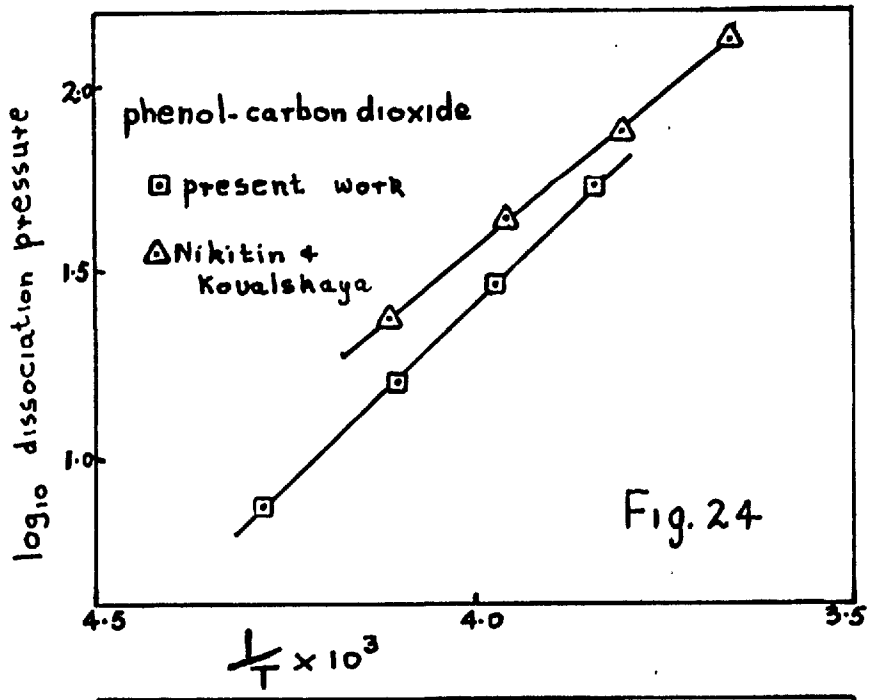
phenol-carbon dioxide
present work
Nikitin + Kovalskaya
log10 dissociation pressure
2·0
1·5
1·0
4·5
4·0
3·5
1/T x 10³

Fig. 24

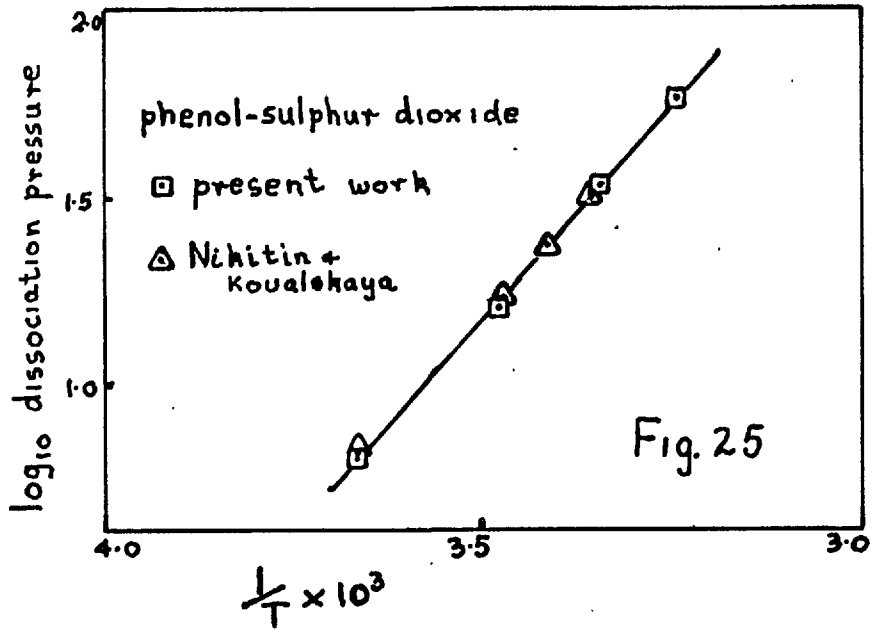
phenol-sulphur dioxide
present work
Nikitin + Kovalskaya
log10 dissociation pressure
2·0
1·5
1·0
4·0
3·5
3·0
1/T x 10³

Fig. 25

III. 3. The Measurement of the Maximum Sorption of Gas by the Quinol Crystals

The method used for the measurement of the maximum sorption of gas by crystals of the host material has been described on page 73. Only an approximate value of the dissociation pressure of a quinol clathrate at any particular temperature is known but this was used as a guide and the maximum sorption was measured over a range of pressure above this value. From the maximum sorption found at a particular temperature the isotherm was constructed by plotting V, the mls. of gas sorbed at s.t.p. per gram of host material against P, the pressure in cms. of mercury.

Three krypton isotherms at temperatures of $0^{\circ}C.$ $-12.3^{\circ}C.$ and $-29.5^{\circ}C.$ were measured. Each point on the isotherm was found independently of the others using a fresh sample of quinol. Fig. 26 shows a plot of these three isotherms. The investigation of the dissociation pressures of the quinol clathrates had suggested the presence of a hysteresis effect in the region of the dissociation pressure and this was investigated as described below for the 0° isotherm and is shown in Fig. 26.

A point on the isotherm was found at a fairly high pressure and then the pressure was lowered in a series of steps at each of which shaking was continued until no further gas would desorb and the new equilibrium had thus been reached. It was found that this "desorption" isotherm followed the "adsorption" isotherm until just below a pressure of 20 cms. of mercury where there was a sharp increase in the amount of gas desorbed. The "desorption" isotherm continued as shown in Fig.26 until at a pressure just below 10 cms. of mercury all the previously sorbed gas had been desorbed. Points were then found by desorption in this region. It was found that no reaction would take place until the pressure was about 6 cms. of mercury above the point at which all gas had previously been desorbed. As shown in Fig. 26, the amount of gas sorbed then rose rapidly with increase in pressure joining the "desorption" isotherm at a pressure of about 18 cms. of mercury and then retracing the original isotherm above a pressure of 20 cms. of mercury.

From the theory discussed on pages 37-39 and 39-41 it was expected that above the region showing a hysteresis effect these isotherms would have the form suggested by Langmuir and could thus be expressed as $KP = \frac{\theta}{1-\theta}$. In this equation θ is given by $\frac{V}{V_m}$, V being the

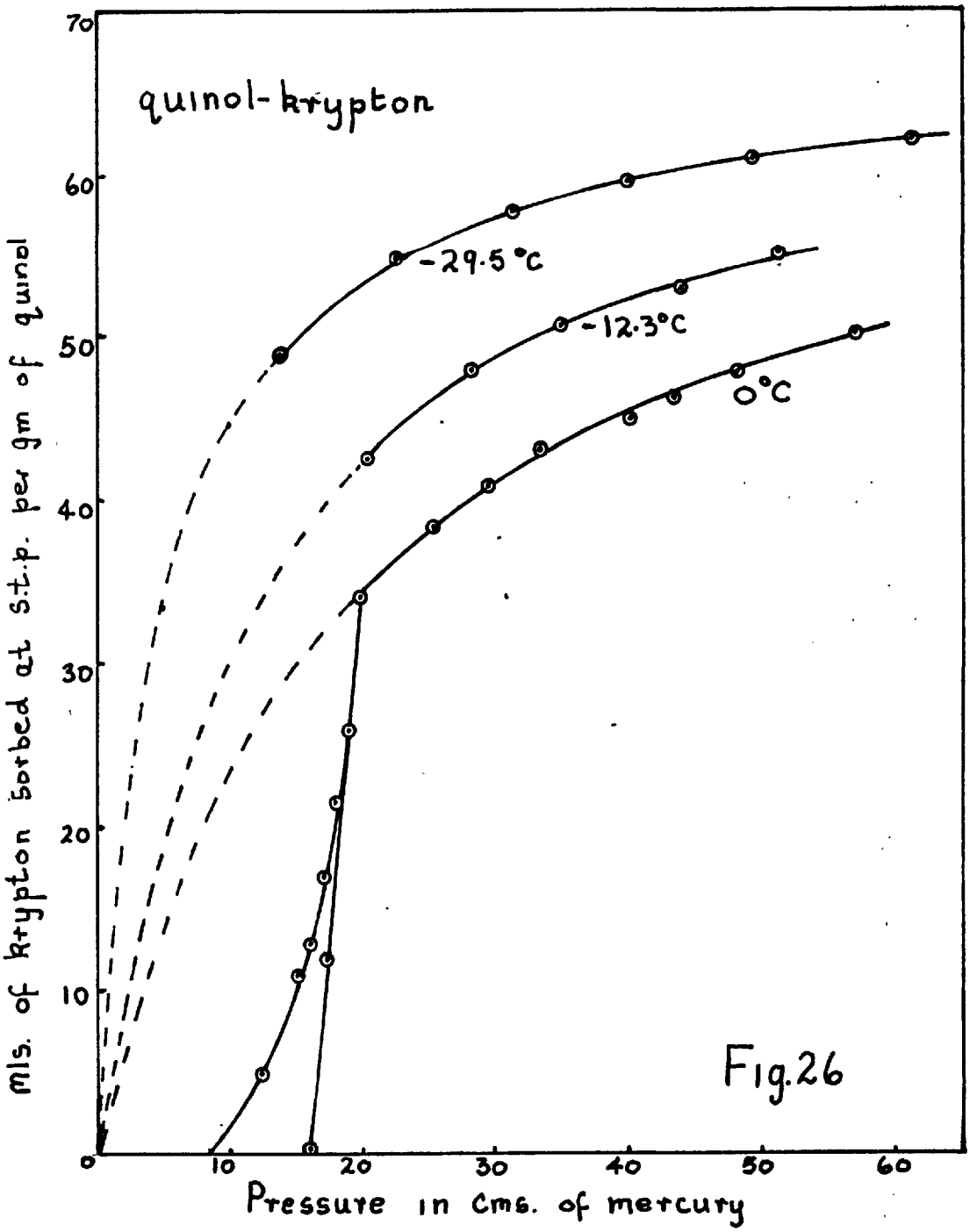
quinol-krypton
-29.5 °C
-12.3°C
0°C
Mls. of krypton sorbed at s.t.p. per gm of quinol
Pressure in Cms. of mercury
0
10
20
30
40
50
60
70

Fig.26

amount of gas sorbed at pressure P and V_m the limiting value to which V tends as P becomes large. K is the Langmuir equilibrium constant. The equation may then be written as

$$KP = \frac{V}{V_m - V}$$

or, on rearranging

$$\frac{P}{V} = \frac{1}{V_m} \cdot P + \frac{1}{KV_m}$$

Thus a plot of $\frac{P}{V}$ against P should be a straight line if the isotherm is a Langmuir isotherm. The slope of the line is the reciprocal of V_m and the negative intercept on the P axis equalto the reciprocal of the Langmuir equilibrium constant.

Fig. 27 shows plots of $\frac{P}{V}$ against P for the three isotherms and it may be seen that they do approximate very closely to straight lines. V_m was found for each isotherm and the values are given in Table IV. In all three cases the values are very close to the theoretical maximum , 67.81 mls. at s.t.p. per gram of host.

$\frac{\theta}{1-\theta}$ was next found for each point on the isotherm and plotted against P as shown in Figs. 28 and 29. The plots approximate well to straight lines passing through the origin. From the slopes of these lines the value of K, the equilibrium constant, was found for each isotherm.

Two further measurements of the maximum sorption of krypton by quinol were made at two further temperatures. It was assumed that V_m was given by the theoretical maximum, and K was calculated for the two points. All the values of K found for the krypton-quinol clathrate are given in Table IV.

From the Clausius-Clapeyron equation ΔH_z the heat evolved when 1 mole of gas is taken from the gas phase and sorbed by the host lattice, can be shown to be related to the Langmuir equilibrium constant by

$$\frac{-\Delta H_z}{R} = \frac{\partial \ln K}{\partial \frac{1}{T}}$$

Fig. 30 shows a plot of Log. $_{10}$ K against $\frac{1}{T}$ for these quinol krypton results. The plot approximates well to a straight-line graph and from the slope ΔH_z may be calculated. ΔH is given by, $\Delta H_z = 2.303.R \times$ slope.

The value found for ΔH_2 is -6.0$_3$ K cals./mole.

Measurements were next made of the uptake of xenon by quinol. At a temperature of -78°C. and a pressure of 55 cms. of mercury the maximum uptake was found to be 67.7 mls. at s.t.p. per gram of quinol, very close to the theoretical maximum. Measurements were then made at the two much higher temperatures of 0°C. and 10.6°C. The results are tabulated in Table IV, and the isotherms shown in Fig. 31. The dissociation pressure of the quinol-xenon clathrates is very small at both 0°C. and 18.6°C., and the pressures at which the measurements were made were much less than those for the krypton and methane clathrates. The hysteresis effect for quinol-xenon at 0°C. was investigated in the same way as for quinol-krypton and is shown in Fig.31

The results give good approximations to straight-line graphs for plots of $\frac{P}{V}$ against P as shown in Fig. 32. The apparent value of V_m found in both cases is higher than the theoretical maximum. At 0°C., V_m is 71 mls. at s.t.p. per gram of quinol and at 10.6°C. V_m is 73.3 mls. at s.t.p. per gram.

Plots of $\frac{\theta}{1-\theta}$ against P were made, Fig. 33, and the Langmuir equilibrium constants calculated. A measure of the maximum sorption of xenon by quinol at 5.3°C. and at a

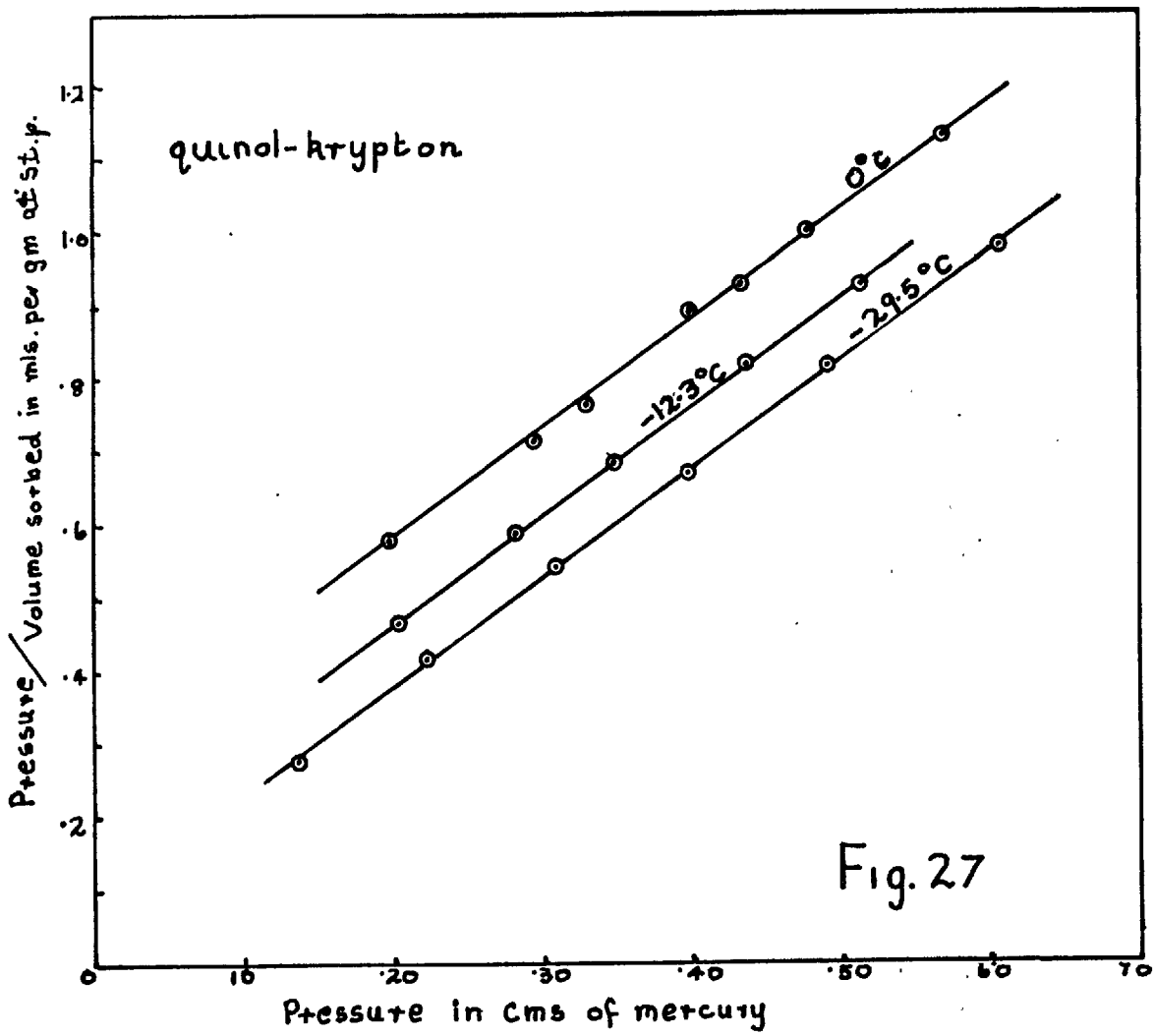
quinol-krypton
0°C
-12.3°C
-29.5°C
Pressure/Volume sorbed in mls. per gm at S.T.P.
Pressure in Cms of mercury
1·2
1·0
·8
·6
·4
·2
0
10
·20
·30
·40
·50
·60
70

Fig. 27

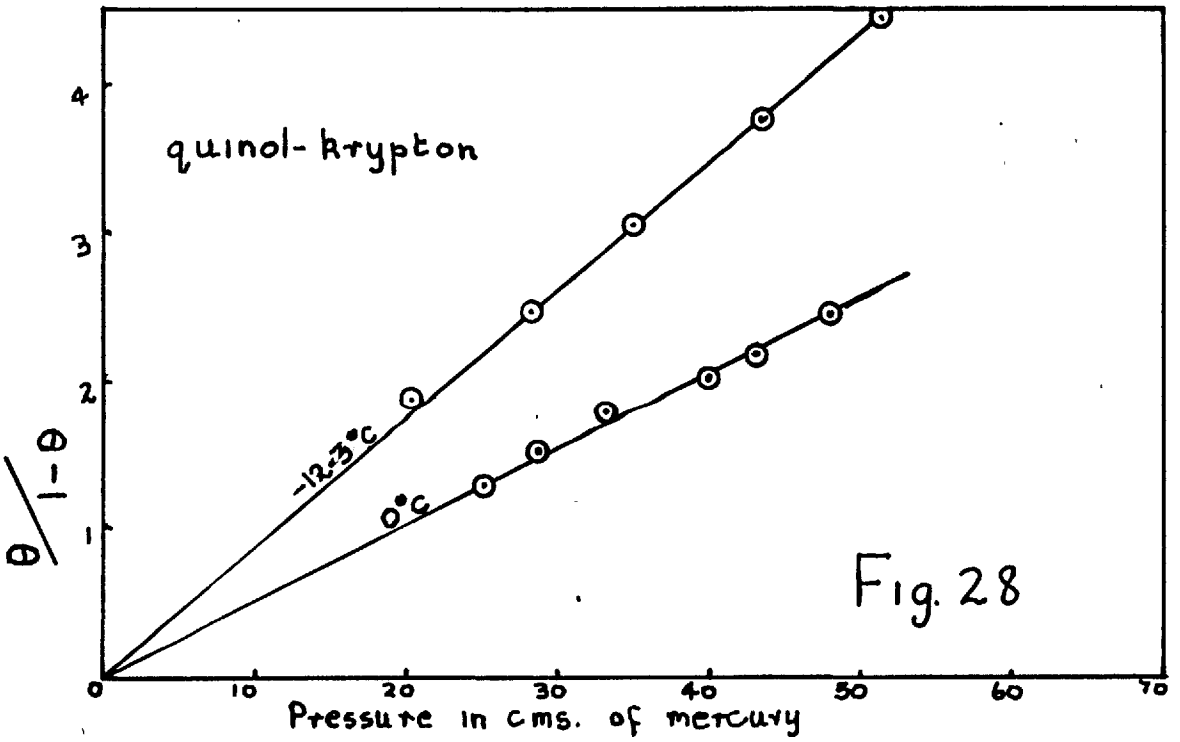
quinol-krypton
-12.3°C
0°C
θ/1-θ
0
1
2
3
4
10
20
30
40
50
60
70
Pressure in cms. of mercury

Fig. 28

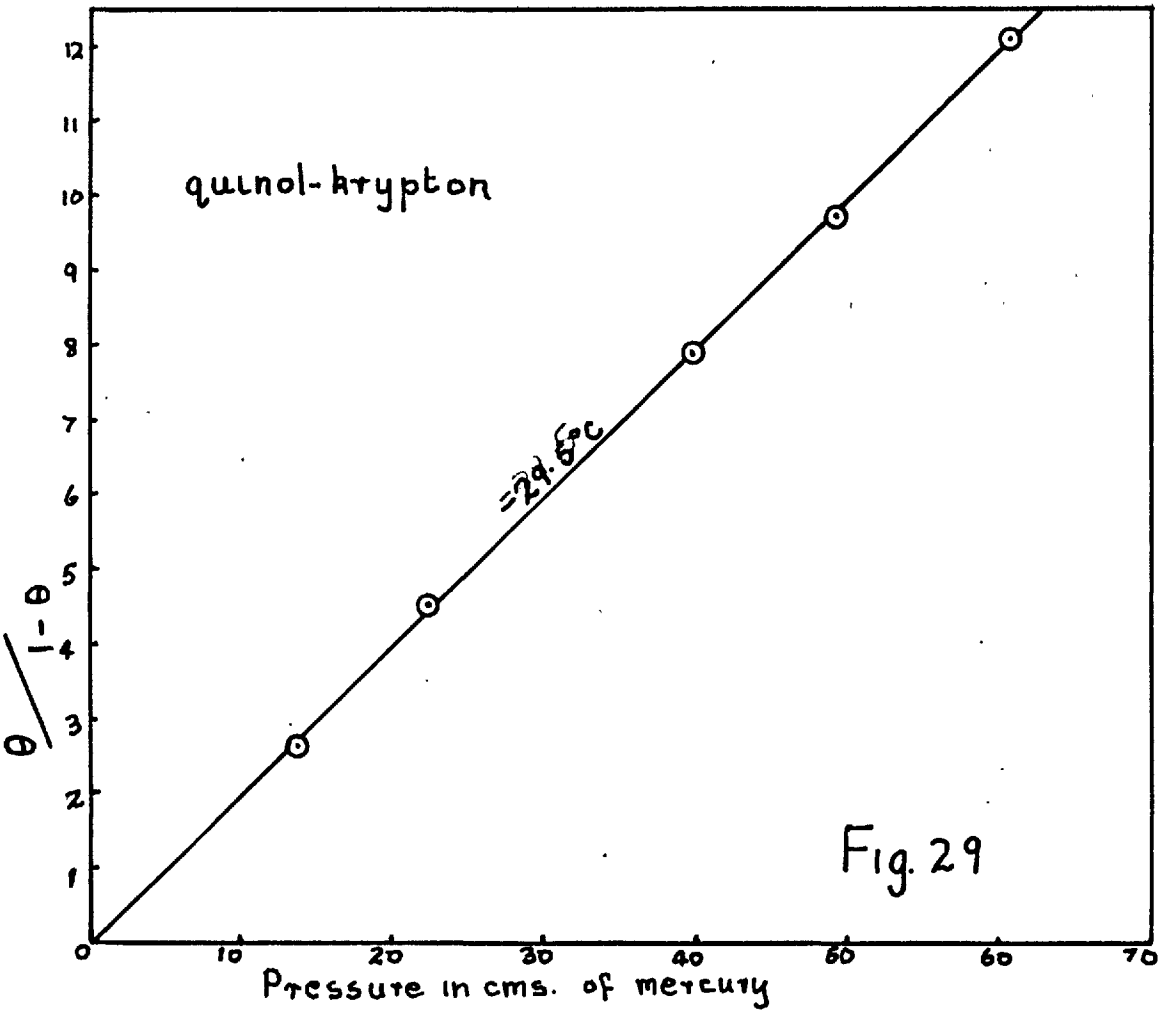
quinol-krypton
-29.6°C
θ/1-θ
0
1
2
3
4
5
6
7
8
9
10
11
12
10
20
30
40
50
60
70
Pressure in cms. of mercury

Fig. 29

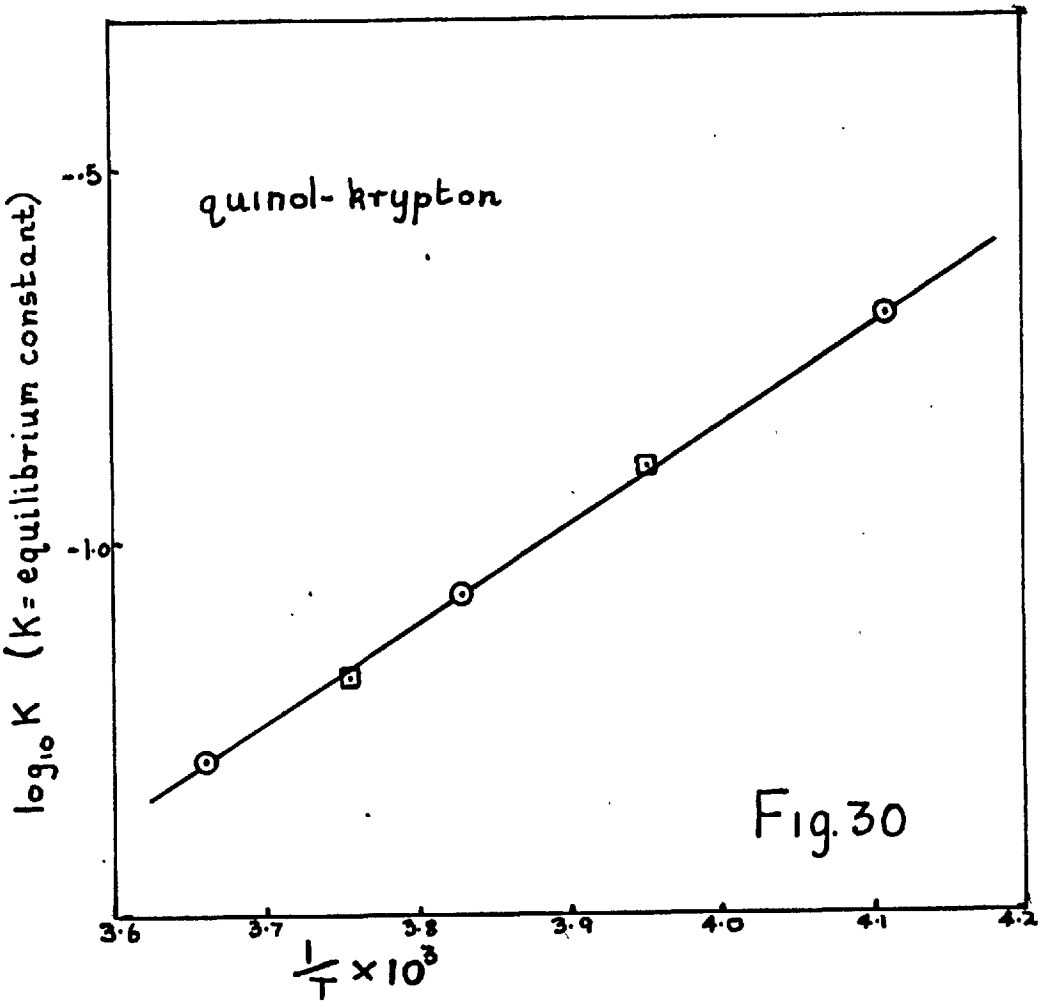
quinol-krypton
-·5
-1·0
$\log_{10} K$ (K = equilibrium constant)
3·6
3·7
3·8
3·9
4·0
4·1
4·2
$\frac{1}{T} \times 10^3$

Fig. 30

pressure of 21.6 cms. of mercury was made. V_m was taken as lying midway between 71 and 73.3 mls. at s.t.p. per gram and K calculated. The values of K found were plotted as Log._{10} K against $\frac{I}{T}$ as shown in Fig. 34.

The plot is a reasonable approximation to a straight line. ΔH_2 was calculated to be -9.8 K cals./mole.

Measurements of the maximum uptake of methane by quinol were also made, at -20.5°C. The isotherm is shown in Fig. 35, and the results are tabulated in Table IV. A plot of $\frac{P}{V}$ against P, Fig. 36, was again found to approximate closely to a straight line and the value of V_m, 68 mls. at s.t.p. per gram again very close to the theoretical maximum. $\frac{\theta}{1-\theta}$ was plotted against P (Fig. 36a) and the Langumuir equilibrium constant found to be 4.26×10^{-2}.

Single measurements of the maximum sorption of methane were made at a number of temperatures over a range from 0°C. to -50°C. V_m was taken to be equal to the theoretical maximum in each case and K calculated at each temperature. The values of K are given in Table IV Fig. 37 shows a plot of Log._{10} K against $\frac{I}{T}$. There is some scatter, but the plot approximates reasonably well to a straight-line graph. ΔH_2 was calculated from the slope and found to be -6.1 K cals./mole.

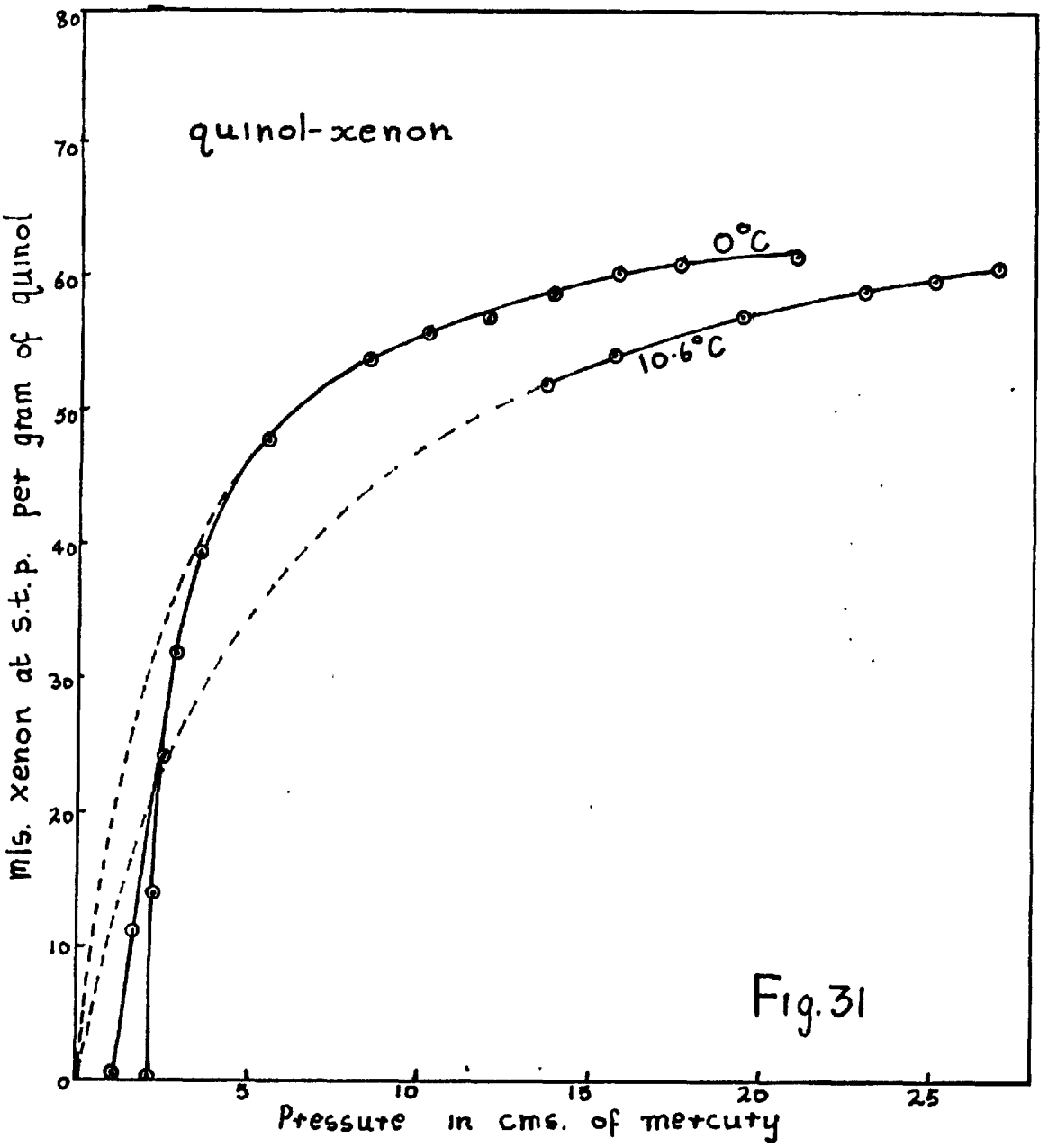
quinol-xenon
0°C
10·6°C
mls. xenon at s.t.p. per gram of quinol
Pressure in cms. of mercury
0
10
20
30
40
50
60
70
80
5
10
15
20
25

Fig. 31

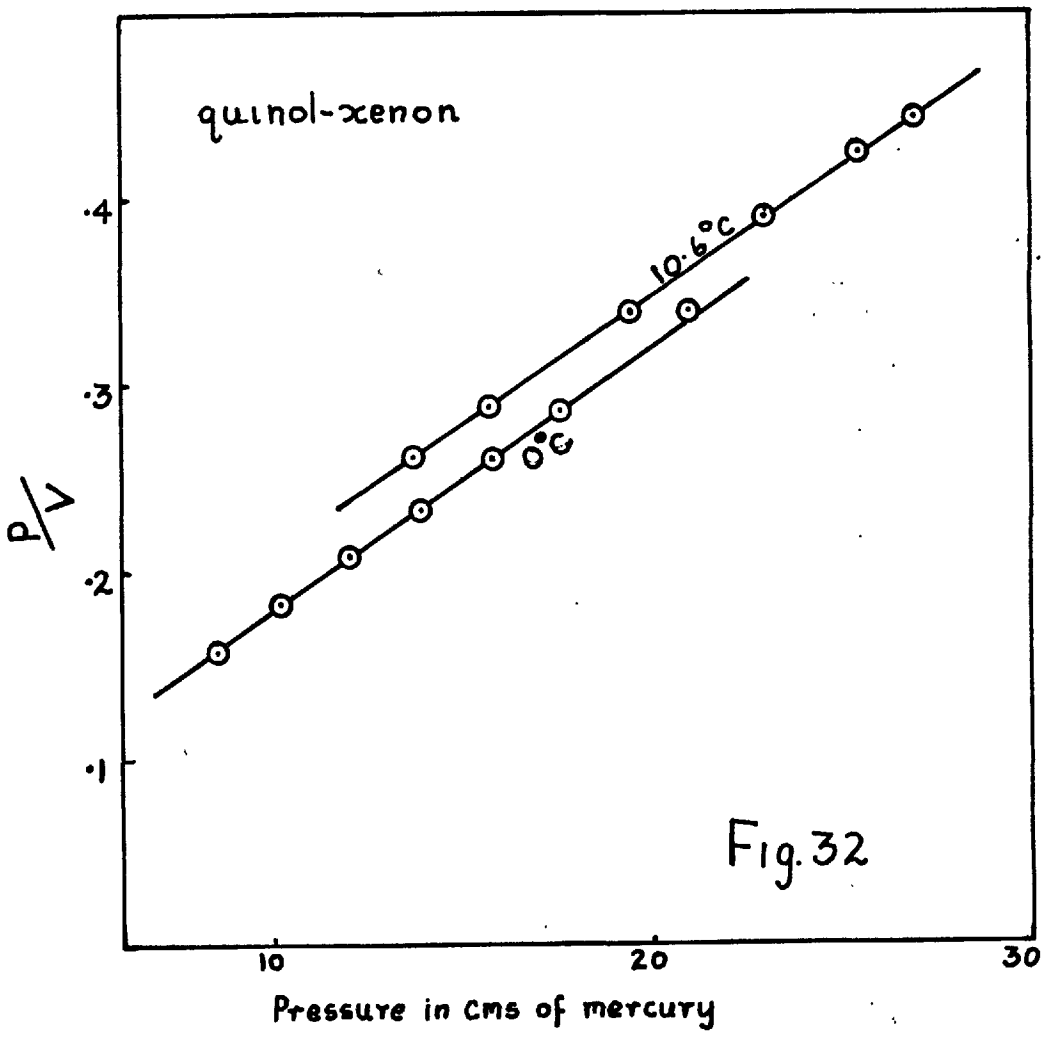
quinol-xenon
10·6°C
0°C
P/V
·4
·3
·2
·1
10
20
30
Pressure in cms of mercury

Fig. 32

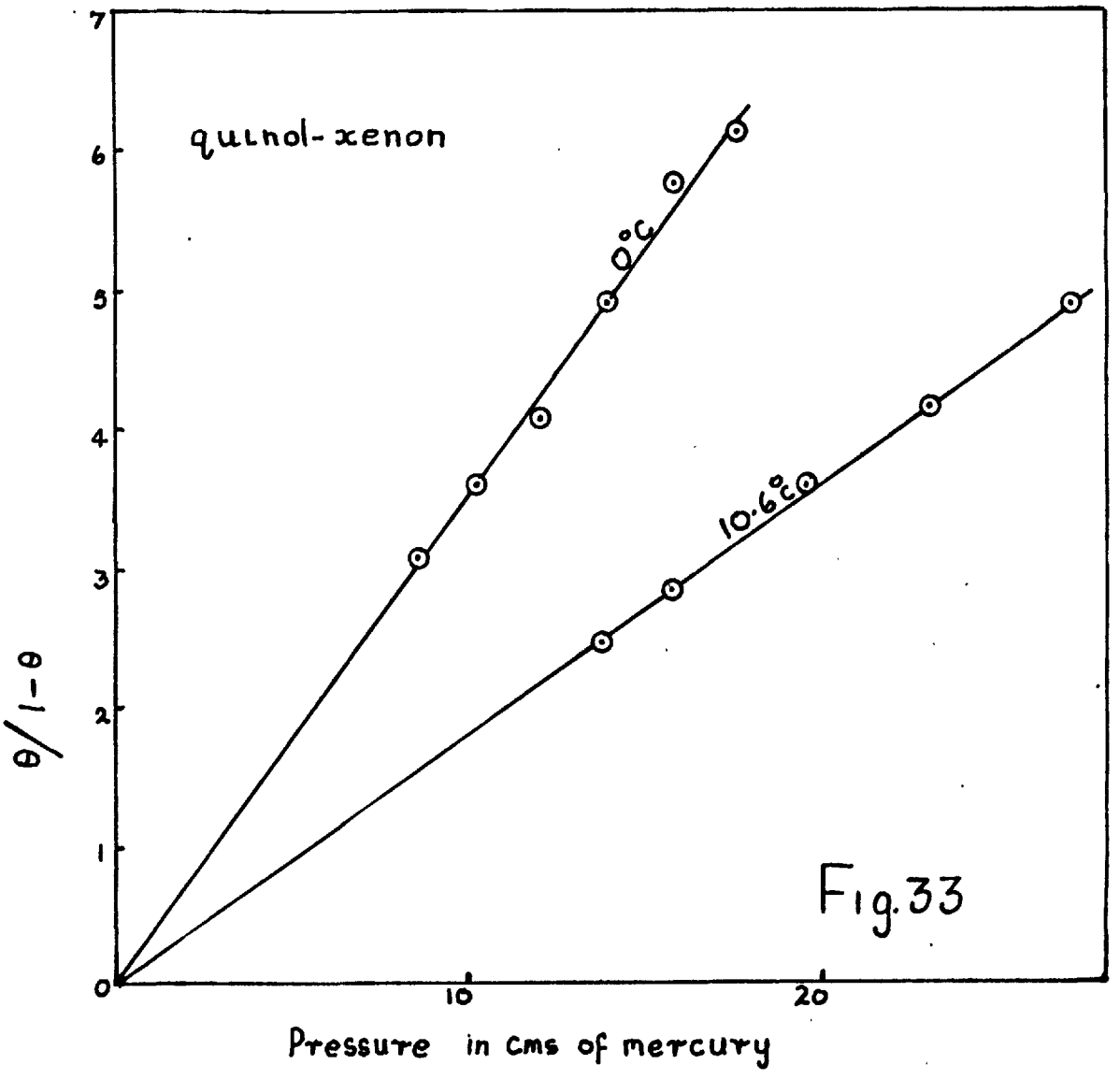
quinol-xenon
0°C
10.6°C
θ/1-θ
Pressure in cms of mercury
0
1
2
3
4
5
6
7
10
20

Fig. 33

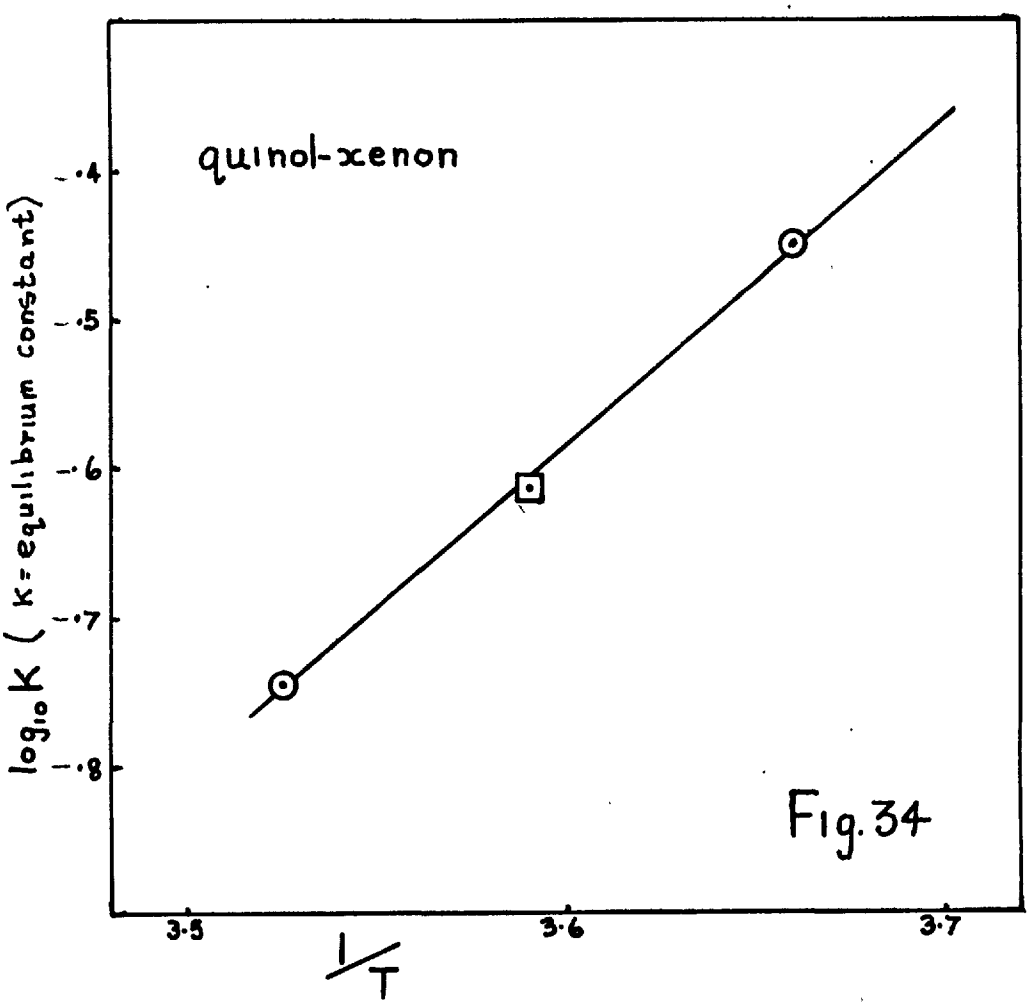
quinol-xenon
$\log_{10} K$ (K = equilibrium constant)
-·4
-·5
-·6
-·7
-·8
3·5
3·6
3·7
1/T

Fig. 34

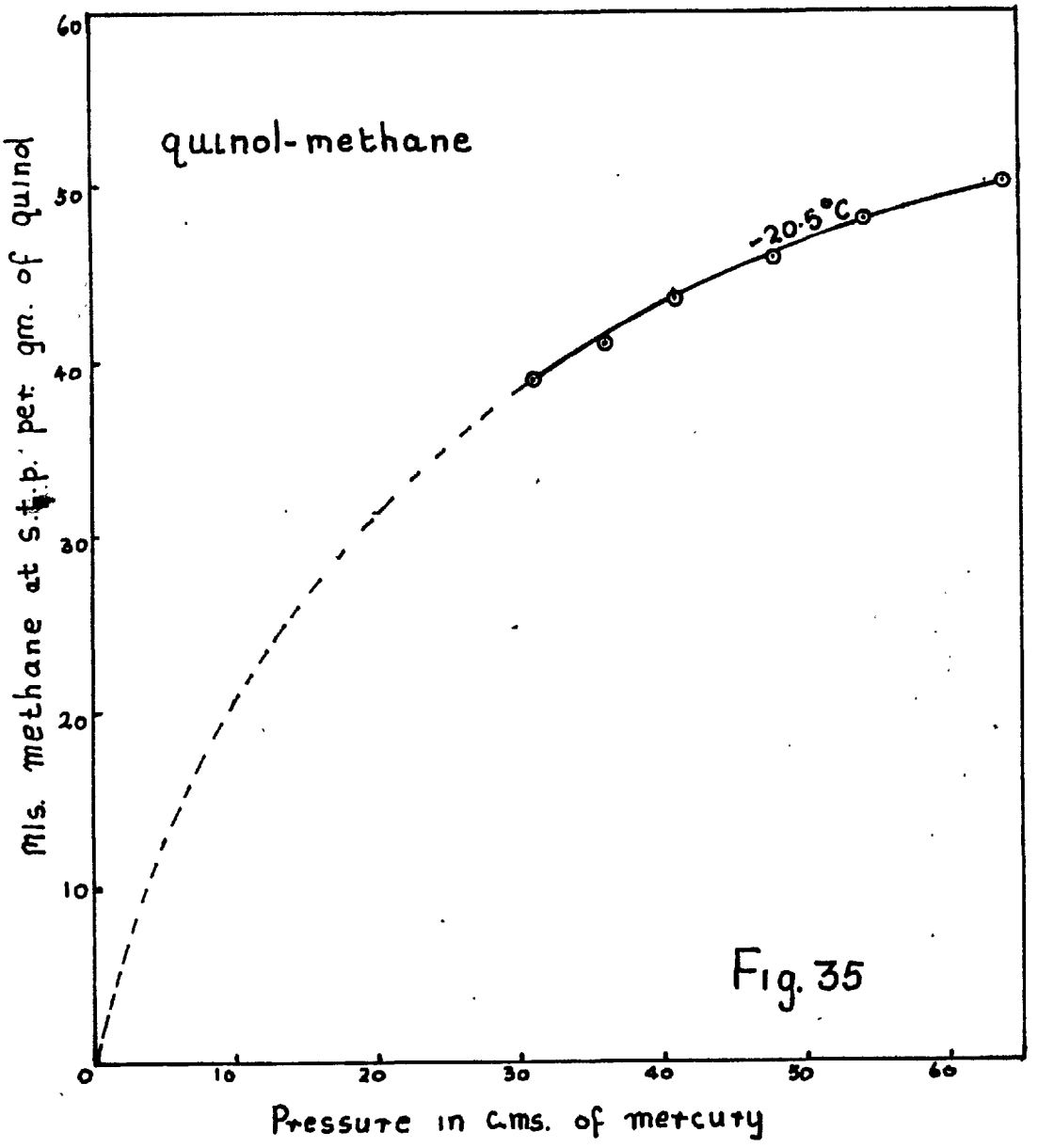
quinol-methane
-20·5°C
Mls. methane at S.T.P. per gm. of quinol
Pressure in cms. of mercury
0
10
20
30
40
50
60

Fig. 35

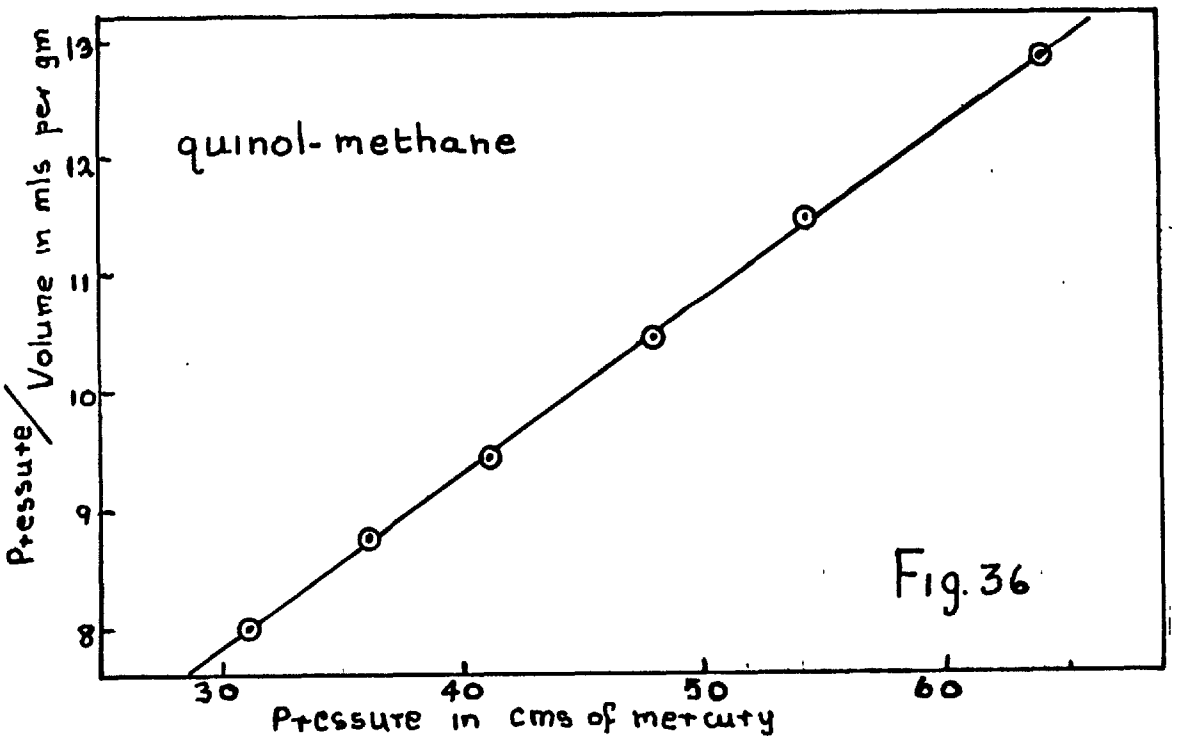

Fig. 36

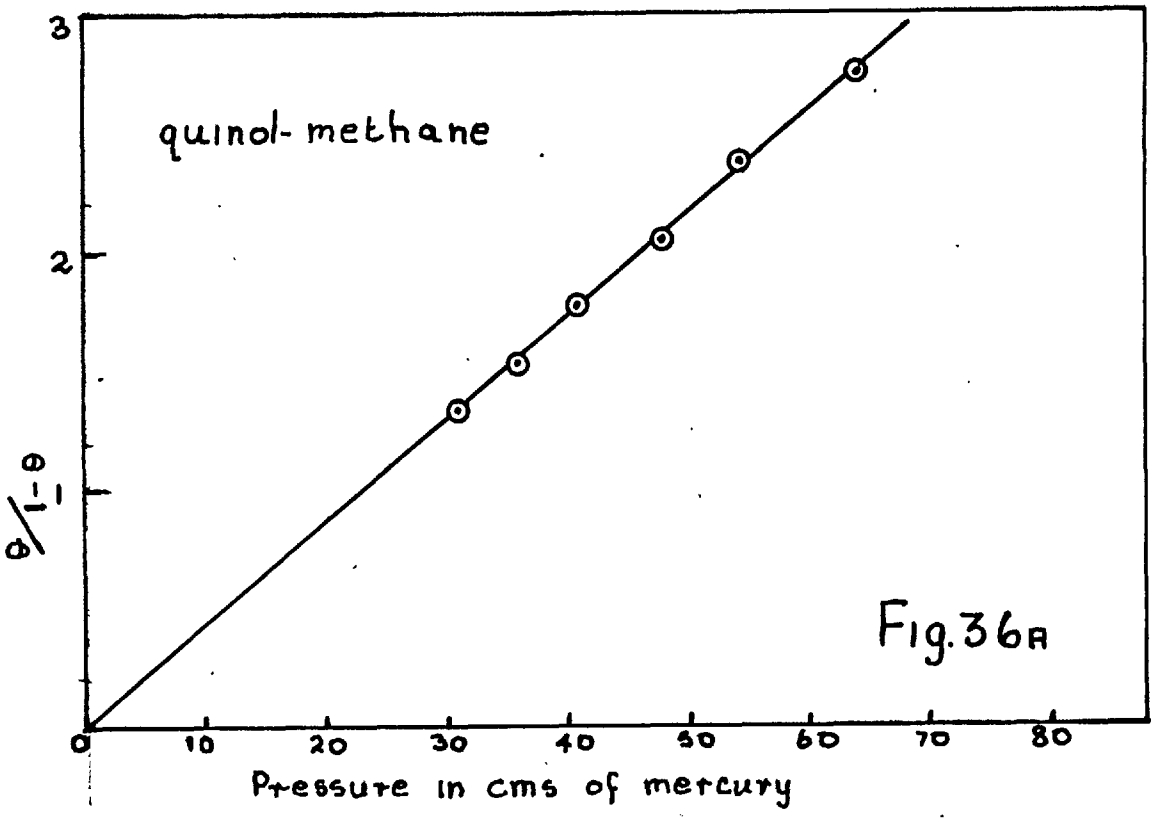

Fig. 36A

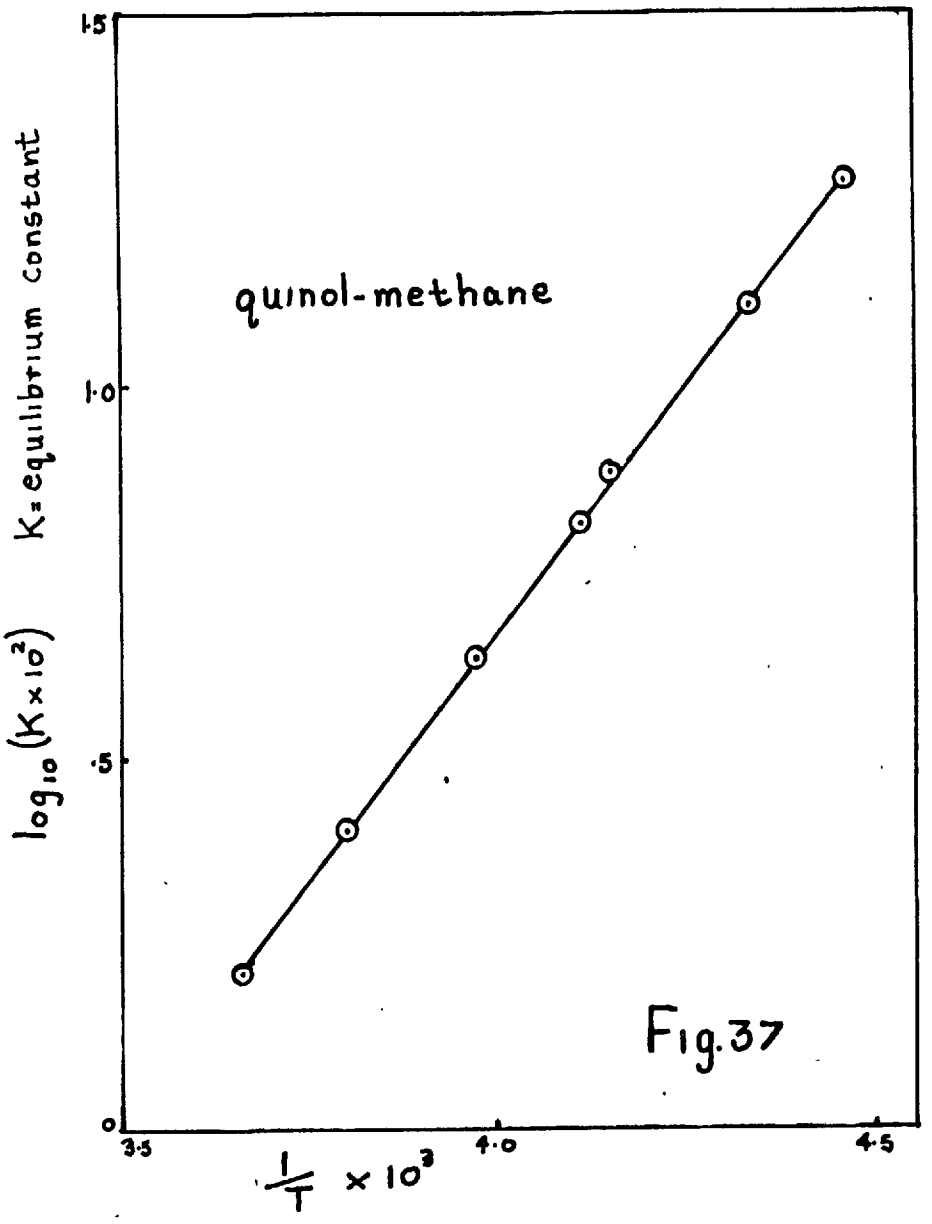
quinol-methane
$\log_{10}(K \times 10^2)$ K = equilibrium constant
1·5
1·0
·5
0
3·5
4·0
4·5
$\frac{1}{T} \times 10^3$

Fig. 37

Table IV

KRYPTON					
T=0°C.		T=-12.3°C.		T=-29.5°C.	
P	V	P	V	P	V
19.6	36.0	20.2	42.4	13.6	48.8
25.0	38.3	28.0	48.0	22.5	54.8
29.2	40.8	34.7	50.5	31.2	57.6
33.2	43.0	43.7	52.8	40.0	59.5
40.0	45.0	51.0	55.0	49.1	60.5
43.3	46.2			61.1	62.0
48.0	47.8				
57.0	50.0				
V_m= 67.4		V_m= 67.2		V_m= 67.5	
$K=5.13\times10^{-2}$		$K=8.5\times10^{-2}$		$K=2.0\times10^{-1}$	
T = -6.7°C $K = 6.5 \times 10^{-2}$				T = -20.2°C. $K = 1.26 \times 10^{-1}$	
ΔH_2= -6.0$_3$ K cals./mole.					

METHANE			
T=-20.5°C.			
P	V	T°C.	$K\times10^2$
31.0	38.8	0	1.62
36.0	40.9	-10	2.5^1
40.8	43.5	-30.2	6.45
47.6	45.7	-33.0	7.57
54.0	47.9	-43,7	12.6
61.0	50.0	-49.2	13.6
V_m	68		
$K = 4.26\times10^2$			
ΔH_2= -6.1 K cals./mole.			

XENON			
T=0°C.		T=10.6°C.	
P	V	P	V
5.5	47.8	13.6	52
8.4	53.6	15.6	54.1
10.1	55.7	19.3	57.1
11.9	57.0	22.9	59.0
13.8	58.6	25.0	59.9
15.6	60.3	26.9	60.8
17.5	61.0		
20.9	61.6		
V_m = 71		V_m = 73	
K = .35		K = .18	
T = 5.3°C.			
K = .242			
ΔH_2 = -9.8 K cals./mole.			

III.4 The Measurement of the Maximum Sorption of Gas by Phenol Crystals

The measurement of the maximum sorption of a gas by phenol crystals to form the phenol clathrate was made in a similar way to that already described for quinol.

For each gas the maximum sorption was measured at several different pressures at a particular temperature and the resultant isotherm plotted. A number of such isotherms were determined. Each point on an isotherm was found separately using a fresh sample of phenol. In order to check for hysteresis effects the reaction was allowed to proceed to completion at one point on an isotherm and the pressure was then lowered in a series of steps to just above the dissociation pressure. At each step shaking was continued until the new equilibrium had been established and no more gas would desorb. The isotherm found by this method was the same as that found by plotting the points found separately and for all the gases investigated there was no evidence of any hysteresis effect.

For the two gases krypton and methane, isotherms were obtained at -78°C. For the other gases the maximum sorption at -78°C. corresponded within experimental error, to the theoretical maximum sorption 79.34 mls. per gram of phenol at s.t.p., and suitable isotherms were obtained only at higher temperatures.

The gases krypton, xenon, methane, ethane, ethylene and carbon dioxide were investigated. Table IV lists the maximum sorption in mls. of gas per gram of phenol at s.t.p. at each pressure. Figs. 38-43 show plots of maximum sorption against pressure for each gas at each particular temperature. The dissociation pressures at each temperature have been included in the plots.

As may be seen, except for gases methane and krypton, the isotherms are very rectangular and the fractional occupancy of the cavities high.

Since the dissociation pressures are accurately known, extrapolation of the isotherms enables the fractional occupancy at the dissociation pressure to be found. This particular value of θ will be designated as $\theta_{crit.}$ As decribed in the discussion of the theory of the phenol clathrates, provided the structure is undistorted and guest-guest intermolecular interactions are small, then the phenol clathrates correspond approximately to a Langmuir model with two different sets of identical sorption sites. The large β -phenol cavity is considered as being composed of three identical smaller cavities and the small β -phenol cavity as a single cavity. If the fractional occupancy of each of the

three cavities making up the large β-phenol cavity is θ_1, and of the small β-phenol cavity is θ_2, then

$$\theta = \frac{\text{equilibrium amount of gas M sorbed}}{\text{theoretical maximum sorption of M}} = \frac{3}{4}\theta_1 + \frac{1}{4}\theta_2$$

If now K_1 is the Langmuir equilibrium constant for each site of the large cavity and K_2 is the Langmuir equilibrium constant for the small cavity and P is the pressure, then:

$$K_1 = \frac{1}{P}\,\frac{\theta_1}{1-\theta_1} \qquad \cdot \qquad K_2 = \frac{1}{P}\,\frac{\theta_2}{1-\theta_2}$$

and therefore

$$\theta = \frac{P}{4}\left[\frac{3K_1}{1+K_1P} + \frac{K_2}{1+K_2P}\right]$$

rearranging and letting $4\theta = C$

$$K_1(1-C) + K_2(3-C) + K_1K_2(4P-CP) = \frac{C}{P}$$

Since θ is known, an attempt may be made using the above equation to calculate K_1 and K_2 and hence θ_1 and θ_2 for each isotherm.

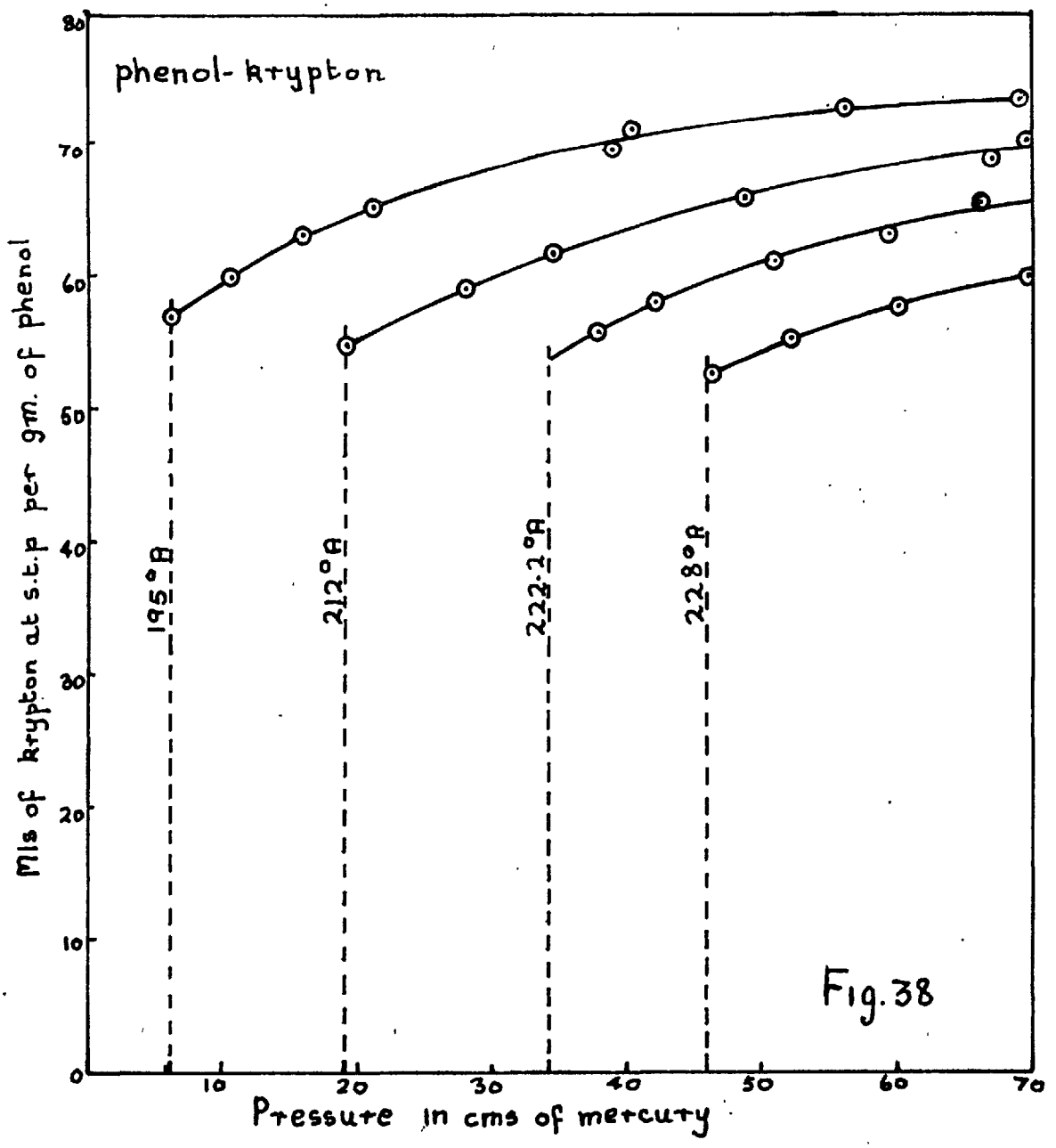
phenol-krypton
Mls of krypton at s.t.p per gm. of phenol
Pressure in cms of mercury
195°A
212°A
222·2°A
228°A
0
10
20
30
40
50
60
70
80

Fig. 38

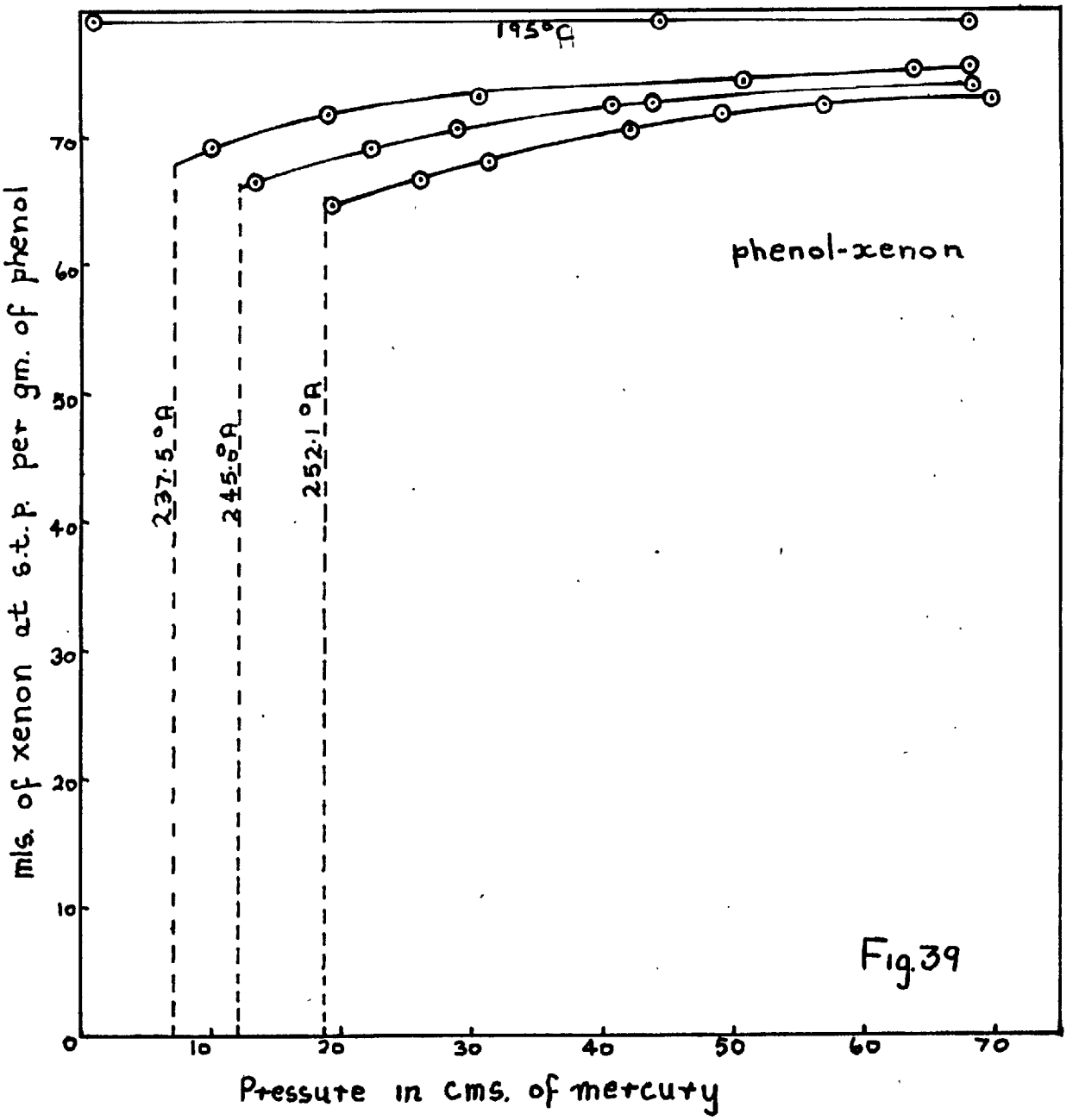
195°A
237.5°A
245.0°A
252.1°A
phenol-xenon
mls. of xenon at s.t.p. per gm. of phenol
Pressure in cms. of mercury
0
10
20
30
40
50
60
70

Fig. 39

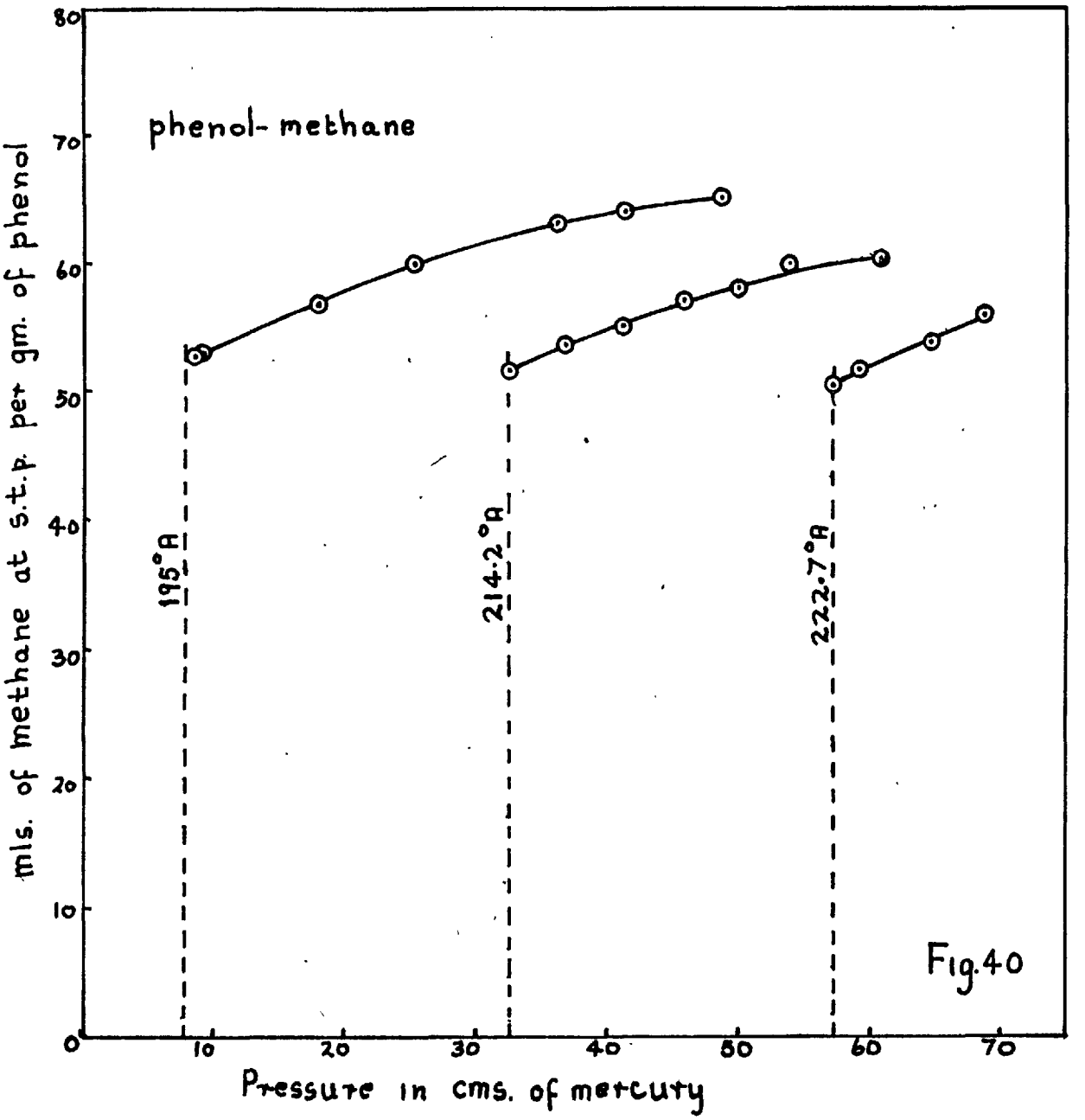
phenol-methane
mls. of methane at s.t.p. per gm. of phenol
Pressure in cms. of mercury
195°A
214.2°A
222.7°A
0
10
20
30
40
50
60
70
80

Fig.40

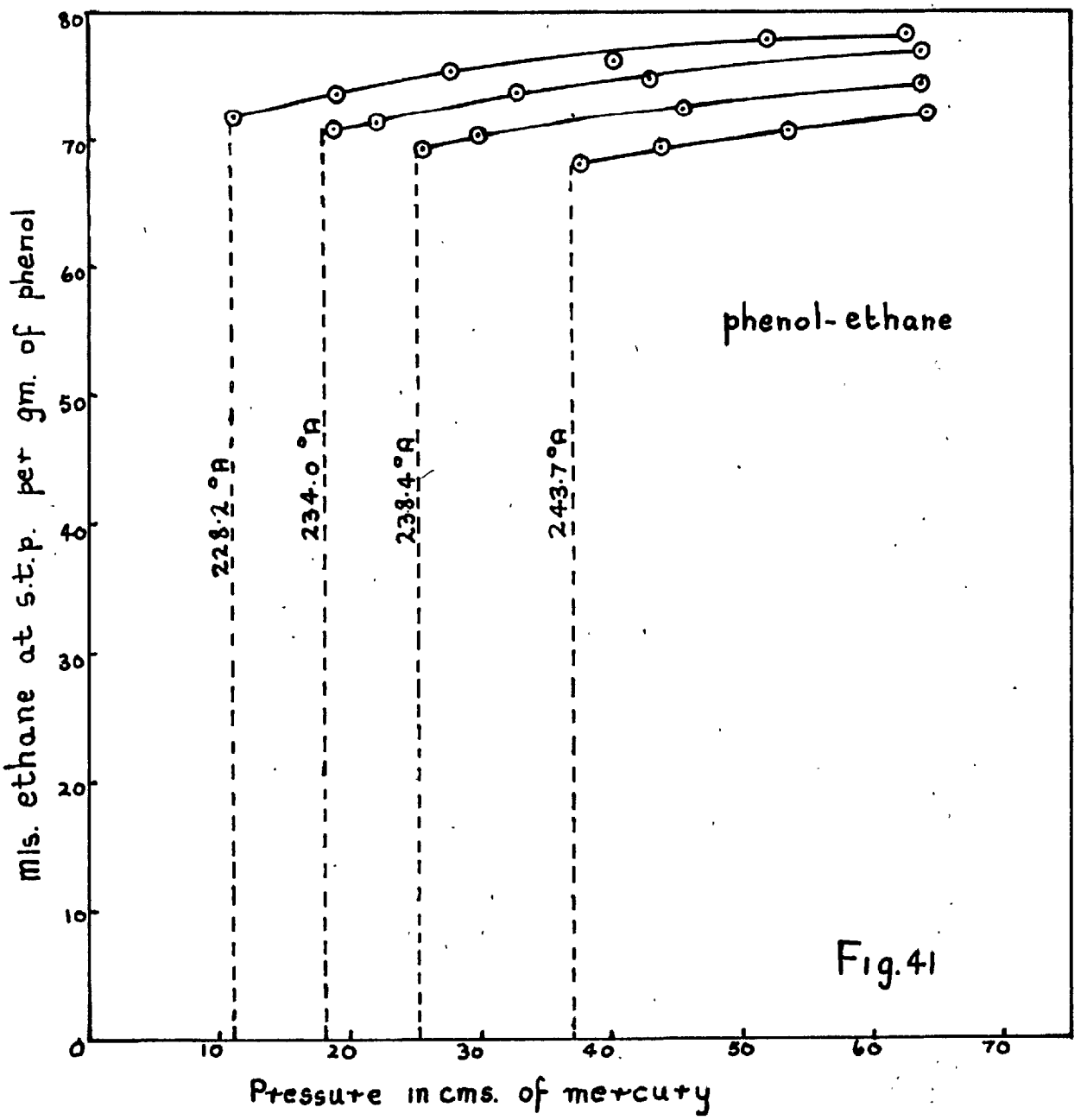
phenol-ethane
228·2 °A
234·0 °A
238·4 °A
243·7 °A
mls. ethane at s.t.p. per gm. of phenol
Pressure in cms. of mercury
0
10
20
30
40
50
60
70
80

Fig. 41

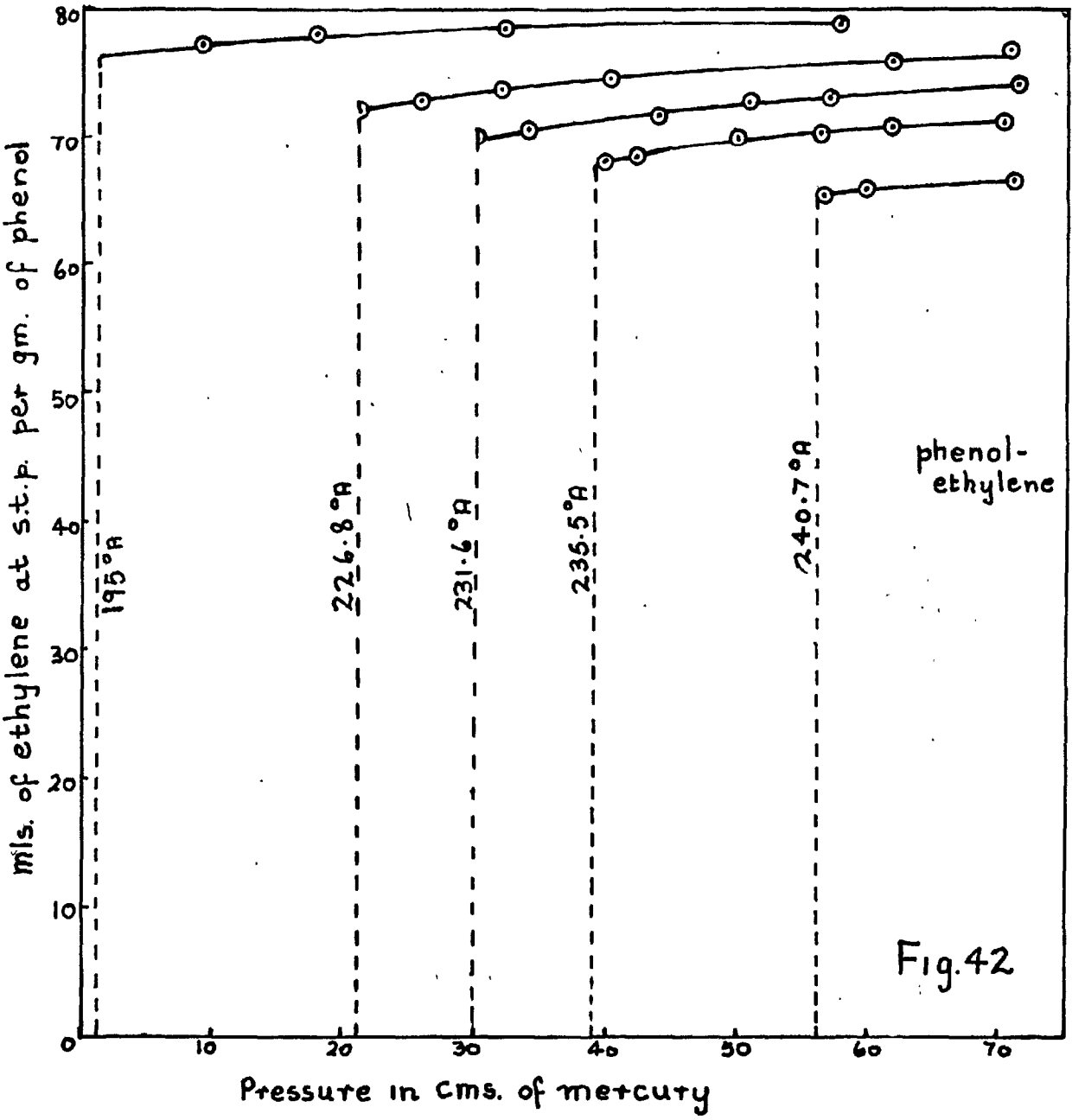
mls. of ethylene at s.t.p. per gm. of phenol
0
10
20
30
40
50
60
70
80
10
20
30
40
50
60
70
Pressure in cms. of mercury
195°A
226.8°A
231.6°A
235.5°A
240.7°A
phenol-
ethylene

Fig. 42

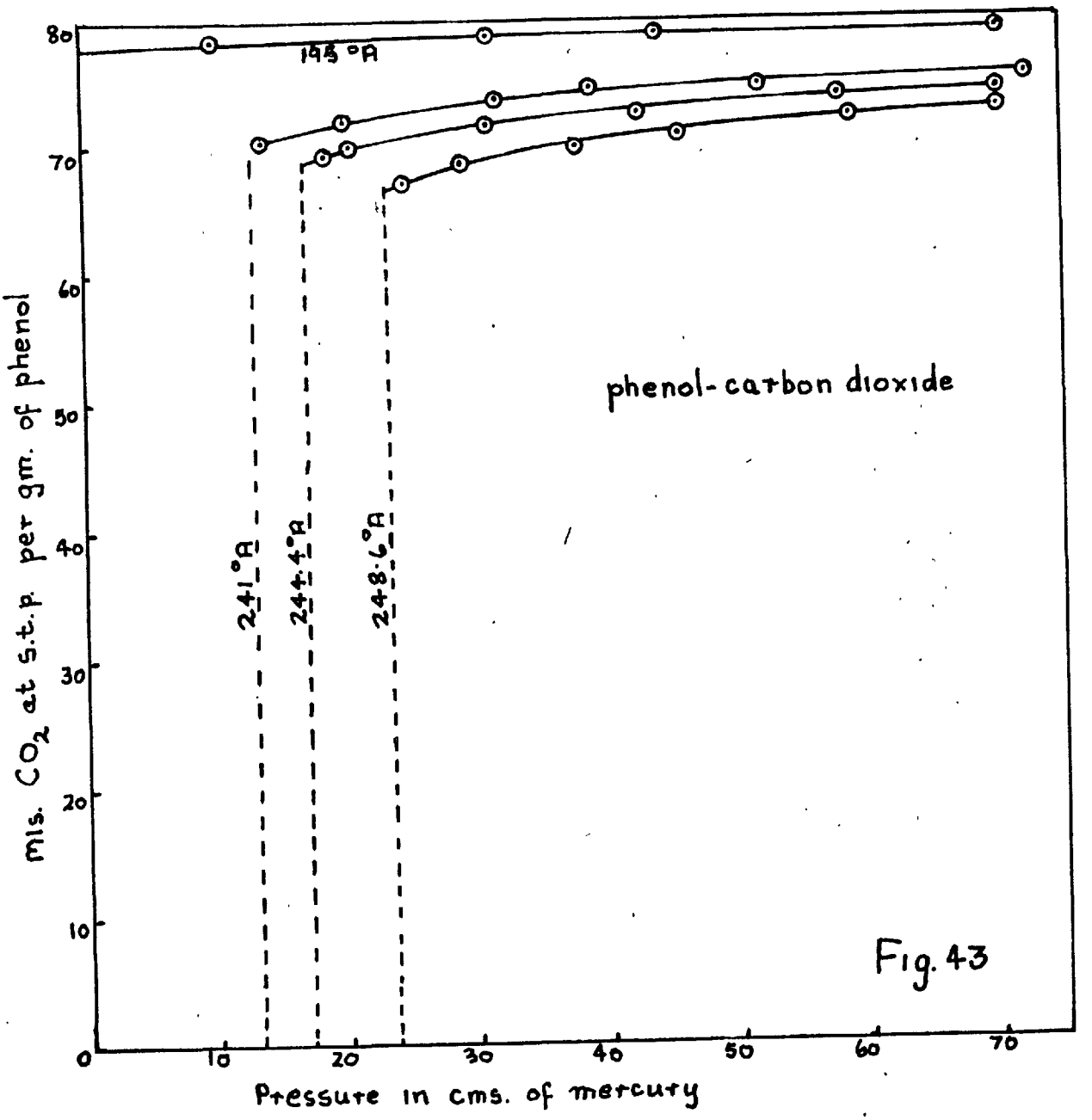
195 °A
241 °A
244.4 °A
248.6 °A
phenol-carbon dioxide
mls. CO_2 at s.t.p. per gm. of phenol
Pressure in cms. of mercury
0
10
20
30
40
50
60
70
80

Fig. 43

Also, if θ_1 and θ_2 are calculated at $\theta_{crit.}$ for each isotherm then $\left(\frac{d\theta_1}{dT}\right)_{crit.}$ and $\left(\frac{d\theta_2}{dT}\right)_{crit.}$ may be found. By substituting these values in equation (31) of page 41, i.e.

$$\Delta H_{\alpha\rightarrow\beta} = \frac{-RT^2}{m(n+1)} \left[\frac{n}{1-\theta_1} \frac{d\theta_1}{dT} + \frac{1}{1-\theta_2} \frac{d\theta_2}{dT} \right]$$

one should, in principle, be able to find a value of $\Delta H_{\alpha\rightarrow\beta}$, the heat difference between the α- and β-crystalline forms of phenol.

It was found, however, that values of K_1 and K_2 could be found only for the two krypton isotherms at -78°C. and -61°C. The equations in C_s, K_1 and K_2 for the other two isotherms were insoluble. In general for the gases with larger molecules and with even more rectangular isotherms, only for the isotherm at the lowest temperature when the range of pressure was greatest was it possible to obtain K_1 and K_2. This indicated that the experimental isotherm was considerably different from a theoretical isotherm fitting the equations above. Therefore $\Delta H_{\alpha\rightarrow\beta}$ cannot be found by the above method.

The difference was further shown if the following values of K_1 and K_2, for two isotherms for which the

equations in C, K_1 and K_2 were soluble, were used to calculate the isotherms, and these were compared with the experimental isotherm (Fig. 44).

	K_1	K_2
krypton (-78°C.)	0.048	1.08
ethane (-45°C.)	0.44	1.4

The experimental isotherm is considerably more rectangular than the calculated one.

Although the two curves can only be regarded as very approximate the above values of K_1 and K_2 were used to calculate the separate isotherms for sorption of gas in the large and small β -phenol cavities, Fig. 45. These indicate considerably greater fractional occupancy of the large cavity, the difference increasing as overall total sorption becomes smaller.

These results and the indication of high fractional occupancy of the large cavity suggest that considerable distortion of the host lattice and also guest-guest interaction takes place, especially by the larger guest molecules. This could account in part for the departure from the theoretical isotherm.

An estimate of the heat of intercalation, ΔH_2, of one mole. of gas by the phenol host lattice may, however, be made. It may be shown that at constant fractional occupancy θ, and for an ideal gas.

$$\left(\frac{\partial \ln P}{\partial T}\right)_{\theta} = \frac{-\Delta H_2}{RT^2}$$

If ΔH_2 may be treated as a constant over a difference in temperature, then

$$\Delta H_2 = 2.303\ R.\ \text{Log.}_{10}\ \frac{P_1}{P_2} \cdot \frac{T_1 T_2}{T_2 - T_1}$$

P_1 and P_2 are the pressures for constant θ on two isotherms at temperatures T_1 and T_2.

The rectangular shape of these isotherms and the small range in temperature covered by a considerable rise in dissociation pressure especially for the more condensable gases means that a small experimental error in the isotherm would give a fairly large error in the calculated result. Mean values of ΔH_2 at the dissociation pressure were, however, calculated and are given in Table V.

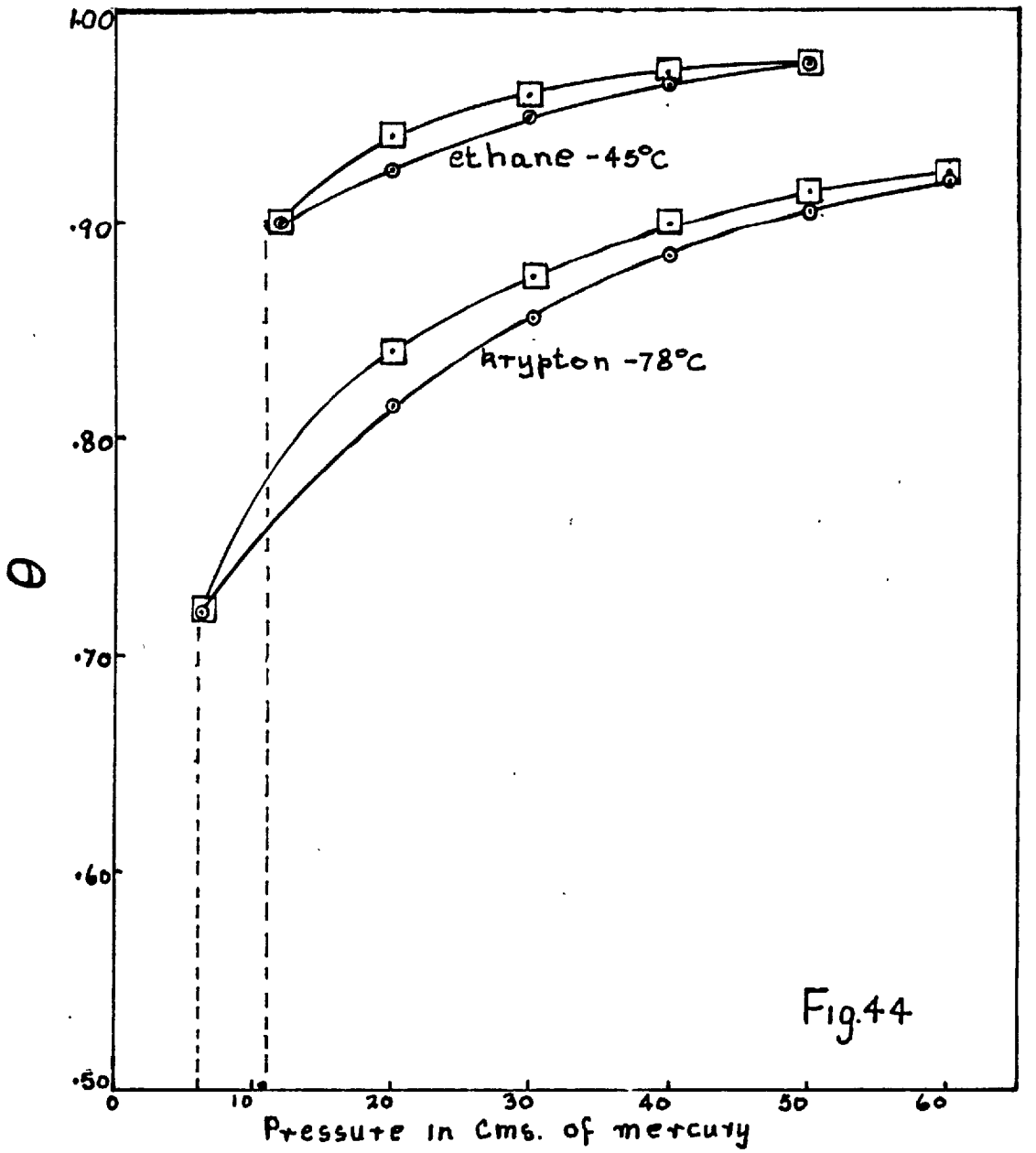
1·00
·90
·80
·70
·60
·50
θ
ethane -45°C
krypton -78°C
0
10
20
30
40
50
60
Pressure in Cms. of mercury
calculated points
expetimental points

Fig.44

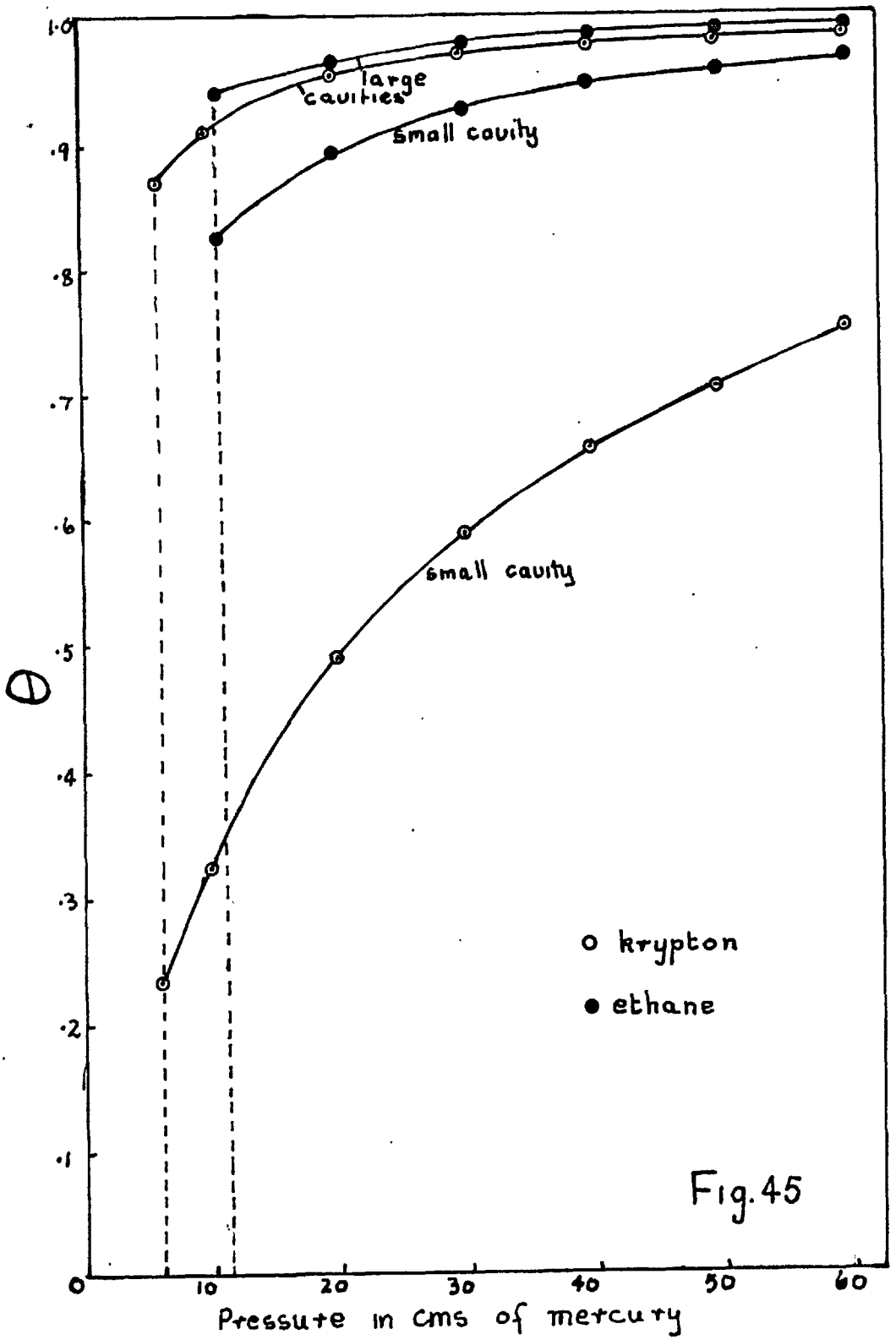
1·0
·9
·8
·7
·6
·5
·4
·3
·2
·1
0
θ
large cavities
small cavity
small cavity
o krypton
● ethane
10
20
30
40
50
60
Pressure in cms of mercury

Fig. 45

Table V

Gas	$-\Delta H_2$	Mean $\theta_{crit.}$	Temp.Range $^{o}A.$
krypton	5.9	0.70	195 - 228
xenon	10.6	0.83	237.5- 252.1
methane	6.5	0.65	195 - 222.7
ethane	11.4	0.88	228.2- 243.7
ethylene	14.5	0.89	226.8- 240.7
carbon dioxide	15.5	0.86	241 - 248.6

In general the range in temperature and change in $\theta_{crit.}$ with temperature is too small to enable the change in ΔH_2 with change in temperature to be determined with any accuracy and mean values of ΔH_2 have been found at a mean value of $\theta_{crit.}$.

A plot of these values of ΔH_2 against the maximum dimensions of the gas molecules is shown in Fig. 46. As predicted in the theoretical discussion on page 27, the value of ΔH_2 reaches a maximum and then falls off as the size of the molecule increases further.

In the discussion on page 23 it was shown that

$$\Delta G = \frac{n}{\theta_{crit.}} \Delta G_{\alpha \rightarrow \beta} + \Delta G_2$$

and similarly that

$$\Delta H = \frac{n}{\theta_{crit.}} \Delta H_{\alpha \rightarrow \beta} + \Delta H_2$$

or

$$(\Delta H - \Delta H_2) \frac{\theta_{crit.}}{n} = \Delta H_{\alpha \rightarrow \beta}$$

An estimate of $\Delta H_{\alpha \rightarrow \beta}$ may now be made using the above values of ΔH_2 and the values of ΔH calculated from the dissociation pressure data. These values are given in Table VI below.

Table VI

Gas	$\Delta H_{\alpha \rightarrow \beta}$ K cals./mole.
krypton	.14
xenon	0.80
methane	0.064
ethane	.88
ethylene	2.1
carbon dioxide	1.8

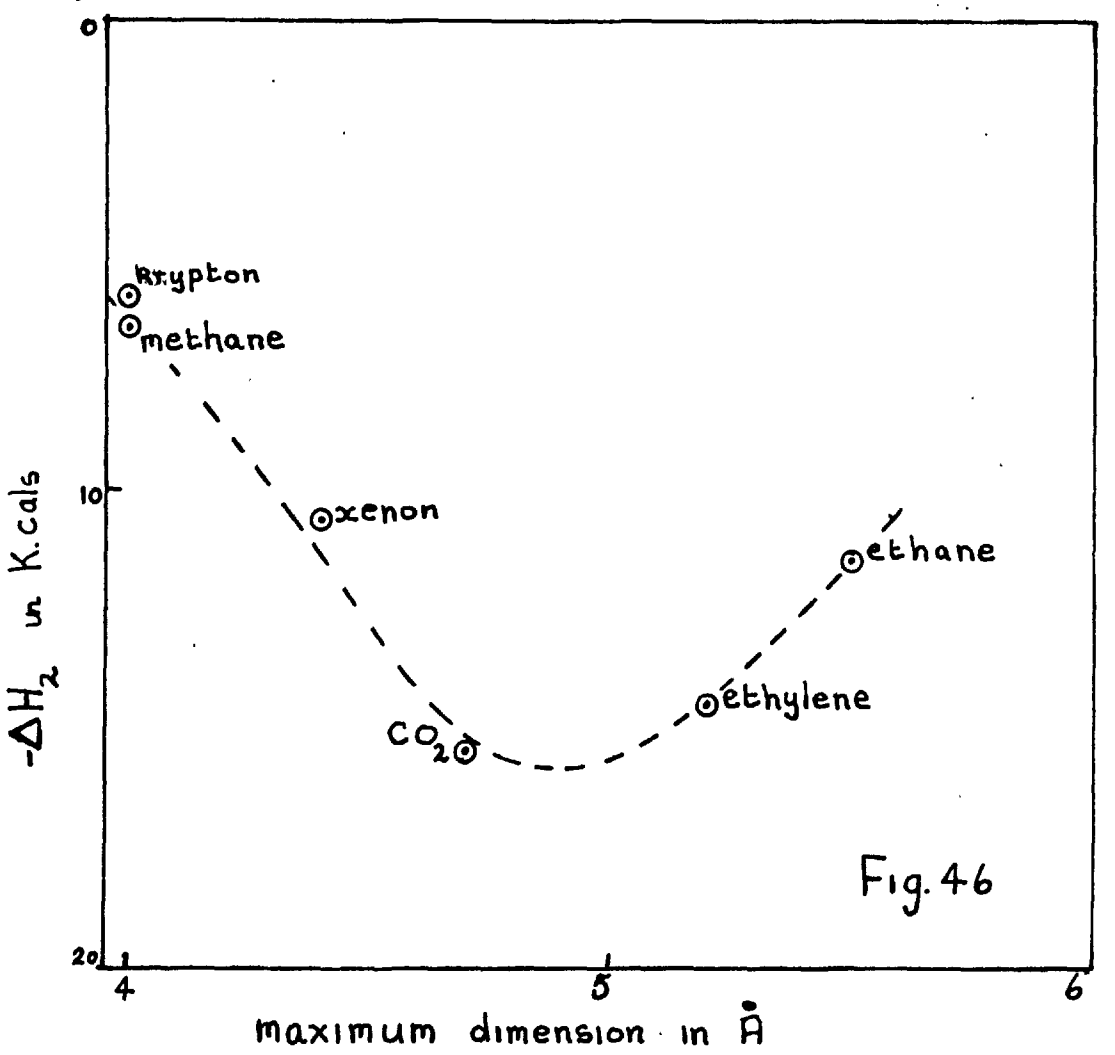
0
10
20
$-\Delta H_2$ in K.cals
Krypton
methane
xenon
CO_2
ethylene
ethane
4
5
6
maximum dimension in Å

Fig. 46

The value of $\Delta H_{\alpha \rightarrow \beta}$ is small as expected for the small guest species krypton and methane, but increases considerably as the size of the guest molecules and degree of occupancy of the cavities increases. This suggests that distortion of the host lattice may be considerable.

In previous calculations of ΔH from experimentally determined values of ΔH_2,[25] the value of $\Delta H_{\alpha \rightarrow \beta}$ has been taken as a constant irrespective of the size of the guest molecule. $\Delta H_{\alpha \rightarrow \beta}$ was taken as the value for the small guest species argon or krypton where no distortion of the lattice takes place. These results for phenol suggest that for the enclathration of larger guest molecules in phenol and probably quinol as well the value of $\Delta H_{\alpha \rightarrow \beta}$ may be significantly larger than the value for the small guest molecules, and ΔH correspondingly smaller than calculated.

The variation of ΔH_2 as the degree of filling of the host lattice cavities varies is shown in Figs. 47 and 48 for phenol-krypton and phenol-methane. For these isotherms the heat of enclathration of a mole of gas falls off as the fractional occupancy of the cavities rises. From the dissociation pressures it was found that

$\triangle H$ the heat of overall reaction does not vary over a considerable range in temperature including that covered by the isotherms. As already described $\triangle H$ is given by the equation

$$\triangle H = \frac{n}{\theta_{crit.}} \triangle H_{\alpha \rightarrow \beta} + \triangle H_2$$

The variation in $\theta_{crit.}$ for the gases krypton and methane over the range in temperature covered by the isotherms is small, and $\triangle H$ may therefore be expected to remain constant. For the other gases the change in $\theta_{crit.}$ is somewhat greater but as $\theta_{crit.}$ increases the numerical values of both $\triangle H_2$ and $\frac{n}{\theta} \triangle H_{\alpha \rightarrow \beta}$ decrease. Since $\triangle H_2$ has a negative value and $\triangle H_{\alpha \rightarrow \beta}$ a positive, this has a compensating effect which accounts for the reasonably constant value of $\triangle H$.

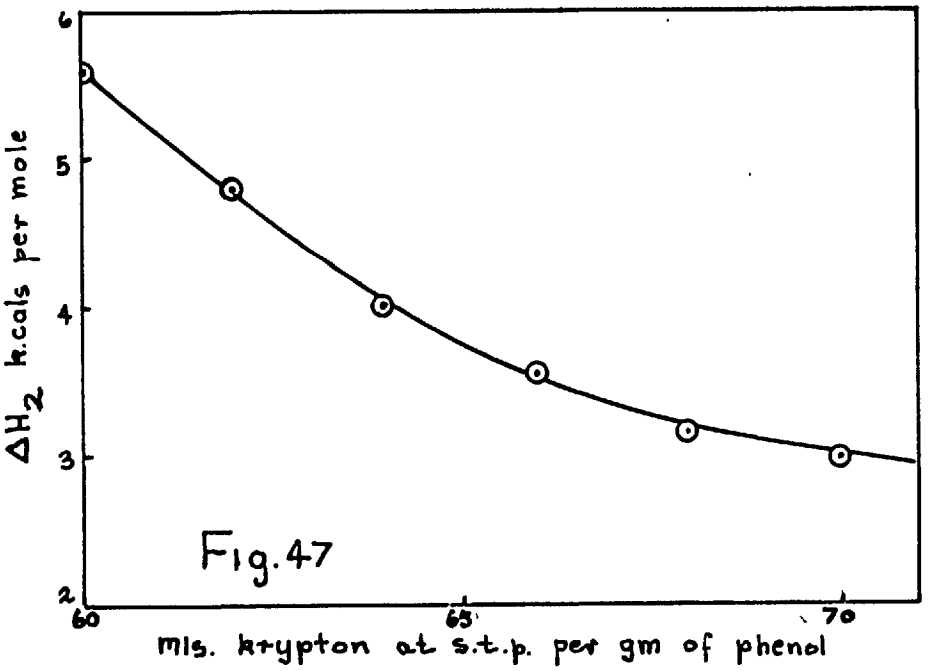
6
5
4
3
2
ΔH_2 k.cals per mole
60
65
70
mls. krypton at s.t.p. per gm of phenol

Fig. 47

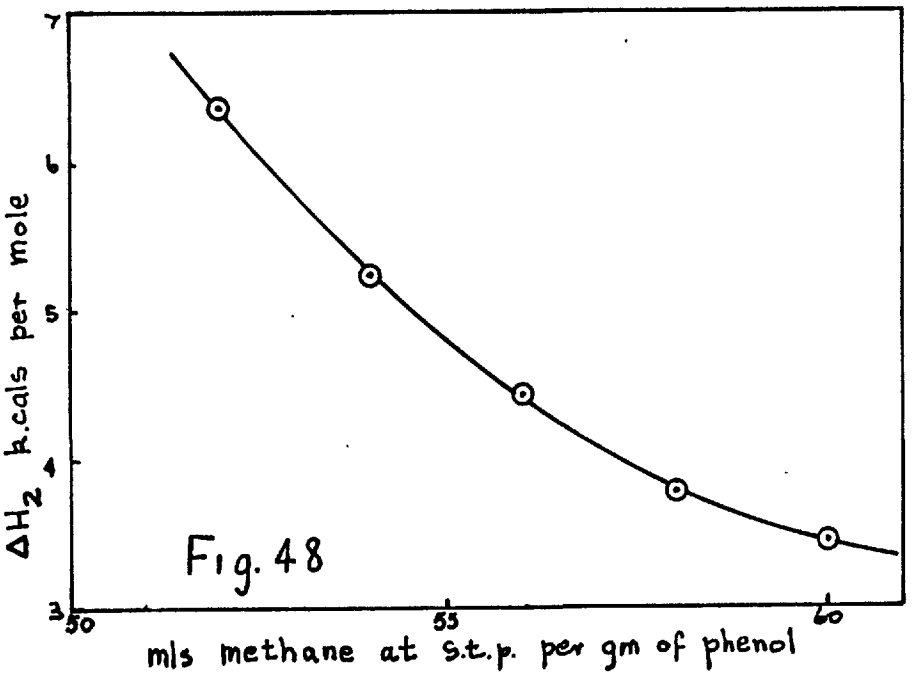
7
6
5
4
3
ΔH_2 k.cals per mole
50
55
60
mls methane at s.t.p. per gm of phenol

Fig. 48

Table IV

Krypton-Phenol

T = 195°A.		T = 212°A.		T = 222.2°A.	
P	V	P	V	P	V
6.0	57.0	19.3	54.8	38.0	55.6
10.5	60.0	28.0	59.0	42.0	58.0
15.8	63.0	34.5	61.6	51.0	61.0
21.1	65.1	48.6	65.8	60.2	63.0
38.8	69.5	67.0	68.7	66.3	65.3
40.3	71.0	69.6	70.3		
56.0	72.5				
69.5	73.6				

T = 228°A.	
P	V
46.3	52.6
52.2	55.2
60.1	57.5
69.7	60.0

Xenon-Phenol

T = 195°A	
P	V
All	79.3

T = 237.5°A	
10.0	69.0
19.0	71.6
30.5	73.0
51.0	74.4
64.5	75.1
68.0	75.4

T = 245°A.	
P	V
13.4	66.5
22.3	69.1
29.0	70.5
40.9	72.4
44.0	72.5
68.5	74.0

T = 252.1°A	
P	V
19.3	64.6
26.0	66.6
31.4	68.0
42.2	7o.4
49.2	71.7
57.0	72.0
70.0	72.8

Methane-Phenol

T = 195°A	
P	V
8.5	53.0
9.0	53.2
16.0	56.9
25.5	60.0
36.2	63.2
41.5	64.0
49.0	65.0

T = 214.2°A.	
P	V
32.5	51.7
37.0	53.7
41.1	55.1
46.0	57.0
50.0	58.0
54.0	60.0
61.0	60.3

T = 222.7°A.	
P	V
57.4	50.3
59.1	51.6
64.9	53.9
69.0	56.0

Ethane-Phenol

T = 22.82°A.		T = 234°A.		T = 238.4°A.	
P	V	P	V	P	V
11.1	71.6	18.8	70.7	25.6	69.1
19.0	73.5	22.0	71.2	30.0	7o.2
27.8	75.1	32.7	73.5	45.5	72.3
40.2	76.0	43.0	74.5	63.6	74.1
52.6	77.5	63.6	76.6		
62.5	78.0				

T = 243.7°A.	
P	V
37.5	68.0
43.9	69.0
53.6	70.5
64.0	71.9

Ethylene-Phenol

T = 195°A.		T = 226.8°A.		T = 231.6°A.	
P	V	P	V	P	V
9.0	79.2	21.0	72.0	30.0	69.8
18.0	78.3	26.0	72.7	34.0	70.5
32.2	78.0	32.0	73.5	43.9	71.5
58.0	77.0	40.3	74.5	51.1	72.6
		62.0	75.7	57.0	73.0
		70.8	76.7	71.4	74.0

T = 235.5°A.		T = 240.7°A.	
P	V	P	V
40.0	68.0	56.5	65.3
42.3	68.3	59.8	65.8
50.0	69.8	71.0	66.5
65.4	70.2		
61.7	70.6		
70.3	71.0		

Carbon dioxide-Phenol

T = 195°A.		T = 241°A.		T = 244.4°A.	
P	V	P	V	P	V
10.2	78.4	14.0	70.2	18.6	69.1
31.4	78.6	20.2	72.0	20.6	69.9
44.5	78.9	32.0	73.5	31.1	71.6
70.5	79.0	39.1	74.5	42.8	72.5
		52.0	74.6	58.1	73.7
		72.5	75.2	70.3	74.1

T = 248.6°A.	
P	V
24.8	67.0
29.0	68.5
38.0	69.8
41.0	70.7
59.0	72.2
70.4	72.6

III.5. Kinetic Measurements of the Formation of the Quinol and Phenol Clathrates

Two curves for the formation of a quinol and a phenol clathrate, showing the uptake of gas in mls. per gram at s.t.p. against time, were shown in Figs. 11 and 12. Shaking was continuous and time was measured from the moment of admission of gas into the reaction vessel. In the measurement of the equilibrium uptake of gas for a particular clathrate, and from such values the construction of isotherms, it was found that the kinetics of clathrate formation were of a similar type for all the gas investigated.

A number of kinetic measurements for the formation of quinol clathrates are shown in Fig. 49. In all cases the main reaction is preceded by a small preliminary uptake which, as previously described, may be clathration of the gas in the α-quinol lattice. This preliminary uptake begins immediately gas is admitted to the shaken sample and rapidly reaches a maximum value. This is followed some time later by the second reaction and much larger uptake of gas. As the pressure increases, however, this initiation time or induction period becomes shorter and the second step may begin before the first plateau has been reached.

A number of kinetic measurements for the phenol clathrates are shown in Fig. 50. In all cases following an initiation-lime of variable length there is a single-step uptake of gas which is generally considerably faster than the quinol clathrate reaction.

It was considered of interest to examine in more detail the two aspects of these kinetics, firstly the initiation time denoted by the symbol τ, and secondly the rate of sorption of gas. By finding the way in which τ and the kinetics varied with temperature and pressure, one may hope to obtain a more complete understanding of the mechanism of these reactions.

III.5.1 The Initiation Time, τ

A number of experiments were undertaken in which the initiation time τ was measured over a range in pressure for the formation of a particular clathrate species. The temperature was kept constant for each set of P, τ measurements. The initiation time for the phenol clathrates may be found very accurately as the uptake of gas starts very sharply and rapidly. In the quinol clathrate reactions the start of the second step cannot be as sharply determined because of the presence of the small preliminary uptake and accordingly only a

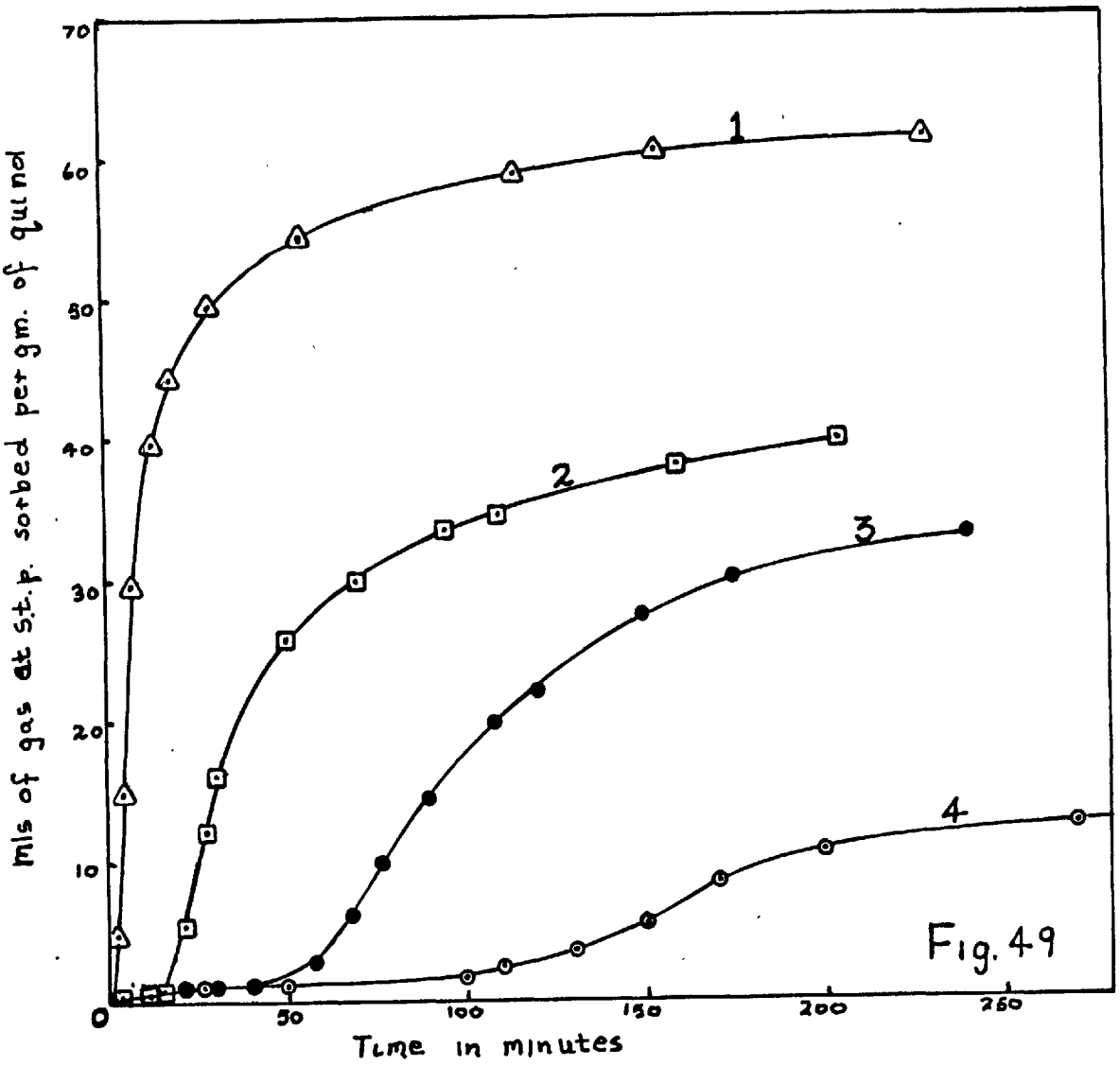

Fig. 49

1 xenon 58 cms of Hg. -6°C. 3 methane 44 cms Hg 0°C

2 krypton 62.8 " " " 0°C. 4 krypton 16 " " 0°C

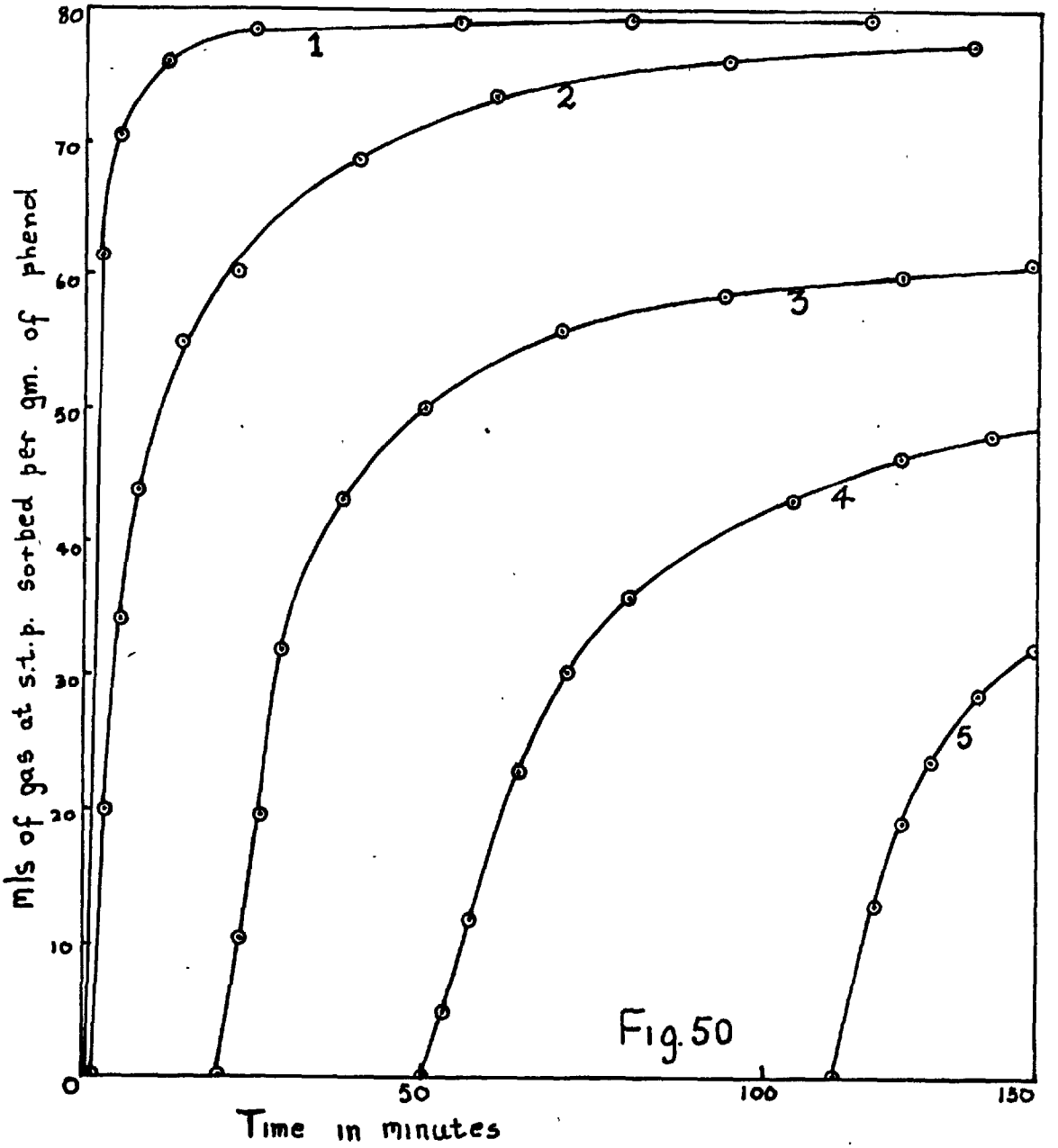

Fig. 50

1 CO_2 70·4 cms Hg, -48·7 °C.
2 xenon 67·7 " " -78 " .
3 methane 67·3 " " -78 " .
4 methane 65 cm Hg -62·5 °C
5 Krypton 9·2 " " -20 °C

best estimate could be made. In Figs. 51 and 52 are shown plots of τ against P for the two systems phenol-carbon dioxide and quinol-xenon. The dissociation pressure of the phenol-carbon dioxide clathrate at the experimental temperature has been included in the plot. The shape of the curve suggested that a relationship of the type $P_e \tau^n = k$, where P_e is the excess pressure given by

P_e = P (overall) - D.P.(dissociation pressure)

and n and k are constants, might describe the variation of τ with pressure.

If $P_e \tau^n = k$, then $\text{Log.}_{10} P_e = -n \text{ Log.}_{10} \tau + \text{Log.}_{10} k$. and a plot of $\text{Log.}_{10} P_e$ against $\text{Log.}_{10} \tau$ is a straight-line plot of slope n.

Fig. 53 and 54 show plots of $\text{Log.}_{10} P_e$ against $\text{Log.}_{10} \tau$ for the phenol-carbon dioxide curve and for two other phenol clathrates, phenol-xenon and phenol-krypton. These plots are good approximations to a straight line showing the validity of the relationship $P_e \tau^n = k$. From the slope of the plots the value of n was obtained.

The dissociation pressures of the quinol clathrates are not known with sufficient accuracy to enable P_e to be found and plots as above made. However, by plotting

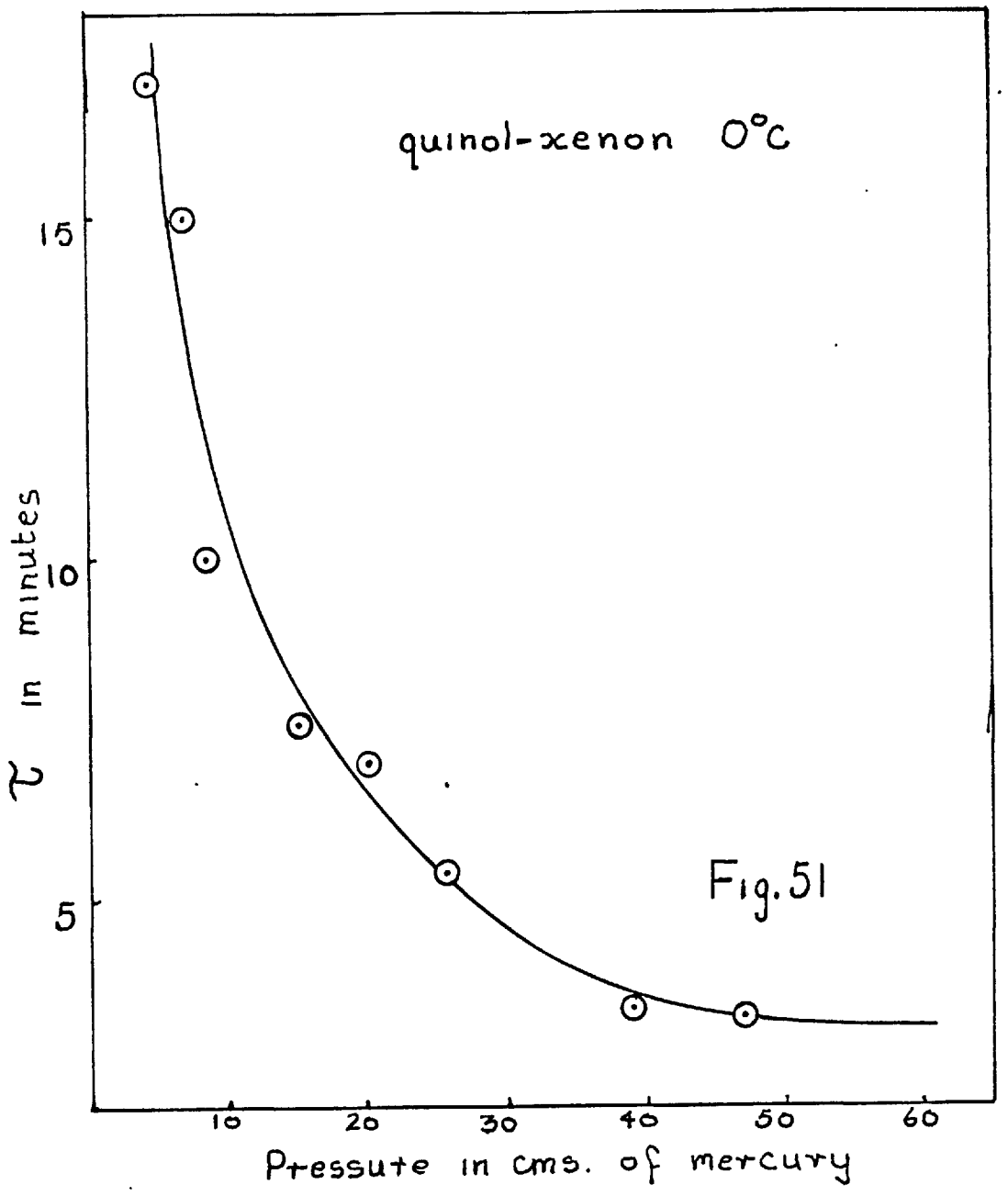
quinol-xenon 0°C
15
10
5
τ in minutes
10
20
30
40
50
60
Pressute in cms. of mercury

Fig. 51

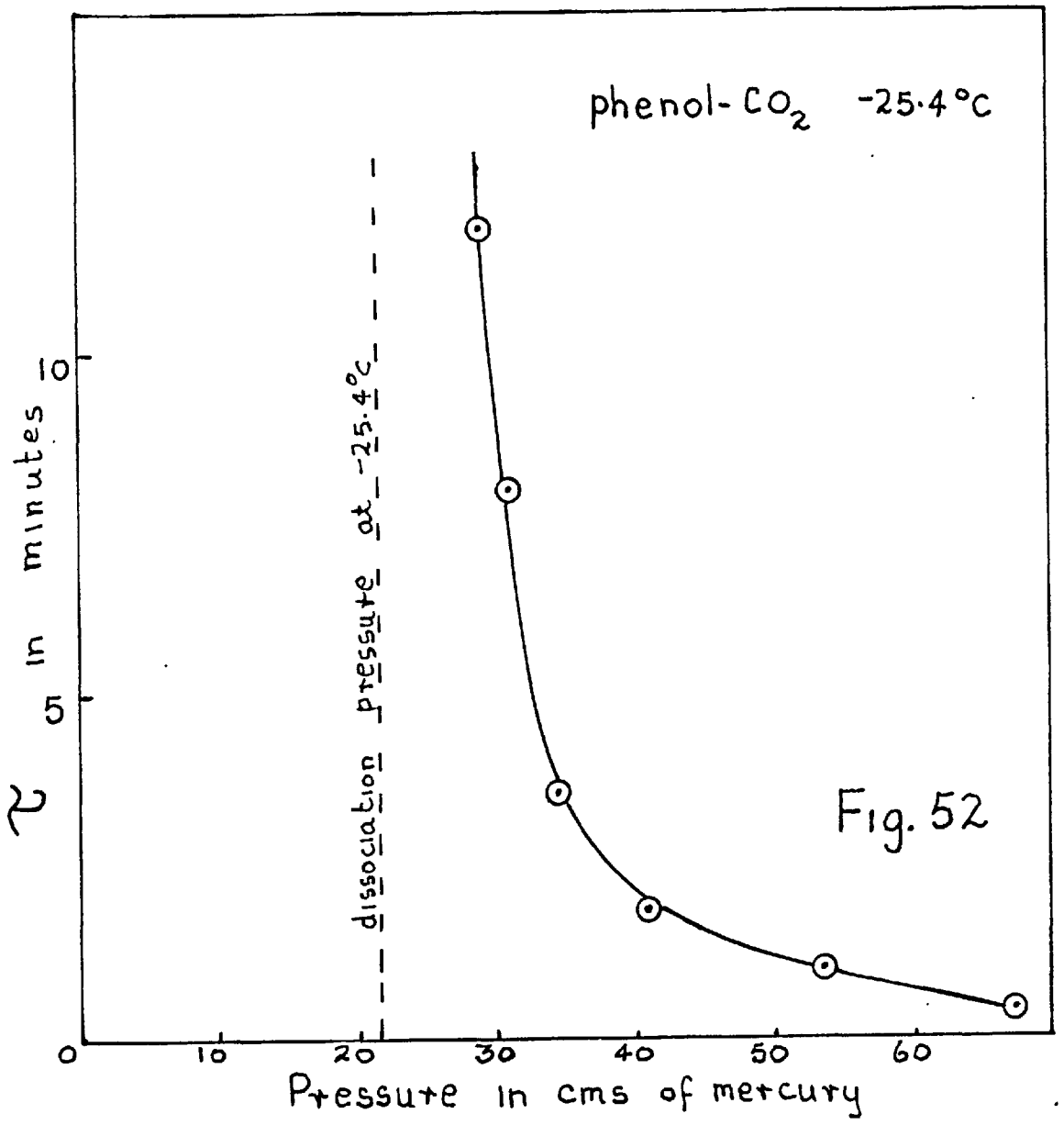
phenol-CO_2 -25·4°C
dissociation pressure at -25·4°C
τ in minutes
0
5
10
0
10
20
30
40
50
60
Pressure in cms of mercury

Fig. 52

the overall pressure P against $\frac{1}{\tau^n}$ for various values of n until the best straight line is obtained, an estimate of the value of n may be made. Figs. 55 and 56 show such plots for quinol-xenon and quinol-krypton. The experimental results for the quinol clathrates show considerably more scatter than those for phenol.

The values of n for the different systems are

	n
phenol-krypton	1.1
phenol-xenon	0.78
phenol-carbon dioxide	0.58
quinol-xenon	1.5
quinol-krypton	1.5

Keeping the excess pressure P_e constant τ was found at a number of points over a range in temperature. This was done for a number of phenol clathrates but for only one quinol clathrate, the quinol-xenon system. Since the dissociation pressure for xenon-quinol is about 2 cms. of mercury at 0°C. then for temperatures below 0°C. it is a reasonable approximation to say P_e = P (overall) if P (overall) is high. In this case the overall pressure for quinol-xenon was kept constant at 54 cms. of mercury. Figs. 57 and 58 show the values of τ found at various temperatures plotted

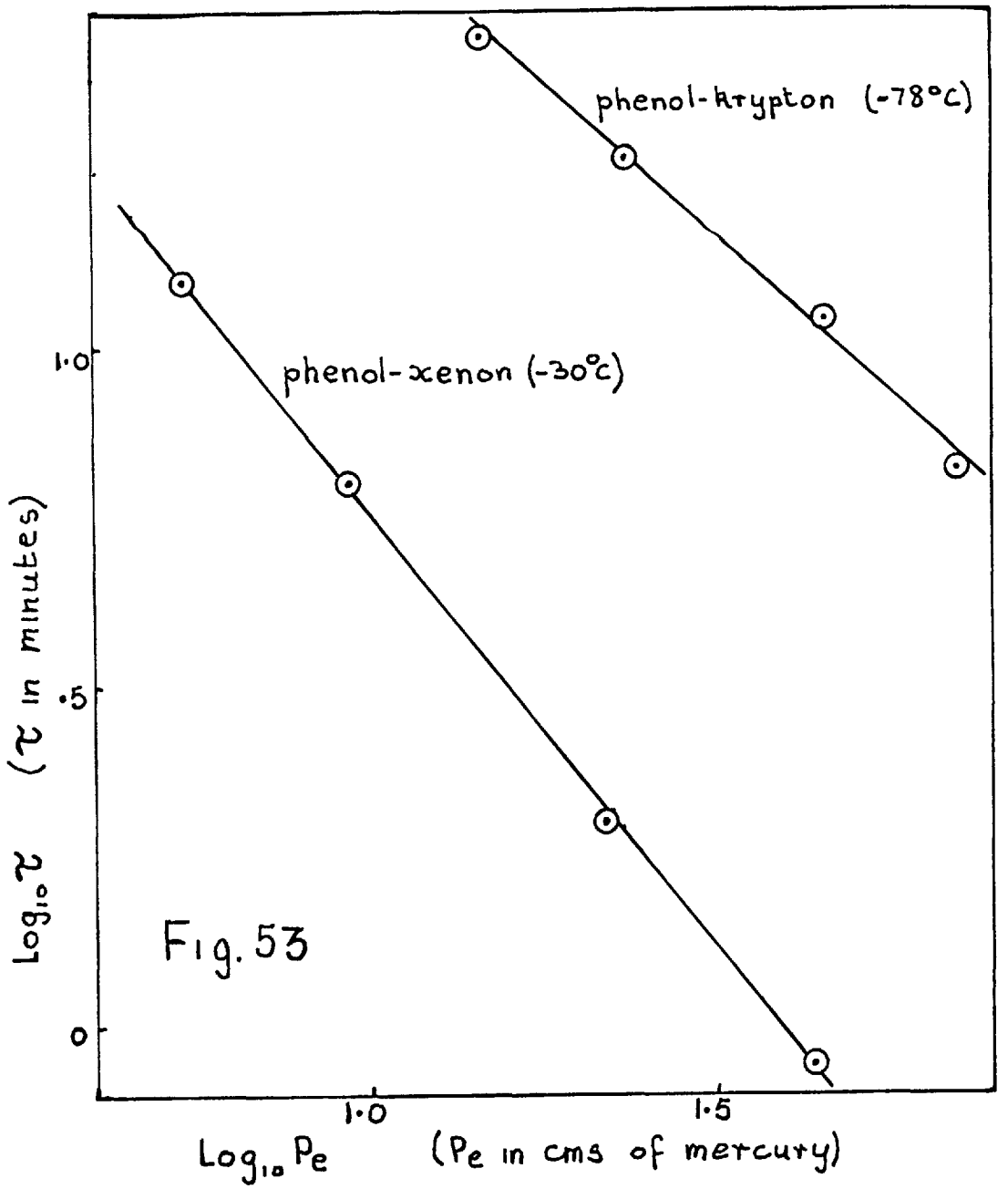
phenol-krypton (-78°C)
phenol-xenon (-30°C)
1·0
·5
0
1·0
1·5
$\log_{10}\tau$ (τ in minutes)
$\log_{10} P_e$ (P_e in cms of mercury)

Fig. 53

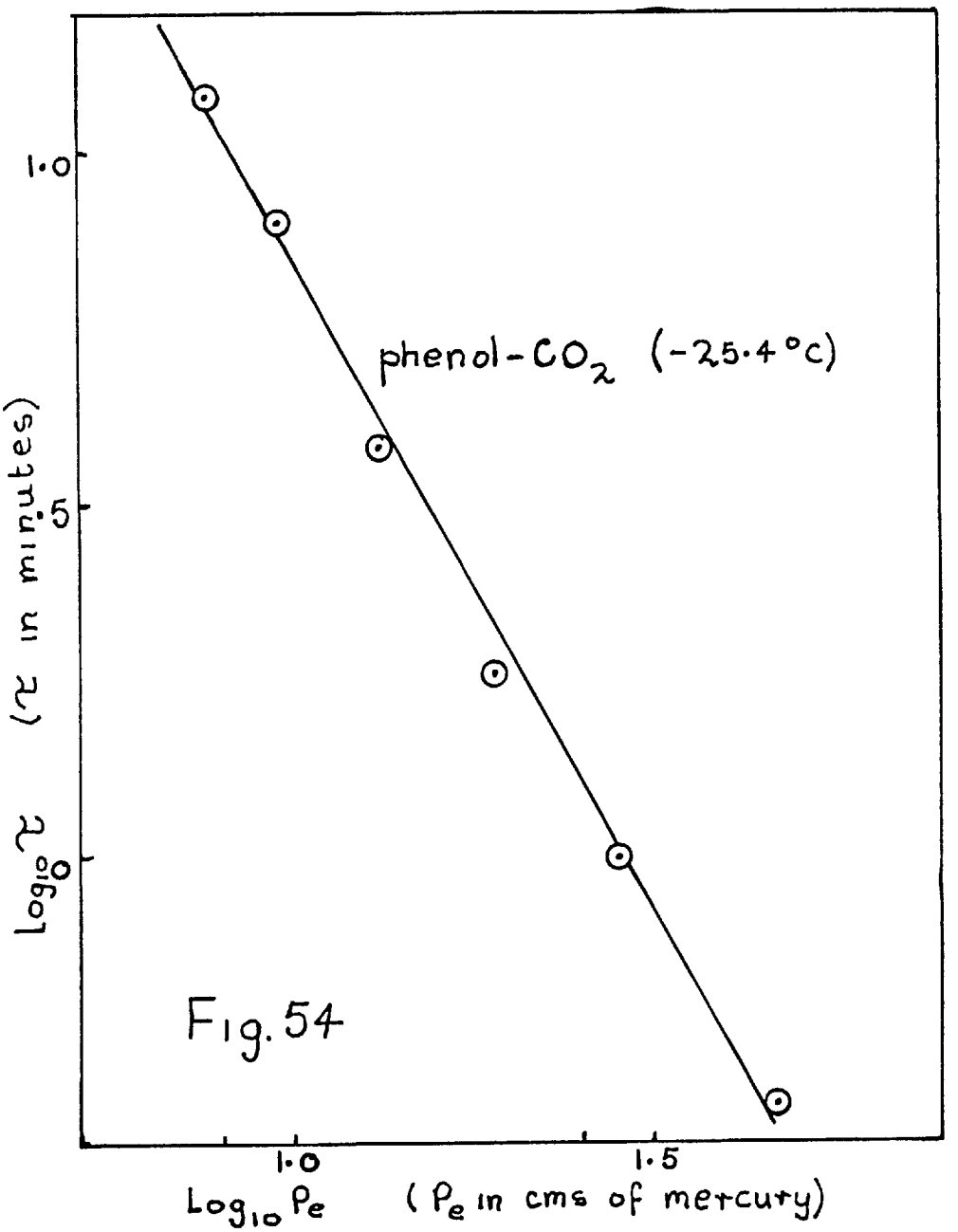
phenol-CO_2 (-25.4°C)
1.0
.5
$\log_{10}\tau$ (τ in minutes)
1.0
1.5
$\log_{10} P_e$ (P_e in cms of mercury)

Fig. 54

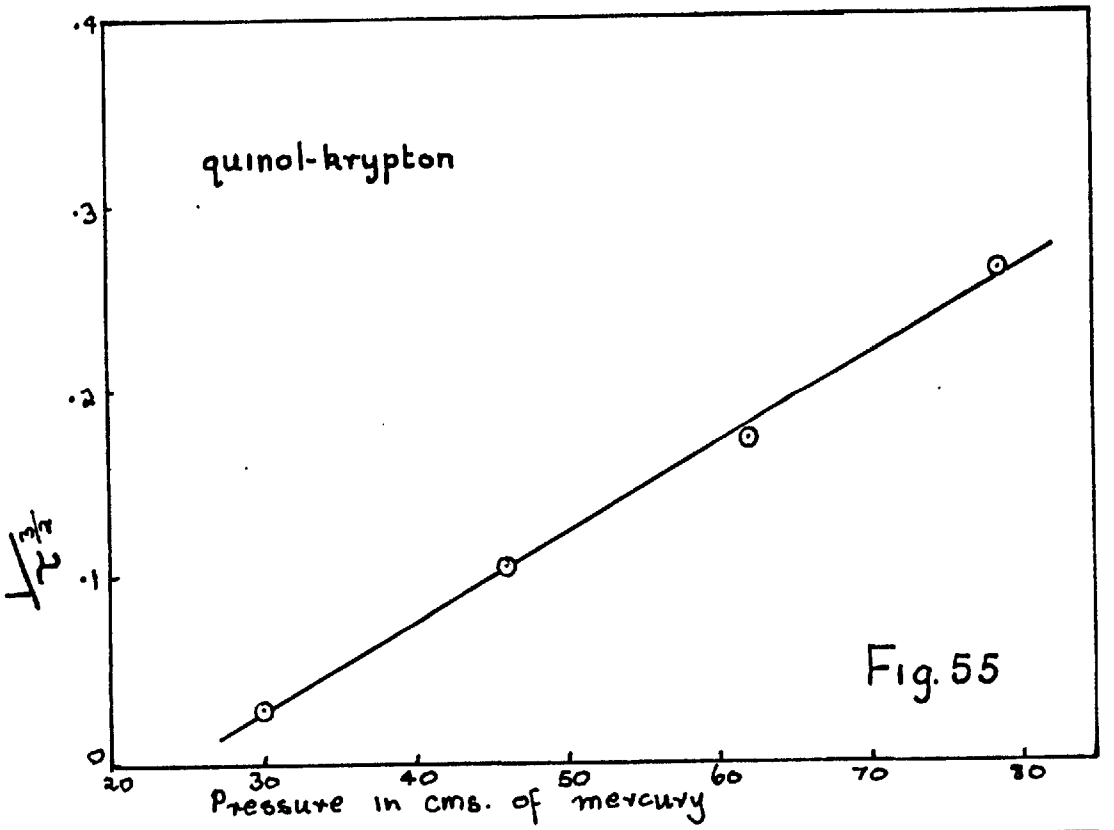
quinol-krypton
$\frac{1}{T^{3/2}}$
·4
·3
·2
·1
0
20
30
40
50
60
70
80
Pressure in cms. of mercury

Fig. 55

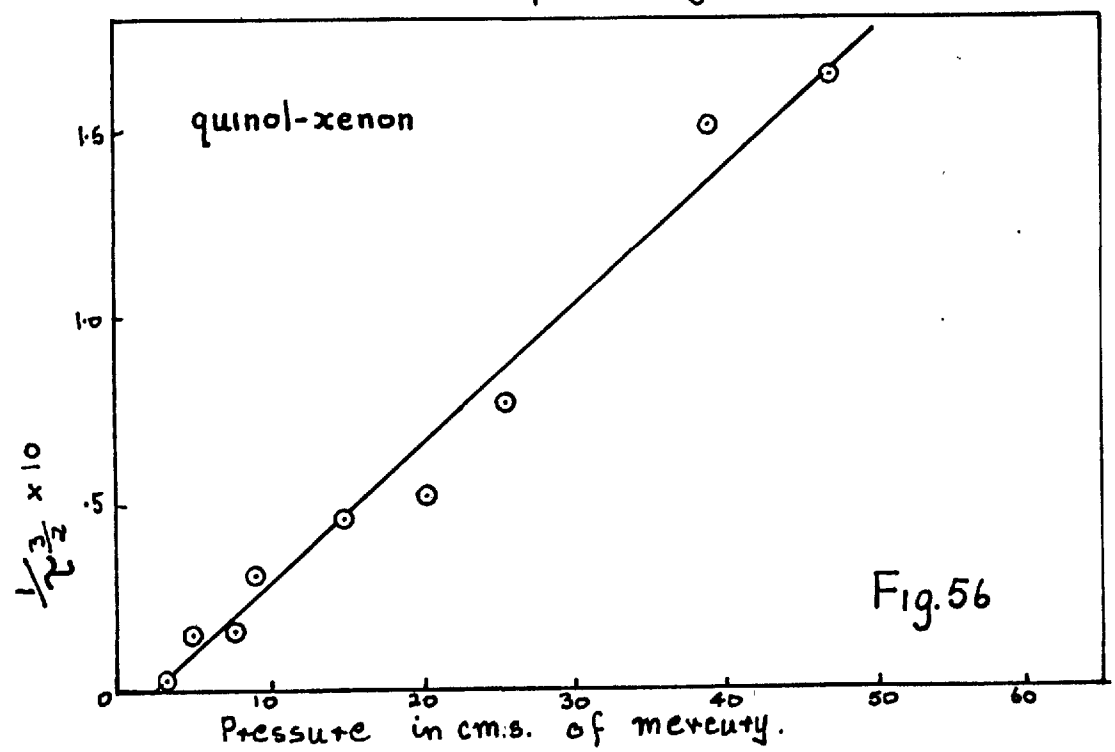
quinol-xenon
$\frac{1}{T^{3/2}} \times 10$
1·5
1·0
·5
0
10
20
30
40
50
60
Pressure in cms. of mercury.

Fig. 56

against temperature. In all cases it may be seen that allowing for slight experimental scatter τ remains constant over a wide range of temperature. n and k are therefore constants for all temperatures at which the clathrate was found.

When a new phase B forms at points in a lattice of A, ΔG_i, the free energy change accompanying the formation of an embryo of B containing i molecules, may be shown to pass through a maximum as i increases.[24] For small embryos where the value of i is less than i at ΔG_i(maximum) the embryo is unstable with respect to the transformation A $\longrightarrow$ B, when i is greater than i at ΔG_i(maximum) the embryo grows with a decrease in free energy and the increase in amount of the new phase B occurs rapidly.

τ may be considered as a measure of time taken for the embryos of clathrate phase to reach the critical size at which ΔG_i is a maximum, after which the detectable uptake of gas begins. The variation of τ with pressure may have two possible explanations. As the pressure increases the rate of growth up to the critical size may be

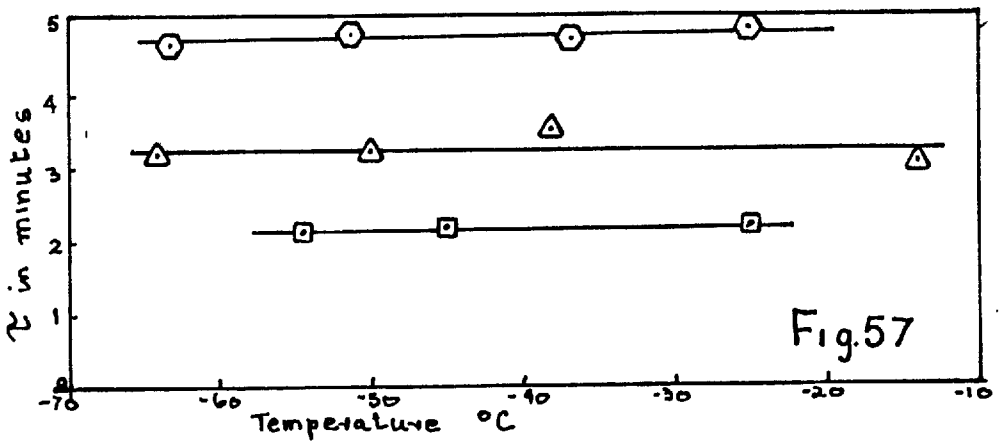

△ phenol-xenon P_e = 10cms. of mercury

□ phenol-xenon P_e = 18 cms. of mercury

○ phenol-CO_2 P_e = 12 cms. of mercury

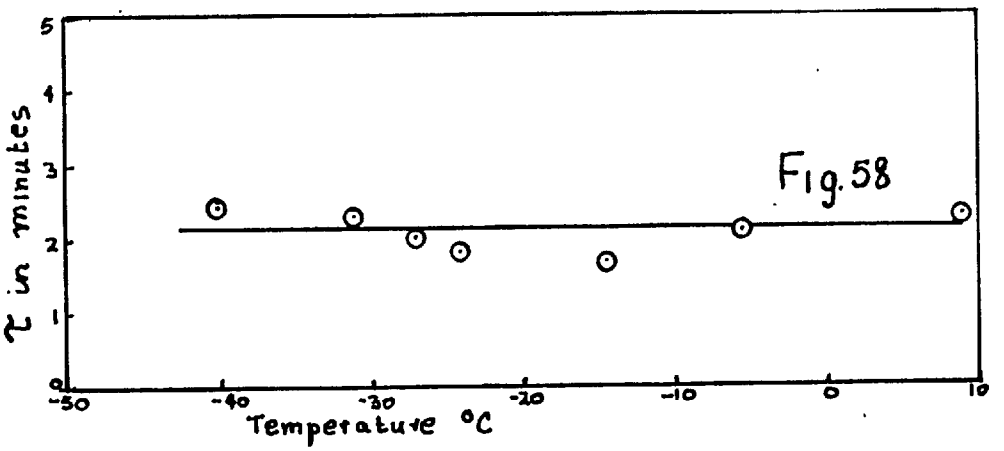

○ quinol-xenon P = 54 cms. of mercury

increased, or the number of molecules constituting the critical size may be reduced and thus a shorter time be required to reach it.

III.5.2 The Rate of Formation of the Clathrate

In observing the rate of the reaction the quantity experimentally determined is V_t, the number of mls. of gas at s.t.p. sorbed per gram of host material at time t. At the end point all the α -phase has been converted to the clathrate β -phase. If V_m is defined as the value of V_t at equilibrium, and V_s as the theoretical maximum sorption, i.e. when all the cavities are occupied by guest molecules then as before $\theta = \frac{V_m}{V_s}$ is the fractional occupancy of the β -lattice at equilibrium. At time t the fraction of β -phase and hence of clathrate formed is given by $\frac{V_t}{V_m}$ which will be designated by ϕ_t.

A number of kinetic runs were made over a range in temperature for the two systems quinol-xenon and phenol-xenon. The overall pressure was kept constant for each system. The results were plotted in the form $\frac{t^1}{V_t}$ against t^1, where $t^1 = t - \tau$, as shown in Figs. 59 and 60.

The plot may be divided into two parts, each approximating reasonably well to a straight line. The

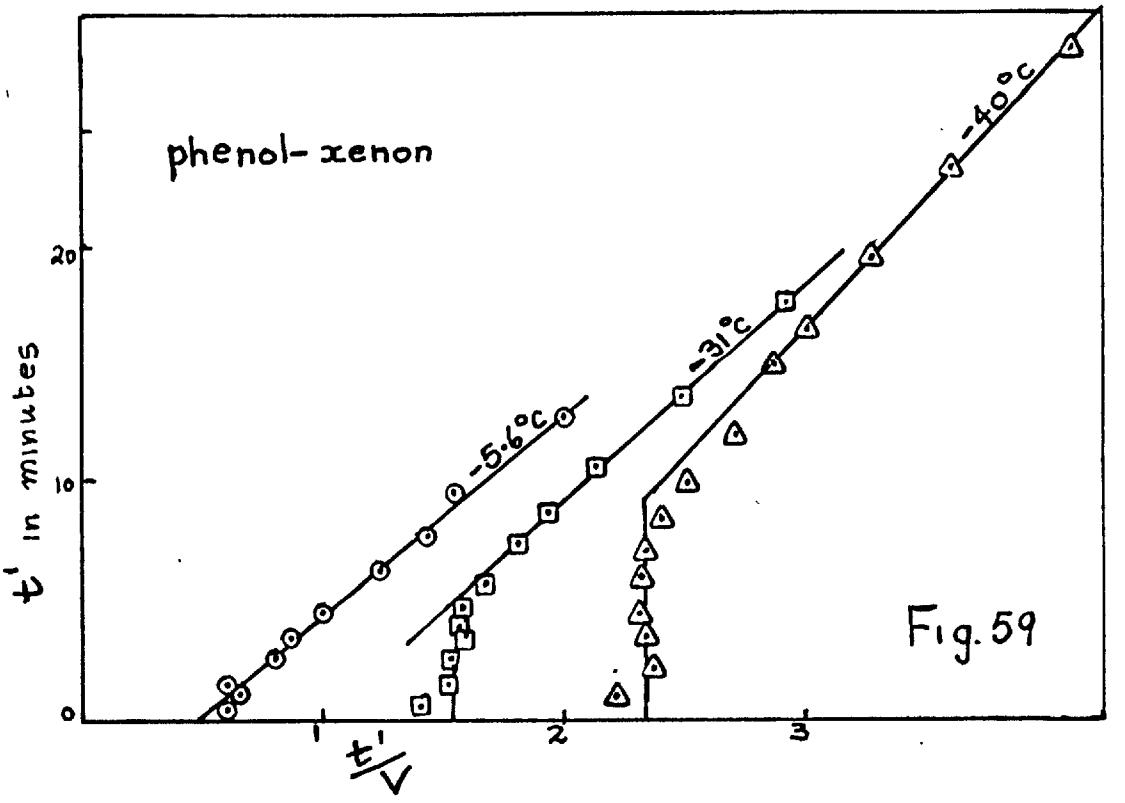
phenol-xenon
-5.6°C
-31°C
-40°C
t' in minutes
t'/V
0
10
20
1
2
3

Fig. 59

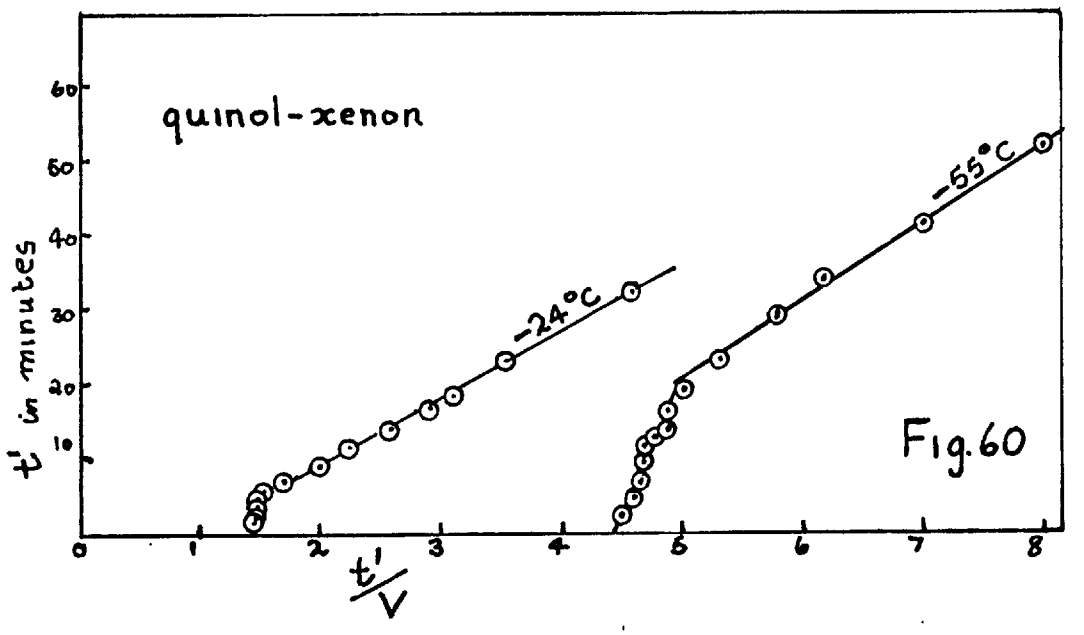
quinol-xenon
-24°C
-55°C
t' in minutes
t'/V
0
10
20
30
40
50
60
1
2
3
4
5
6
7
8

Fig. 60

lower part obeys the relationship $V_t = t^1C$ where C is a constant, while the upper part obeys the relationship $\frac{t^1}{V_t} = A + Bt^1$, where A and B are constants. When t^1 is very large V_t approaches V_m, the maximum sorption of gas at equilibrium, and hence for very large t^1:

$$\frac{t^1}{V_m} = A + Bt^1$$

and also $Bt^1 \gg A$ therefore:

$$\frac{t^1}{V_m} = Bt^1 \text{ or } B = \frac{1}{V_m}$$

V_m may thus be found from the slope of the upper straight line and hence $\frac{V_t}{V_m} = \phi_t$ found for each value of t^1. Figs. 61 and 62 show plots of ϕ_t against t^1 for the two systems.

For the lower part of the curve

$$(48) \quad V_t = t^1C \text{ or } \phi_t = \frac{t^1C}{V_m} .$$

Differentiating with respect to t^1:

$$(49) \qquad \frac{d\phi_t}{dt^1} = \frac{C}{V_m} = C^1 \qquad \text{where } C^1 = \frac{C}{V_m}$$

For the upper part of the curve the equation is

$$(50) \qquad \frac{t^1}{V_t} + A + \frac{t^1}{V_m}, \quad \text{or} \quad \frac{t^1}{\phi_t} = AV_m + t^1$$

On rearranging the last relation one finds

$$(51) \qquad t^1 = \phi_t AV_m + \phi_t t^1 \quad \text{and} \quad t^1 = \frac{\phi_t AV_m}{1-\phi_t}$$

Next, differentiating w r.t. t^1 gives

$$(52) \qquad 1 = AV_m \frac{d\phi_t}{dt^1} + \phi_t + t^1 \frac{d\phi_t}{dt^1}$$

and rearranging the above expression leads to

$$(53) \qquad \frac{d\phi_t}{dt^1} = \frac{1-\phi_t}{AV_m+t^1}$$

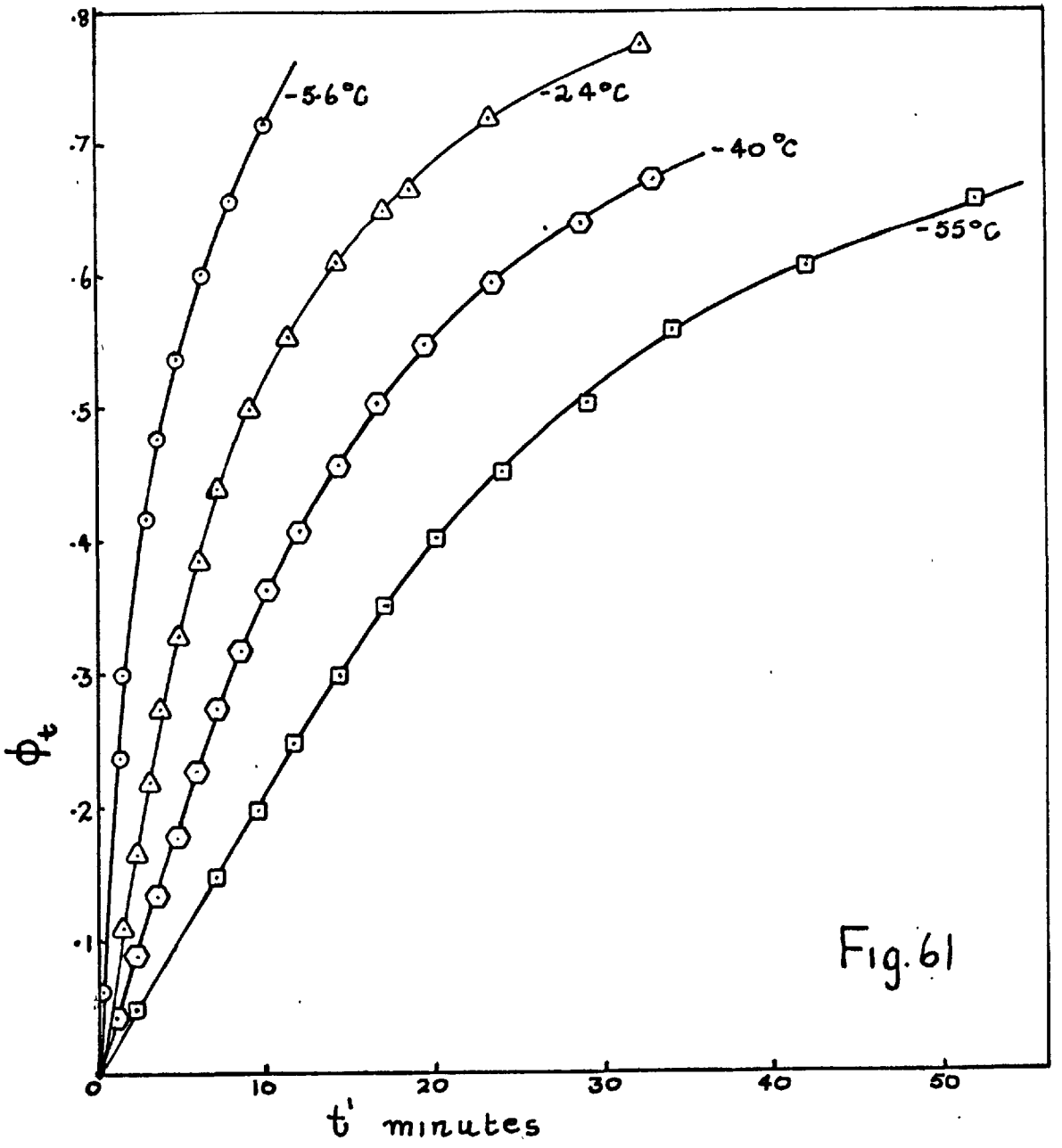

Fig. 61

Quinol-xenon 54·1 cms. of mercury

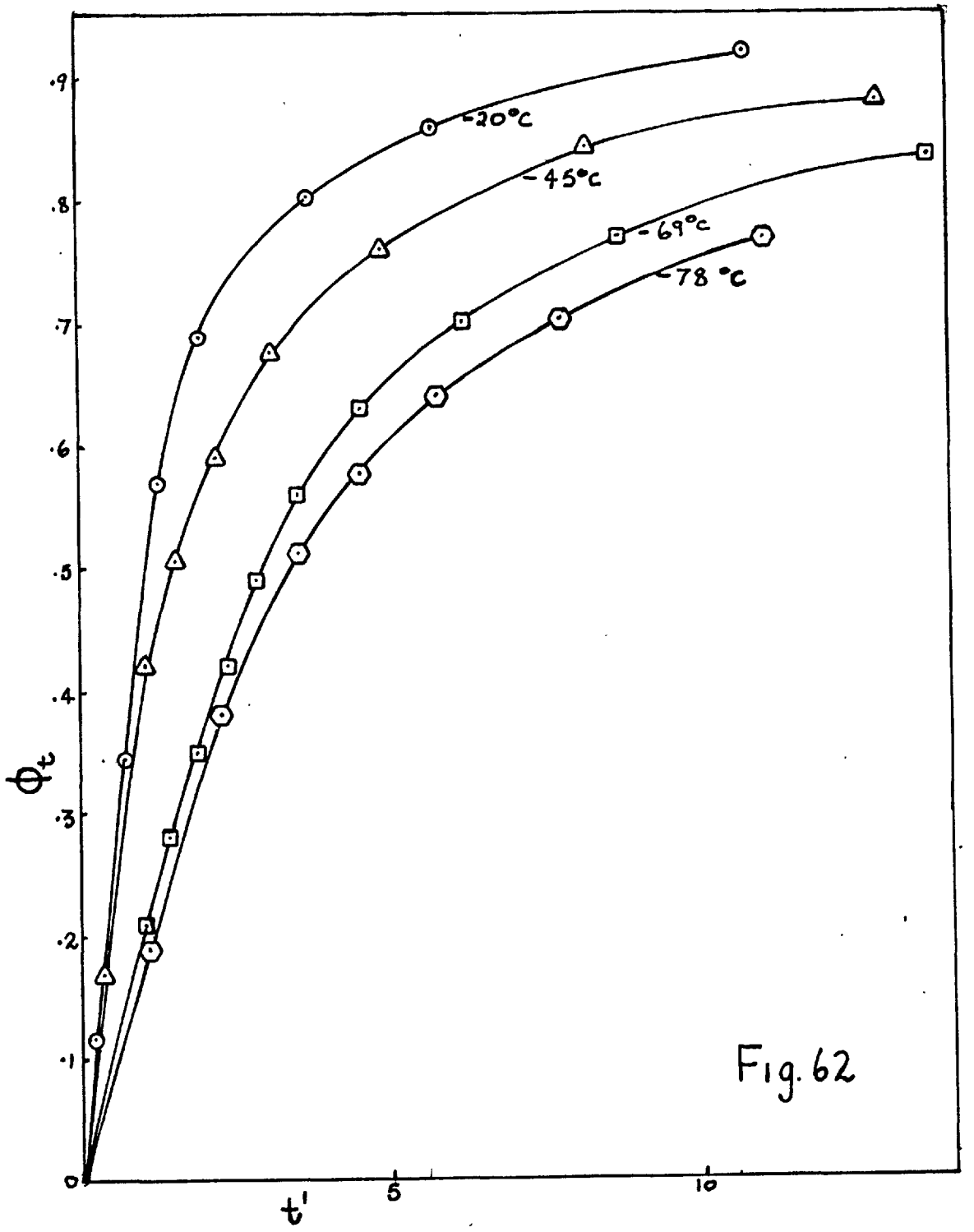

Fig. 62

Phenol-xenon P_e = 37 cms of mercury

Finally substituting for t^1 from equation (51) gives

$$(54) \quad \frac{d\phi_t}{dt^1} = \frac{1 - \phi_t}{AV_m + \frac{\phi_t AV_m}{1 - \phi_t}}$$

$$= \frac{(1 - \phi_t)^2}{AV_m}$$

$$(55) \quad \text{or } \frac{d\phi_t}{dt} = A^1(1 - \phi_t)^2 \quad \text{where } A^1 = \frac{1}{AV_m}$$

The influence of temperature on the reaction velocity is shown by the variation of A^1 and C^1 with temperature. It was of interest to compare these temperature variations with that of the Arrhenius equation, $\ln k = \frac{-E}{RT} + \text{constant}$.

Further kinetic runs were therefore made to obtain more values of A^1 and C^1 and plots were made of $\text{Log.}_{10}A^1$ and $\text{Log.}_{10}C^1$ against $\frac{1}{T}$.

As shown in Figs. 63-66, the phenol-xenon results give a reasonable approximation to a straight line, but the quinol-xenon results show considerably more scatter.

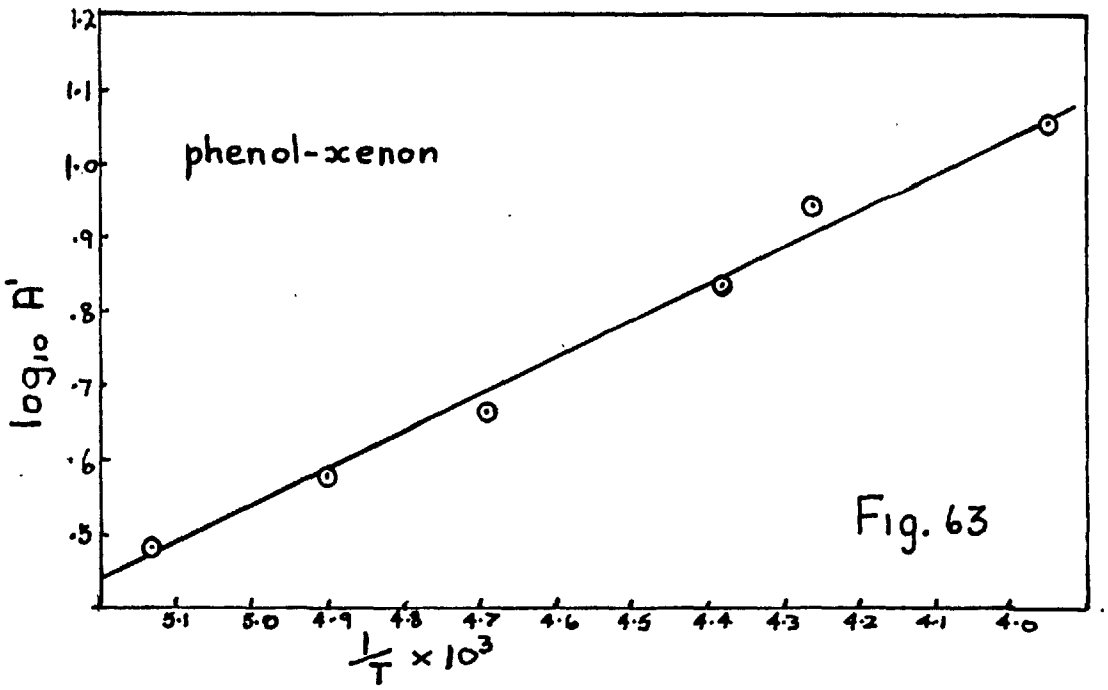
phenol-xenon
$\log_{10} A'$
1·2
1·1
1·0
·9
·8
·7
·6
·5
5·1 5·0 4·9 4·8 4·7 4·6 4·5 4·4 4·3 4·2 4·1 4·0
$\frac{1}{T} \times 10^3$

Fig. 63

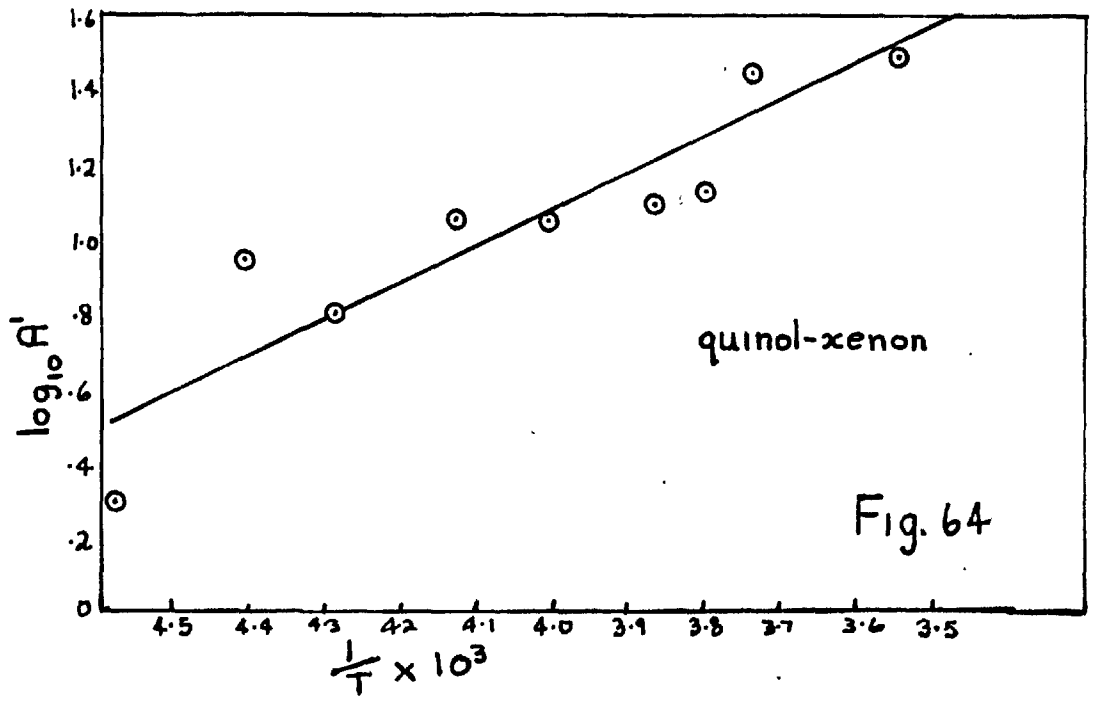
quinol-xenon
$\log_{10} A'$
1·6
1·4
1·2
1·0
·8
·6
·4
·2
0
4·5 4·4 4·3 4·2 4·1 4·0 3·9 3·8 3·7 3·6 3·5
$\frac{1}{T} \times 10^3$

Fig. 64

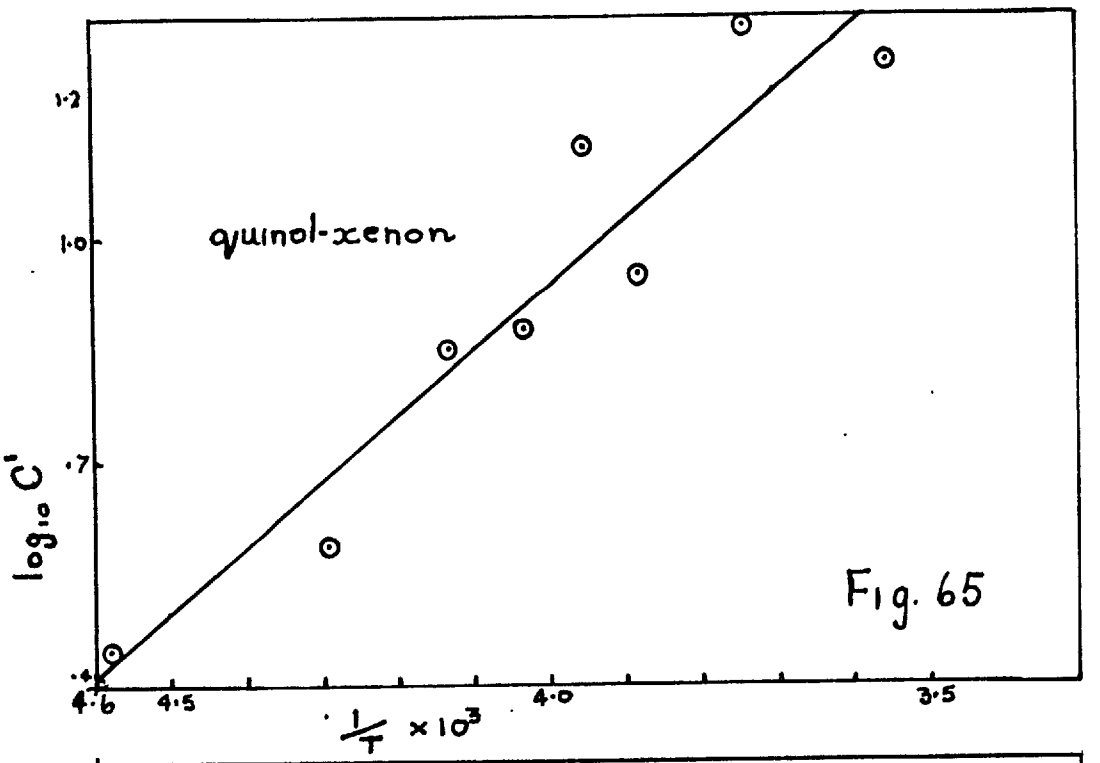
quinol-xenon
$\log_{10} C'$
1·2
1·0
·7
·4
4·6
4·5
4·0
3·5
$\frac{1}{T} \times 10^3$

Fig. 65

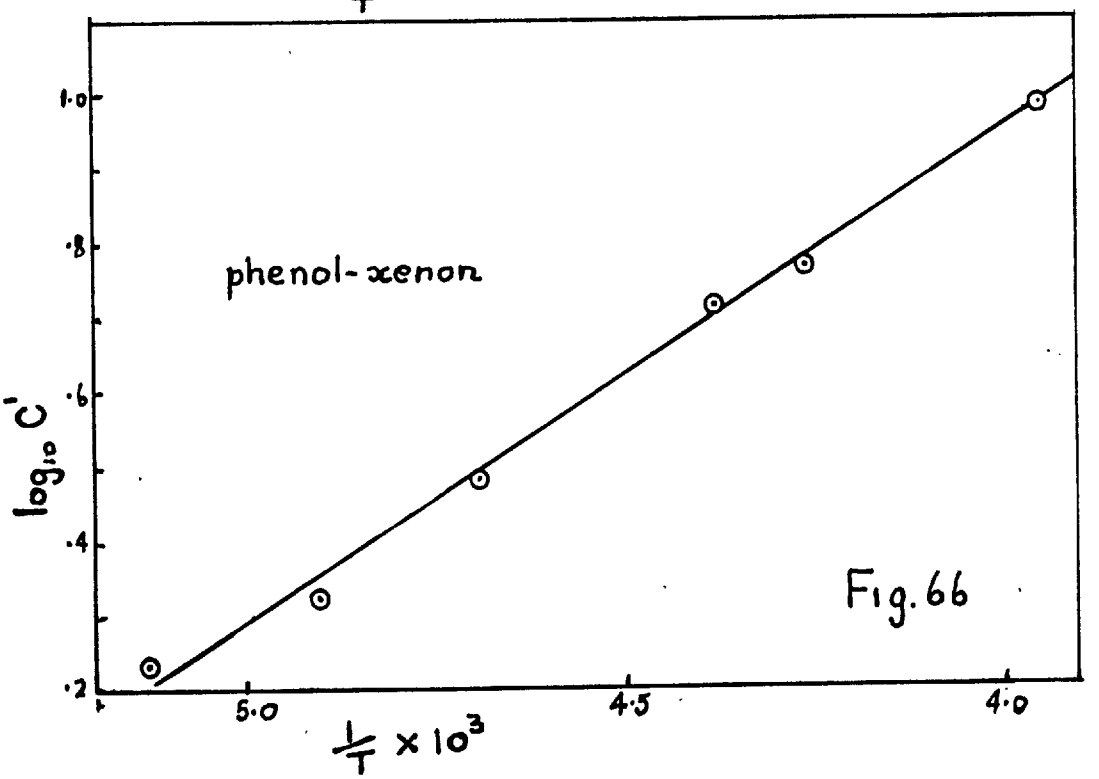
phenol-xenon
$\log_{10} C'$
1·0
·8
·6
·4
·2
5·0
4·5
4·0
$\frac{1}{T} \times 10^3$

Fig. 66

A calculation of E, the apparent "energy of activation" was made, the slope of the straight line being equal to $\frac{-E}{2.303\ R}$. The values found were

	E(K cals./mole)	
	A^1	C^1
quinol-xenon	4.4	4.0
phenol-xenon	2.2	3.4

Isothermal kinetic runs were then made for the phenol-xenon system in which the pressure was kept constant for a given run, but was varied from run to run. The runs were made at -30°C., with two additional runs, at -78°C. Fig. 67 shows plots of ϕ_t against t^1. The rate of the reaction was found to vary very little over a considerable change in pressure.

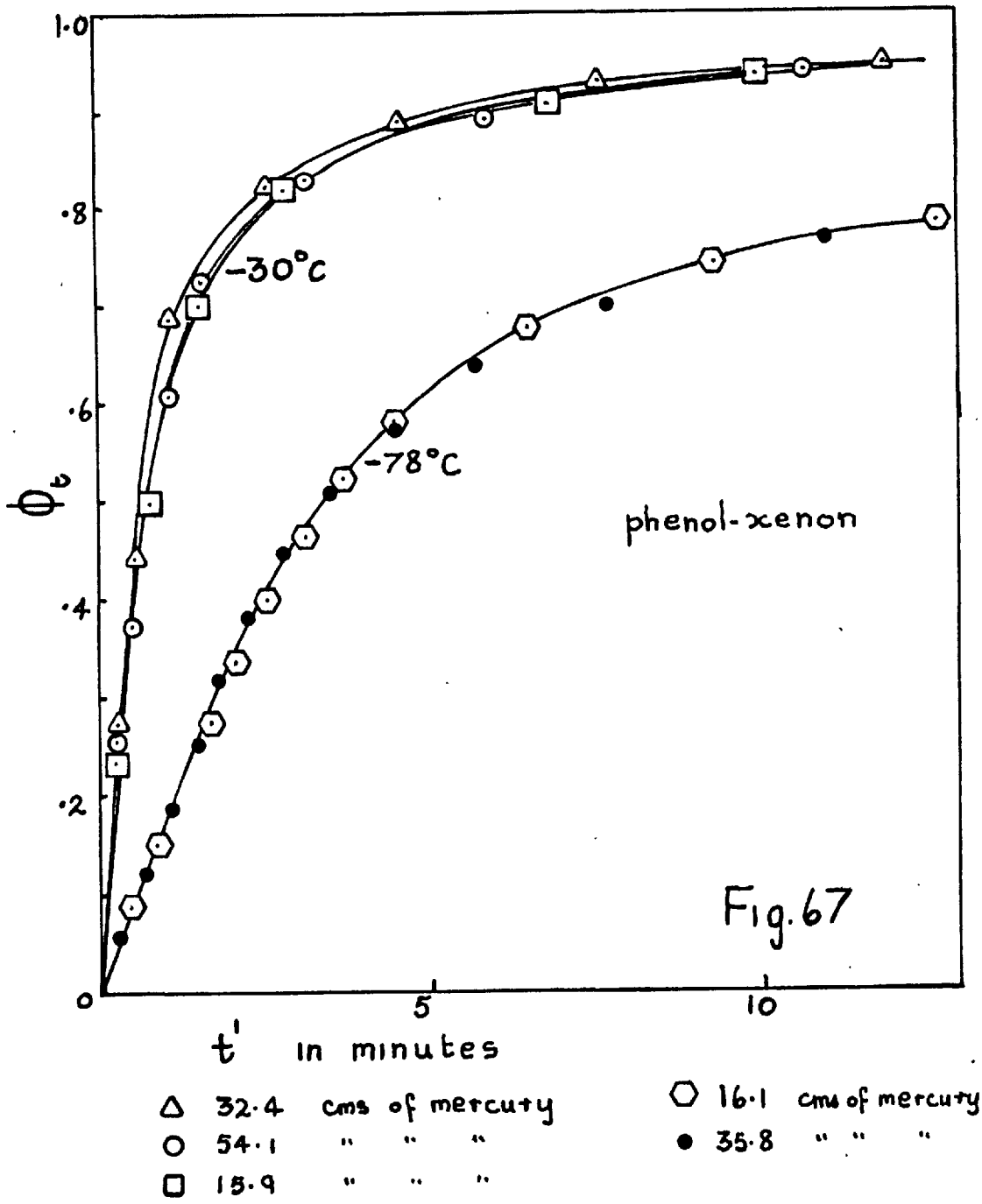
1·0
·8
·6
·4
·2
0
θ
5
10
t' in minutes
-30°C
-78°C
phenol-xenon
△ 32·4 cms of mercury
○ 54·1 " " "
□ 15·9 " " "
⬡ 16·1 cms of mercury
● 35·8 " " "

Fig. 67

III.5.3 Kinetic Runs with Interrupted Shaking

In all the above kinetic runs shaking of the reaction vessel was continuous throughout the course of the experiment. A number of kinetic runs were now made in which shaking was stopped shortly after sorption of gas indicated that the clathrate had started to form. The rate of uptake of gas was now observed to fall off very sharply. If after a time shaking was re-started the uptake of gas rapidly increased and the further kinetics followed the behaviour observed for continuous shaking. Figs. 68-71 show plots of V against t for the four systems, quinol-xenon, quinol-carbon dioxide, phenol-xenon and phenol-carbon dioxide. For the phenol-carbon dioxide the additional uptake of gas after shaking had stopped was proportionately much greater than for the other three systems.

If plots of $\frac{t''}{V''}$ against t" are made, where t" is the time measured from when shaking was stopped and V" is the corresponding further amount of gas sorbed, then as for the kinetics with continuous shaking straight line plots are obtained for the upper part of the curve. V''_m the maximum amount sorbed with no further shaking may be found from the slope of this straight line and

has been included in Figs. 68 and 70. If V" is plotted against $\text{Log.}_{10} \frac{1}{k}(t'' + k)$, where k is a constant, the value of which depends on the particular clathrate species then a good approximation to a straight line graph is obtained for the first part of these kinetics (Figs. 72 and 75). The curve begins to level off as t" becomes large. This relationship is similar to the "logarithmic law" found for the thickening of certain oxide films.[25]

III.5.4 Kinetic Runs With No Shaking

Kinetic investigations were made in which the sample of phenol or quinol was first shaken for a period under vacuum, the shaking stopped and then gas admitted to the reaction vessel. The sample was not shaken at all while in contact with the gas. Over a 24 hour period no sorption of the gases krypton, xenon and methane was found for both quinol and phenol. There was a very small sorption of carbon dioxide by quinol but a considerable uptake of carbon dioxide by phenol was found to have taken place. This sorption of carbon dioxide by phenol was investigated in more detail in two ways.

In the first a sample of phenol was placed in the reaction vessel, the system evacuated and the crystals

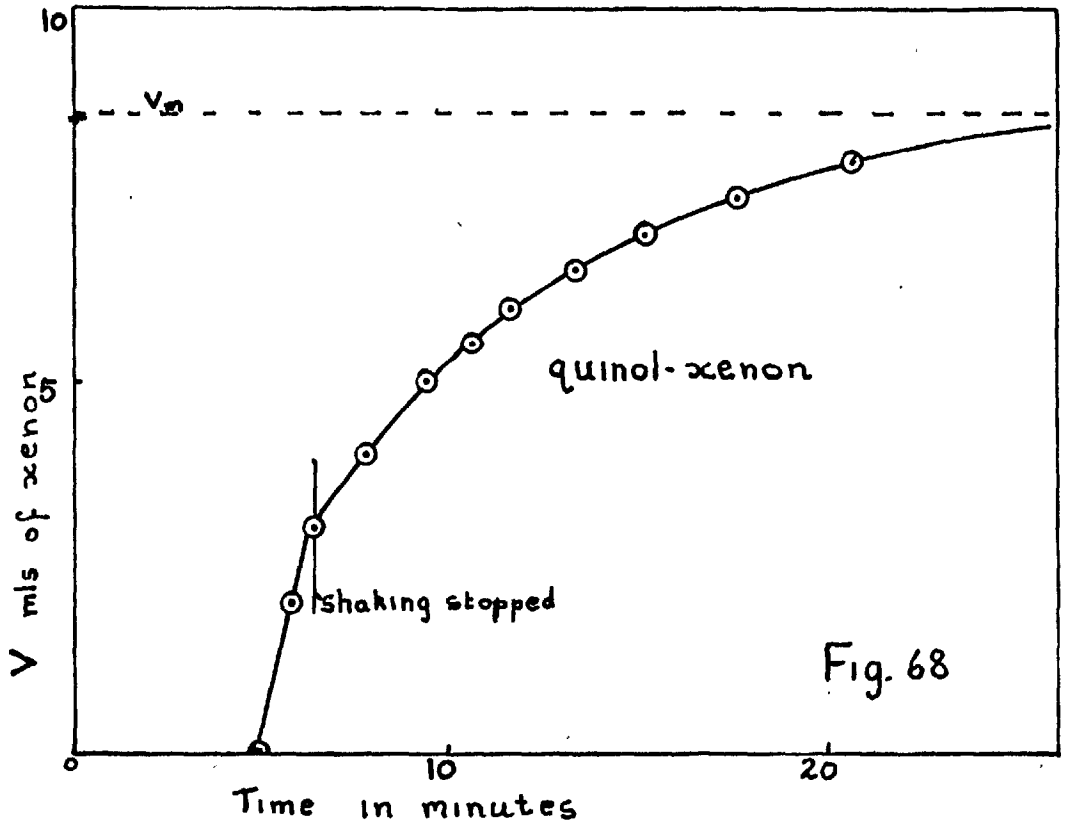
10
V_∞
V mls of xenon
quinol-xenon
shaking stopped
0
10
20
Time in minutes

Fig. 68

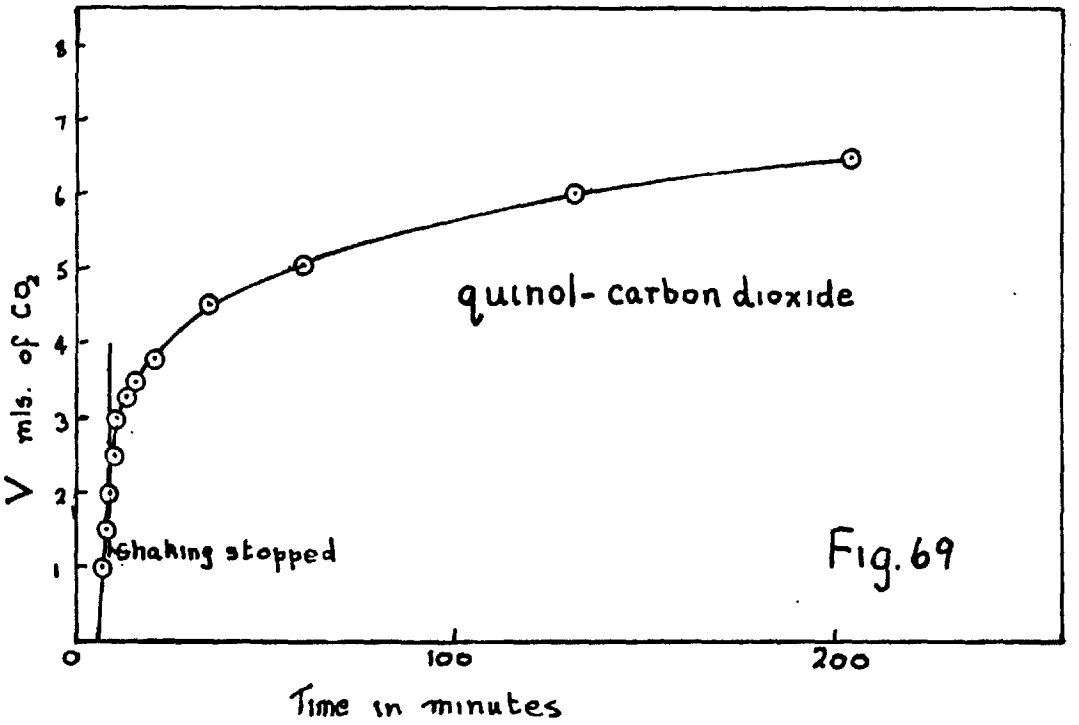
8
7
6
5
4
3
2
1
V mls. of CO_2
quinol-carbon dioxide
shaking stopped
0
100
200
Time in minutes

Fig. 69

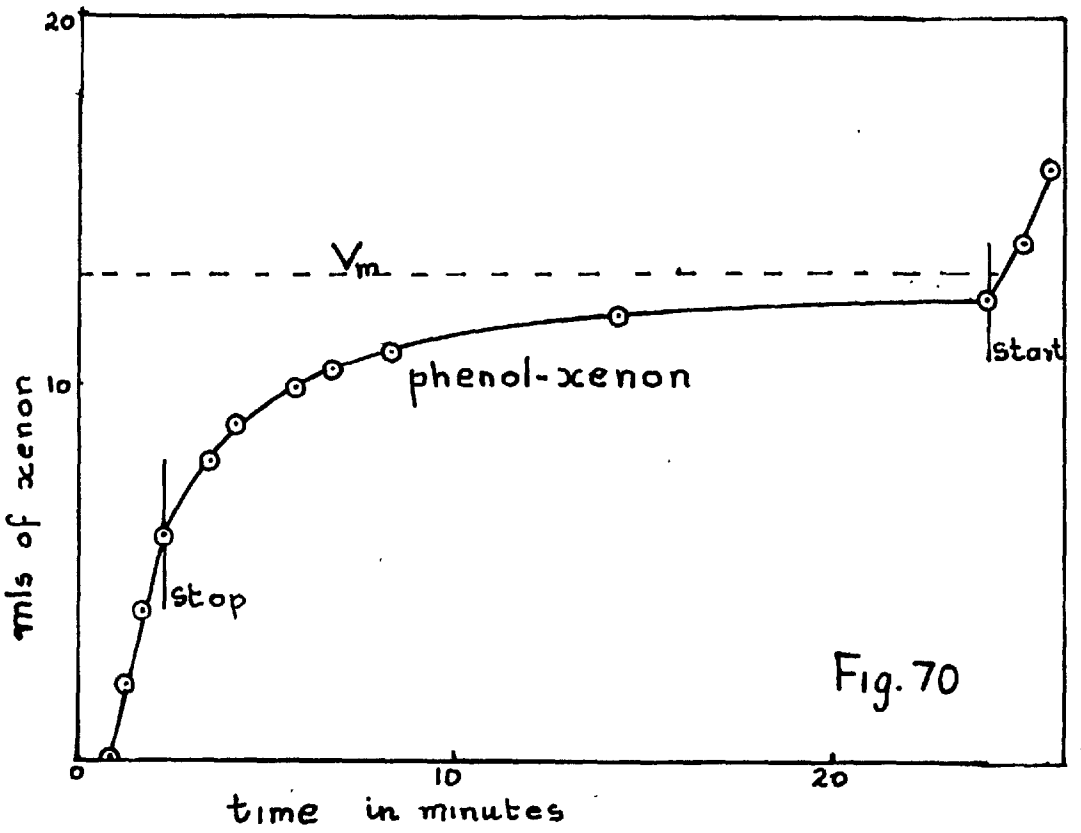
20
10
0
10
20
Vm
start
stop
phenol-xenon
mls of xenon
time in minutes

Fig. 70

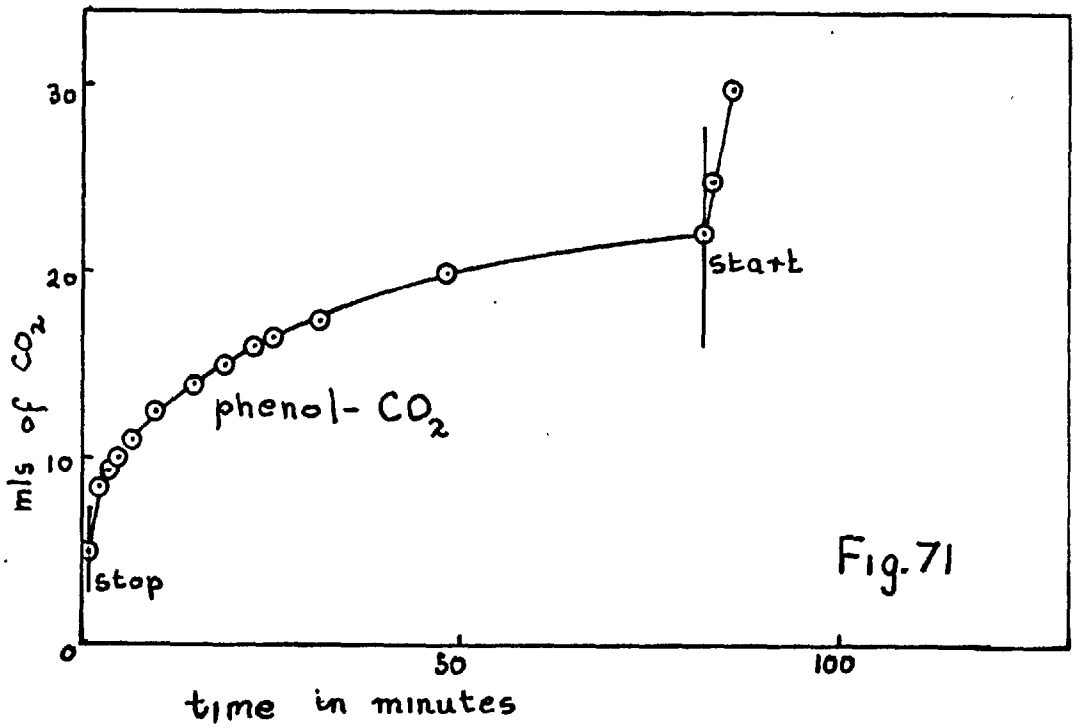
30
20
10
0
50
100
start
stop
phenol- CO_2
mls of CO_2
time in minutes

Fig. 71

shaken under vacuum for two minutes exactly. The sample was then left standing under vacuum for a period of time t_s, and then carbon dioxide was admitted to the reaction vessel. Still without further shaking the rate of sorption of carbon dioxide was measured. This experiment was repeated a number of times, shaking under vacuum for two minutes in each case but varying the "waiting time" t_s. The temperature and pressure were kept constant at -50°C. and 46 cm. of mercury respectively. As for the kinetics in which shaking was continuous, the sorption of gas did not start immediately it was admitted to the reaction vessel but only after an initiation time τ. The rate of sorption was the same in each case and independent of t_s. Fig. 76 shows a plot of τ against t_s. The result shows a large scatter but in general τ increases with increasing t_s. When t_s is zero τ is very close to the initiation time found when shaking is continuous at this temperature and pressure.

In a second series of kinetic runs the reaction vessel was shaken for a different length of time for each run but the "waiting time" t_s was kept constant at ten minutes. These runs were all made at a temperature of -78°C. and a pressure of 53 cms. of mercury. The

upper parts of these kinetic curves also give good straight line plots for $\frac{t^1}{V_t}$ against t^1, and V_m may be found from the slope. $\phi_t = \frac{V_t}{V_m}$ was calculated for each point and plotted against t, the time after the admission of gas, as shown in Fig. 77. The initiation time τ was found to increase as the shaking time decreased, while the initial rate of the reaction was found to decrease with decrease in the shaking time.

For phenol-carbon dioxide at -78°C. the final amount sorbed found with continuous shaking is, within experimental error, the theoretical maximum, 79.34 mls. of carbon dioxide at s.t.p. per gram of phenol. This was also found to be the case for these kinetic runs in which there was no shaking after admission of gas.

A further single experiment was performed at -78°C. in which large uncrushed crystals of phenol were introduced into the reaction vessel, the system evacuated and then carbon dioxide admitted to a pressure of 53 cms. of mercury. A very small uptake of gas was observed to have taken place over a period of 24 hours.

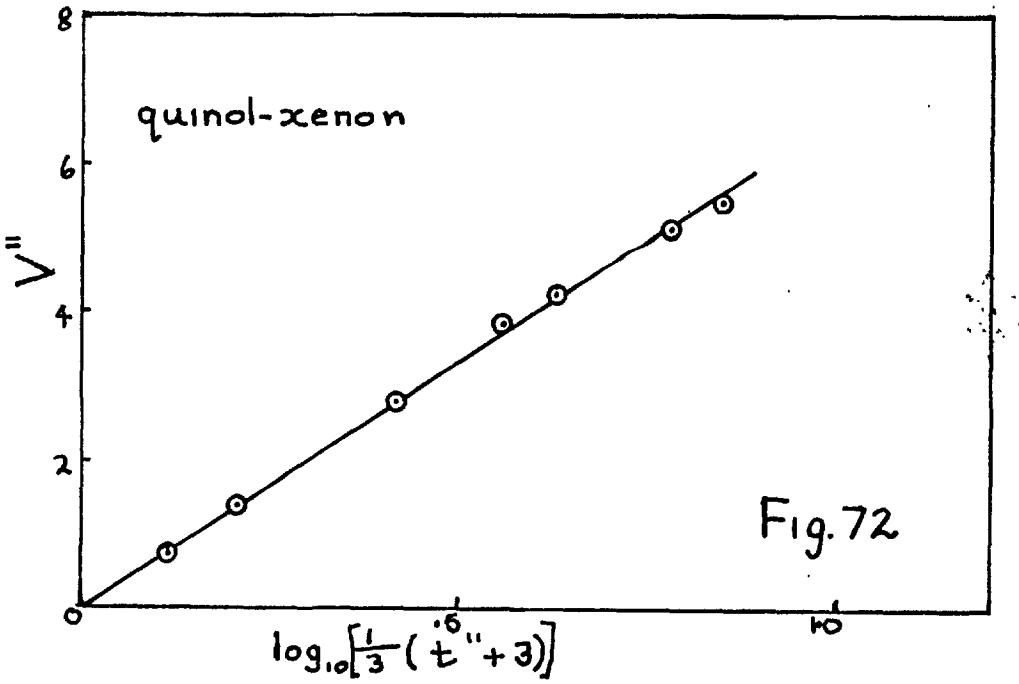
quinol-xenon
8
6
4
2
0
V=
1·0
log10[1/3 (t"+3)]

Fig. 72

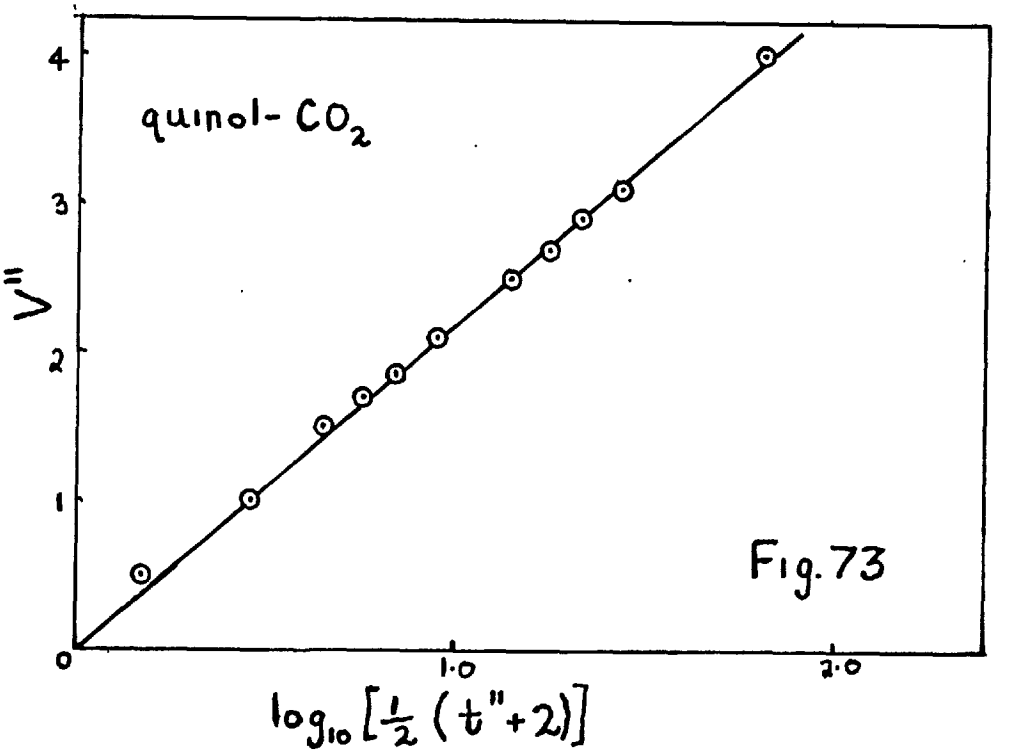
quinol- CO2
4
3
2
1
0
V=
1·0
2·0
log10 [1/2 (t"+2)]

Fig. 73

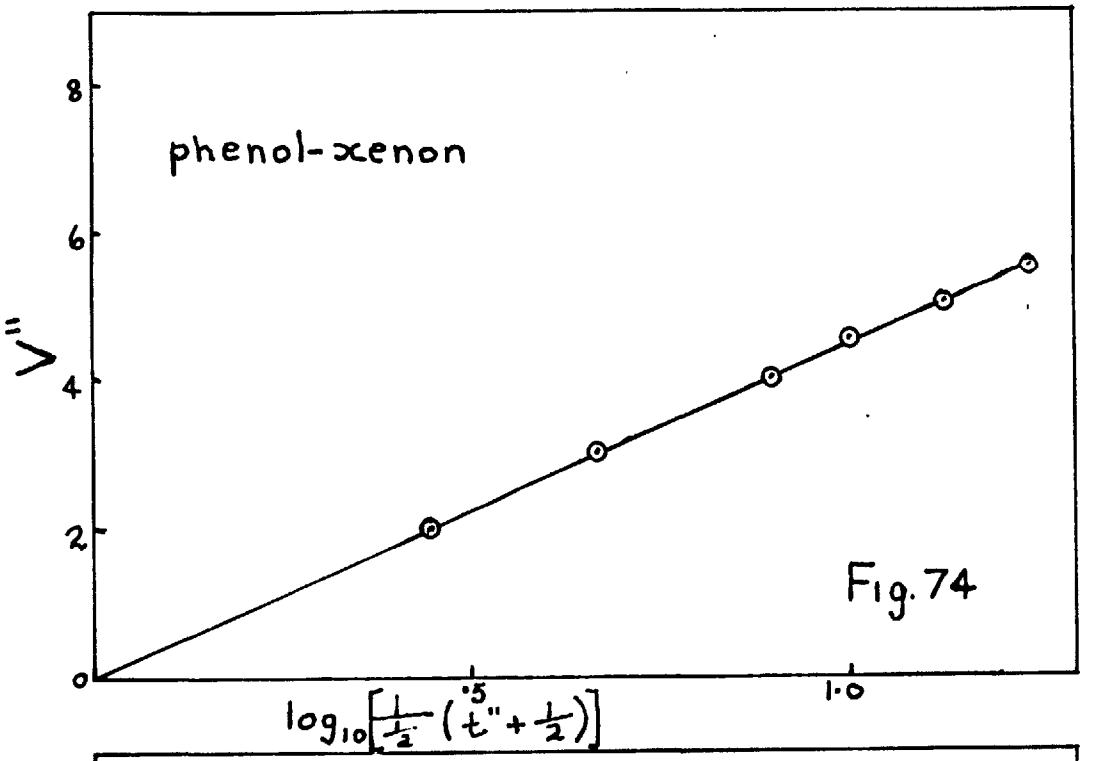
phenol-xenon
8
6
4
2
0
V
·5
1·0
$\log_{10}\left[\frac{1}{\frac{1}{2}}\left(t''+\frac{1}{2}\right)\right]$

Fig. 74

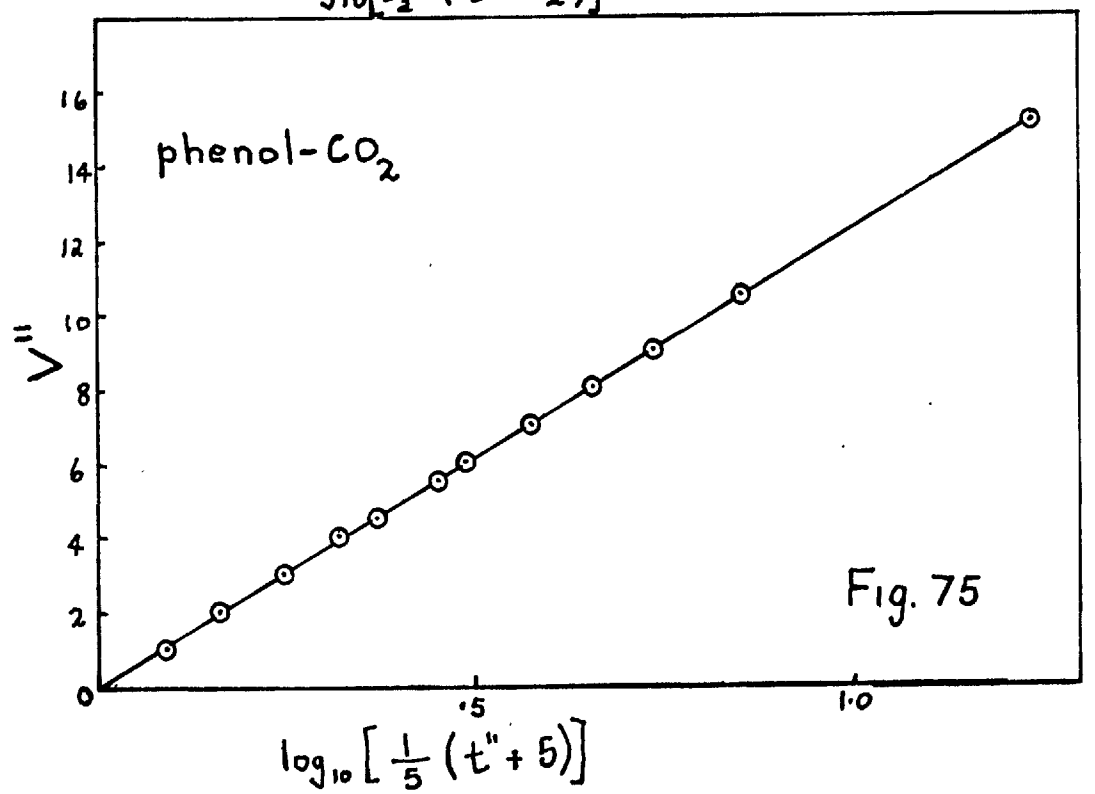
phenol-CO_2
16
14
12
10
8
6
4
2
0
V
·5
1·0
$\log_{10}\left[\frac{1}{5}\left(t''+5\right)\right]$

Fig. 75

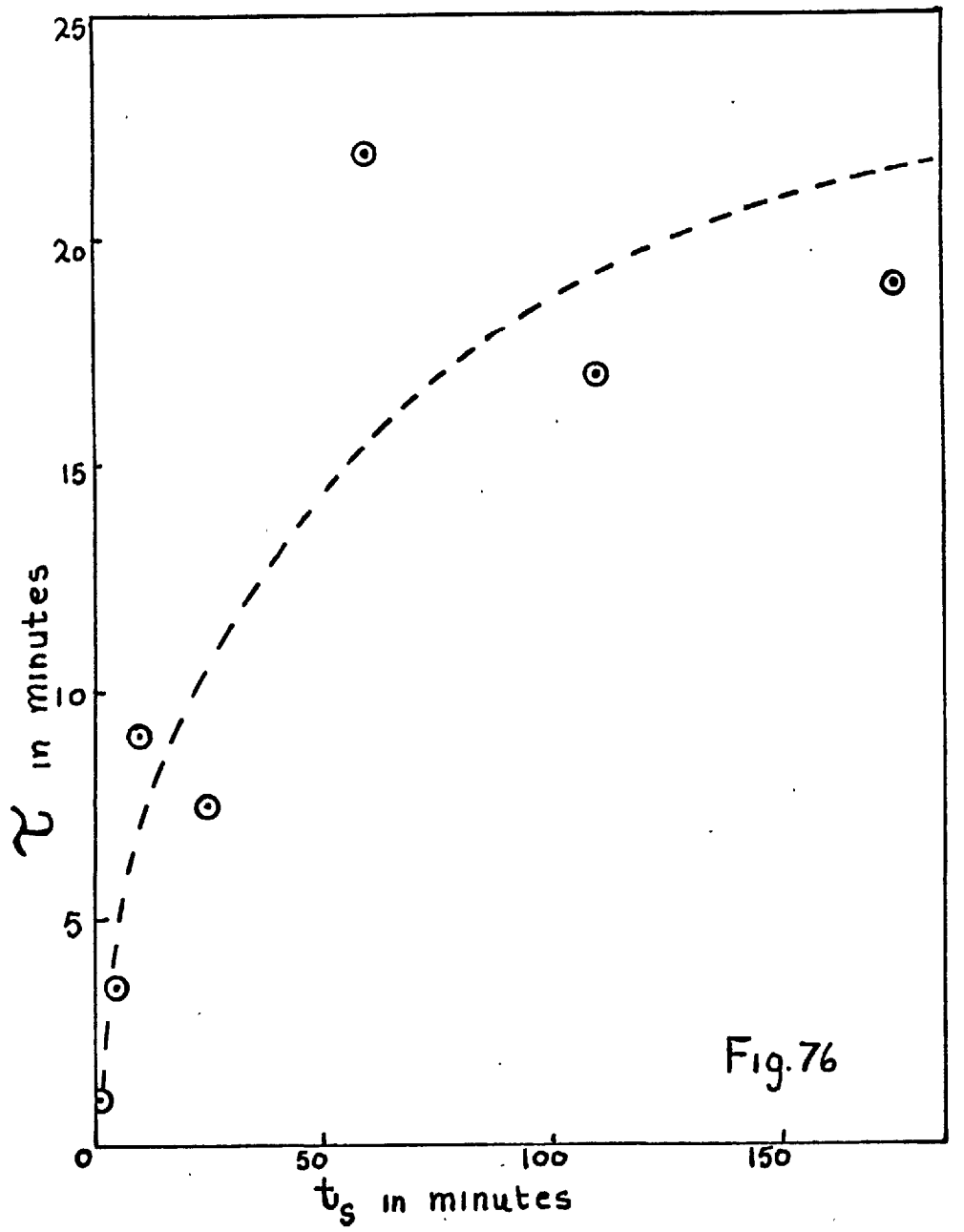

Fig. 76

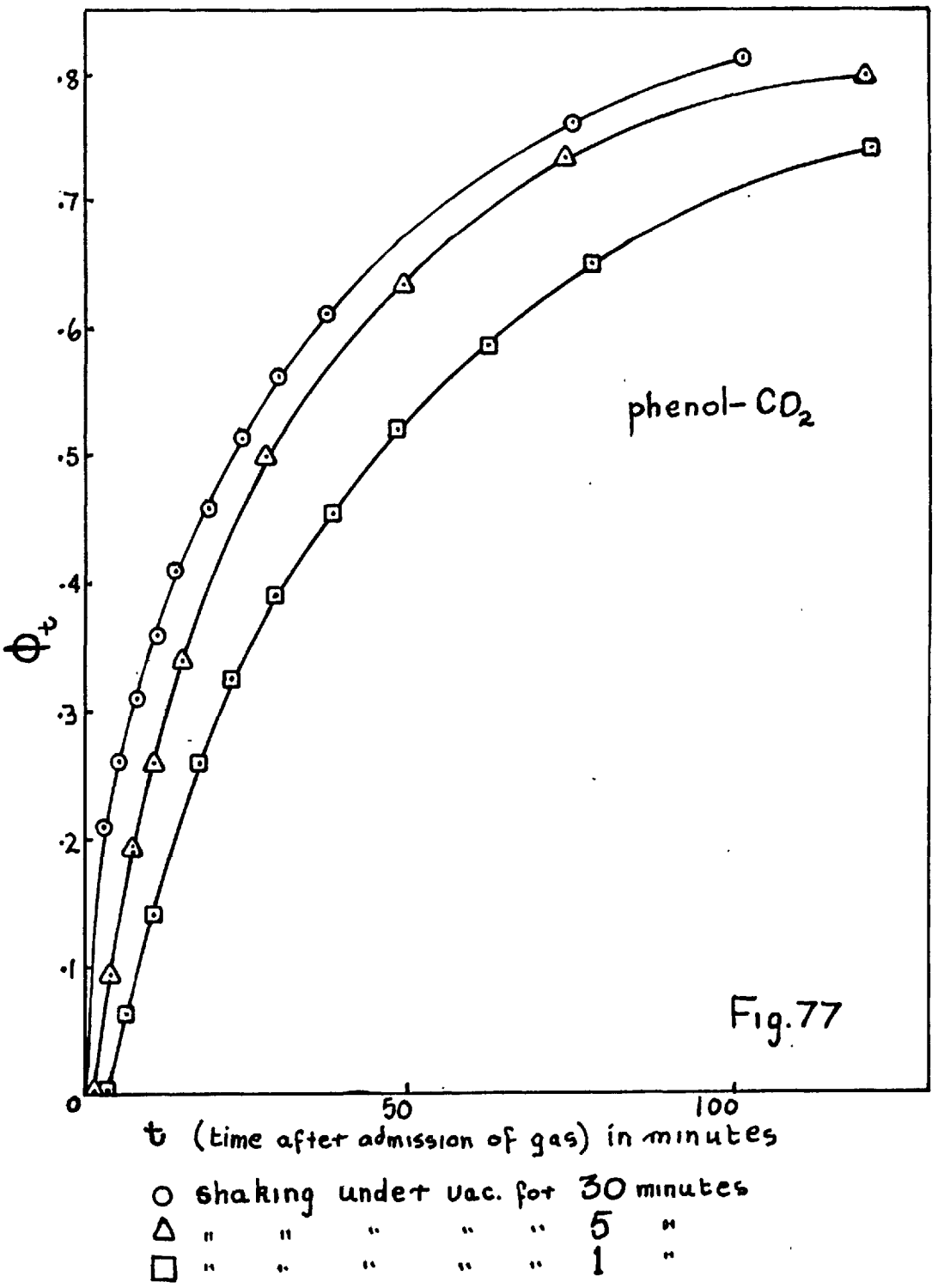
·8
·7
·6
·5
·4
·3
·2
·1
0
ϕ_t
50
100
phenol-CO_2
t (time after admission of gas) in minutes
○ shaking under vac. for 30 minutes
△ " " " " " 5 "
□ " " " " " 1 "

Fig. 77

Nikitin[9] has found similar results for phenol and a number of gases. He observed no reaction between finely powdered and dried phenol and the gases argon, krypton and xenon at pressures of about 1.5 atmospheres and over a temperature range between room temperature and -185°C. He found however an immediate reaction between phenol and hydrogen sulphide. Nikitin reported that the crystals of phenol-hydrogen sulphide compound could act as nucleii for a phenol-xenon reaction.

III. 5.5 The Effect of Shaking on the Reaction

These kinetic experiments have shown the importance of the shaking and crushing action in the reaction of crystals of quinol and phenol with various gases to form clathrates. The formation of the clathrates would seem to depend on shaking and crushing in two ways, firstly for the initiation of the reaction and secondly to allow the reaction to proceed to equilibrium.

Without shaking, of the gases investigated, only carbon dioxide gave any reaction at all, suggesting that the shaking creates or greatly enhances the conditions necessary for the embryos of the β -phase to form. If

shaking is stopped once the reaction has been initiated the rate of reaction falls off rapidly and, except for phenol-carbon dioxide, comes to a stop. Clathrate formation can take place where a surface of α -phase is exposed to the gas. It would be expected that this surface would rapidly become covered with a layer of clathrate as the reaction proceeds, preventing access of the gas to the remaining α -phase and "poisoning" the reaction. Shaking would crack or break off this clathrate layer continuously exposing unreacted α -phase to the gas and allowing the reaction to proceed to completion.

The anomalous behaviour of carbon dioxide with phenol has a possible explanation suggested by the structure of the phenol clathrate lattice. As described in the discussion of crystal structure on page 16 there are windows between the large cavities of the β -phenol structure. The carbon dioxide molecules might diffuse through these windows to reach the surface boundary between the two solid phases allowing the formation of the clathrate to proceed to completion.

R E F E R E N C E S

1. Mylius, F., Ber., 19,999 (1886).

2. Palin, D.E. and Powell, H.M., J.Chem.Soc., 1947, 208.

3. Powell, H.M., J.Chem.Soc., 1948, 61.

4. Palin, D.E. and Powell, H.M., J.Chem.Soc., 1948, 571.

5. Caspari, W.A., J.Chem.Soc., 1926, 2944.

6. Caspari, W.A., J.Chem.Soc., 1927, 1093.

7. Palin, D.E. and Powell, H.M., J.Chem.Soc., 1948, 815.

8. Terres, E. and Vollmer, W., Petroleum Z., 31, (19), 1, (1935).

9. Nikitin, B.A., J.Gen.Chem.(U.S.S.R.), 9, 1167 (1939).

10. Nikitin, B.A. and Kovalskaya, M.P., Bull.Acad.Sci. U.S.S.R., Div. Chem. Sci., 1952, 23.

11. Stackelberg, M. von, Hoverath, A., and Schringer, C., Z.Elektrochem., 62, 129 (1958).

12. Mandelcorn, L., Chem.Rev., 59, 827 (1959).

13. Stackelberg, M. von, "Proc.Inter.Conf. on Coordination Compounds, Amsterdam, 1955", p. 408.

14. Van der Waals, J.H., Trans. Faraday Soc., 52, 184 (1956).

15. Van der Waals, J.H. and Platteeuw, J.C., "Advances in Chemical Physics", ed. by I. Prigogine, Vol. 2, p.1, London, Interscience Press Inc., 1959.

16. Barrer, R.M. and Stuart, W.I., Proc.Roy.Soc.(London) A243, 172 (1957).

17. Barrer, R.M. and Rees, L.V.C., Trans. Faraday Soc., 50, 852 (1954).

18. Van der Waals, H.H. and Platteeuw, J.C., Rec.Trac. Chim., 75, 912 (1956).

19. Van der Waals, J.H. and Platteeuw, J.C.,,unpublished result.

20. Powell, H.M., Rec.Trav.Chim., 75, 885 (1956).

21. Evans, D.F. and Richards, R.E., Proc.Roy.Soc. (London) A223, 238 (1954).

22. Lahr, P.H. and Williams, H.L., J.Phys.Chem., 63, 1432 (1959).

23. Barrer, R.M. and Ruzicka, D.J., Trans.Faraday Soc., 58, 2239 (1962).

24. Barrer, R.M. and Ruzicka, D.J., Trans.Faraday Soc., 58, 2262 (1962).

25. Child, W.C., Quart Rev. (1964) 18, 321-346.

26. Evans, U.R., Trans.Faraday Soc., 41, 365 (1945).